To The Graduate Council

I am submitting herewith a thesis written by Kelly E McDougall entitled "Flight Testing Flow Diverting Devices On an OH-58A+ For Applications To An MH-6 Helicopter " I have examined the final copy of this thesis for form and content and recommend that it be accepted in partial fulfillment of the requirements for the degree of Master of Science, with a major in Aviation Systems

Dr W Lewis, Major Professor

We have read this thesis and recommend its acceptance

Dr R Kimberlin

F Stellar

Accepted for the Council

Interim Vice Provost and
Dean of the Graduate School

FLIGHT TESTING FLOW DIVERTING DEVICES ON AN OH-58A+ FOR APPLICATIONS TO AN MH-6 HELICOPTER

A Thesis

Presented for the

Master of Science

Degree

The University of Tennessee, Knoxville

Kelly E. McDougall

December 2000

DEDICATION

This thesis is dedicated to my wife and children who, because of their love, patience, unselfish support, and encouragement throughout this endeavor have made this manuscript possible.

ACKNOWLEDGMENTS

The author wishes to express sincere appreciation to Doctor William Lewis, Doctor Ralph Kimberlin, and Professor Fred Stellar for their assistance in the preparation of this manuscript. Additionally, a special thanks to Colonel Rick Bowman and the rest of the men of the 160th SOAR, not only for their support to this project but also for their tireless support for this country.

ABSTRACT

This study investigates the use of Flow Diverting Devices to reduce passenger fatigue and parasite drag (specifically equivalent flat plate drag) for the 160th Special Operations Aviation Regiment MH-6 Helicopters. Due to cost, scheduling, and airworthiness release (AWR's) issues this manuscript focuses on the actual flight test data of a similar helicopter, the OH-58A+. The flight-testing investigated the level flight performance, and handling qualities with doors removed, with and without the Flow Diverters installed. Consideration was also given in the design to discover ways of minimizing the airflow on the external passengers (amount of deflection), changes in noise level, and to the reduction in the field of view measured from the Design Eye Position. The baseline aircraft (with doors removed) was tested against 3 different types of Flow Diverting Devices (6 inch Sawtooth, 6 inch Flat Plate with Vortex Generators installed, and 8 inch Flat Plate with Vortex Generators installed).

It was determined that the airflow can be deflected away from the passengers a maximum of 16 inches with no adverse impact on handling qualities. This is important for several reasons:

1. Possible increase in performance.
2. Passenger comfort.
3. Mission envelope expansion.

This mission envelope expansion would include the ability to fly in colder temperatures, feasible to fly in precipitation, as well as possibly having the ability to maintain faster enroute speeds without causing undue fatigue on the passengers. This deflection was achieved with an average increase of 4.0 square feet of equivalent flat plate drag. This is much less than the effect flat plate drag on the MH-6 due to passengers and equipment installed for the mission. Additionally, during the flight testing it was noted that there were no detectable changes to the handling qualities or the noise level inside the test aircraft.

Hence, the author concluded that the 8 inch Flat Plate, with Vortex Generators, Flow Diverting Device will successfully divert the airflow around the upper body of the external passengers thus reducing passenger fatigue and increasing their safety during flight. It is reasonable to assume that the MH-6 helicopter will realize a performance enhancement during flight in high drag configurations (with external passengers). Additionally, it is also possible that the MH-6 in the baseline configuration (doors off, external passenger system installed) could realize a slight performance increase.

The author made the following recommendations:

1. Develop a set of flow diverters specifically for the MH-6.
    a. 8" Flat Plate with Vortex Generators.
    b. The angle should be between 40° and 50°.

c. The Flow Diverter should be capable of 2 positions, full open (maximum deflection) and fully closed (no Deflection). However, if there is a performance increase with the flow diverters installed over the baseline MH-6 there would be little reason to use the fully closed position.

2. Conduct Flight Tests with an MH-6 in its typical mission configuration.

   a. These tests should include flights with and without external ballast.

   b. At least two of the flight tests should be with an FTE as an external passenger. For a qualitative comparison evaluation one flight test should be with no deflection and the other with maximum deflection.

3. Recommend that all doors are removed at all times with Flow Diverters installed.

4. Recommend the use of the Smoke Generator System with a greater volume of smoke. This can be done by either a specialized smoke canister or with a portable smoke generator.

TABLE OF CONTENTS

List of Figures vii
List of Tables ix
List of Abbreviations x
Chapter 1: Introduction 1
Background 1
Early Contingencies 3
160th Special Operations Mission Requirements 5
MH-6 Mission Profile 7
Chapter 2: Theory of Performance Flight-Testing 10
General 10
Purpose 11
Level Flight Performance 13
Test Methods 26
Chapter 3: Aircraft Description 29
MH-6 Development History 29
Description of MH-6 32
Description of OH-58A+ (Model Tested) 36
Differences Between the OH-58A+ and the MH-6 43
Chapter 4: Designing of the Flow Diverters 49
Research Motivation 49
Systems Engineering Process 51
Chapter 5: Flight Test Results and Data Analysis 60
Purpose 60
General 60
Instrumentation and Data Acquisition 62
Pitot Static Calibrations 64
Baseline Level Flight Performance 65
Best Angle Testing 68
6" Sawtooth Level Flight Performance Test 69
6" Flat Plate Level Flight Performance Test 71
8" Flat Plate Level Flight Performance Test 74
8" Flat Plate without Vortex Generators 75
Flow Visualization 76
Airflow Testing with Flow Diverters Installed 80
Noise Level Testing 81
Handling Qualities 83
Comparative Data Analysis 84
Chapter 6: Data Reduction 86
Data Reduction 86

TABLE OF CONTENTS (continued)

Noise Evaluation Data Reduction 92
Chapter 7: Conclusions **94**
160th Mission Requirements 97
Chapter 8: Recommendations **99**
Works Consulted 101
References 102
Bibliography 103
Appendices 106
Appendix A: OH-58A+ and MH-6 Physical Data 107
Appendix B: Pitot Statics 115
Appendix C: Flight Test Data 122
Appendix D: Weight and Balance 149
Appendix E: Test Plan 155
Appendix F: Flow Diverter Installation Illustrations 168
Appendix G: Flow Visualization Installation Illustrations 173
VITA 179

LIST OF FIGURES

Figure		*Page*
1.1.	U.S. Army OH-6A Cayuse Helicopter	1
1.2.	Typical MH-6 Mission Scenario	6
1.3.	MH-6 and AH-6 Special Operations Helicopters	8
2.1.	Typical Power Usage at a Hover	14
2.2.	Analysis of Power Required in Level Flight	15
2.3.	Two-Dimensional Shapes with same Drag	18
3.1.	U.S. Army OH-6A Cayuse Helicopter	29
3.2.	160th SOAR MH-6H Helicopters	31
3.3.	US Army MH-6J Helicopter	32
3.4.	Test Helicopter (OH-58A+)	37
3.5	OH-58A+ Main Rotor Hub Assembly	38
3.6.	OH-58A+ Tail Rotor Assembly	39
3.7.	OH-58A+ Hydraulic System	40
3.8.	OH-58 A+ Flight Control System	42
3.9.	OH-58A+ Station Diagram	43
3.10.	OH-58A+ Forward Transmission Fairing and Resulting Airflow	44
3.11.	MH-6 Station Diagram	45
3.12	MH-6 Profile View	46
3.13	OH-58 Profile View	46
3.14.	Test Aircraft (OH-58A+) Static Port Position	47
3.15.	MH-6 Static Port Position	48
4.1.	MH-6 Helicopter with External Passengers	49
4.2.	The SHEL Model	52
4.3.	Initial Design of 6" Sawtooth Flow Diverters	55
4.4.	6" Flat Plate (with Vortex Generators) Flow Diverters	56
4.5.	8" Flat Plate (with Vortex Generators) Flow Diverters	57
4.6.	MSA Model 80 Noise Dosimeter	59
4.7.	Noise Dosimeter "A" Weighted Scale	59

LIST OF FIGURES (continued)

Figure *Page*

5.1. OH-58A+ Static Port 65
5.2. OH-58A+ Test Aircraft 66
5.3. Test Aircraft Baseline Airflow Diagram 67
5.4. Best Angle Tufted Measuring Device 69
5.5. Test Aircraft Tufted Screen 77
5.6. Experimental Smoke Generating System 78
5.7. Representative 18" Flat Plate Flow Diverter Section 79
5.8. M18 Smoke Canister 80
5.9. MSA "A" Weighted Noise Dosimeter 82
6.1. Equivalent Sound-Level Nomograph 93
A.1. MH-6 Profile View 108
A.2. OH-58A Profile View 108
A.3. MH-6 Major Components 112
A.4. OH-58 Physical Dimensions 114
B.1. N88UT Ship Airspeed Indicator Calibration Chart 116
B.2. N88UT Ship Altimeter Calibration Chart 117
B.3. N88UT Boom Airspeed Indicator Calibration Chart 118
B.4. N88UT Boom Altimeter Calibration Chart 119
B.5. N88UT Position Error Chart 120
B.6. N88UT Instrument Corrected vs. Calibrated Airspeed Chart 121
C.1. Referred Level Flight Performance, Baseline Aircraft 123
C.2. 6" Sawtooth Best Angle Referred Level Flight Performance 124
C.3. 6" Sawtooth Best Angle Airspeed vs. Inches Deflected 125
C.4. 6" Sawtooth Best Angle $ESHP_{ref}$ vs. Inches Deflected 126
C.5 Referred Level Flight Performance, 6" Sawtooth Flow Diverters set at 40° 127
C.6. True Airspeed vs. Inches Deflected, 6" Sawtooth Flow Diverters, set at 40° 128
C.7. $ESHP_{ref}$ vs. Inches Deflected, 6" Sawtooth Flow Diverters set at 40° 129
C.8. Change in Equivalent Flat Plate Drag, 6" Sawtooth Flow Diverters, set at 40° 130

LIST OF FIGURES (continued)

Figure *Page*

C.9. 6" Flat Plate (with VG's) Referred Level Flight Performance 131
C.10. 6" Flat Plate (with VG's) Airspeed vs. Inches Deflected 132
C.11. 6" Flat Plate (with VG's) $ESHP_{ref}$ vs. Inches Deflected 133
C.12. 6" Flat Plate (with VG's) Change in Equivalent Flat Plate Drag 134
C.13. 8" Flat Plate (with VG's) Referred Level Flight Performance 135
C.14. 8" Flat Plate (with VG's) Airspeed vs. Inches Deflected 136
C.15. 8" Flat Plate (with VG's) $ESHP_{ref}$ vs. Inches Deflected 137
C.16. 8" Flat Plate (with VG's) Change in Equivalent Flat Plate Drag 138
C.17. Out of Trim Conditions with 8" Flat Plate Flow Diverters set at 40° 139
C.18. OH-58A+ Lateral Directional Oscillation Root Locus Plot 140
C.19 6" Sawtooth vs. 6" Flat Plate Referred Level Flight Performance 141
C.20. 6" Flat Plate vs. 8" Flat Plate Referred Level Flight Performance 142
C.21. All Diverters, Airspeed vs. Inches Deflected 143
C.22 All Diverters, $ESHP_{ref}$ vs. Inches Deflected 144
C.23. All Diverters, Change in Equivalent Flat Plate Drag 145
C.24. Projected Airflow Inside the OH-58 A+ Test Aircraft 146
C.25. Projected Airflow Around the OH-58 A+ Test Aircraft 147
C.26. OH-58A+ with 8" Flat Plate (with VG's) Installed Rectilinear Graph 148
D.1 Weight and Balance 2 August 2000 150
D.2. Weight and Balance 4 August 2000 150
D.3. Weight and Balance 8 August 2000 151
D.4. Weight and Balance 9 August 2000 151
D.5. Weight and Balance 11 August 2000 152
D.6. Weight and Balance 22 August 2000 152
D.7. Weight and Balance 24 August 2000 153
D.8. Weight and Balance 29 August 2000 153
D.9. Weight and Balance 7 September 2000 154
F.1. Pitot Static Boom. 169

LIST OF FIGURES (continued)

Figure *Page*

F.2. Boom Airspeed and Altimeter Instruments 169
F.3. Data Acquisition Pallet Installation 170
F.4. 6" Sawtooth Flow Diverter 170
F.5. 6" Flat Plate (with Vortex Generators) Flow Diverter 171
F.6. 8" Flat Plate (with Vortex Generators) Flow Diverter 171
F.7. 6" Sawtooth Flow Diverters Installed 172
F.8. 6" Flat Plate Flow Diverters Installed 172
F.9. 8" Flat Plate Flow Diverters Installed 172
G.1. Tufted Screen Installed 174
G.2. Inside and Outside Windscreen Tufts 174
G.3. Best Angle Measuring Device 175
G.4. Smoke Canister Mounting (Left Skid) 175
G.5. Smoke Generator System Installed 176
G.6. Representative 18" Flow Diverter 176
G.7. Smoke Generator System Pin Release Assembly 177
G.8. Smoke Generator System Ground Test 177
G.9. Smoke Generator System Ground Test Car Installation 178
G.10. Smoke Generator System and Tufts for Ground (Car)Test 178

LIST OF TABLES

Table *Page*

5.1. Tests and Test Conditions 63
5.2. 6" Sawtooth Equivalent Flat Plate Drag Calculations 70
5.3. 6" Flat Plate Equivalent Flat Plate Drag Calculations 72
5.4. 8" Flat Plate Equivalent Flat Plate Drag Calculations 75
5.5. Flight Test Noise Level Readings 82
7.1. Flow Diverter Deflection 94
7.2. Mission Scenario Configuration Comparison 95
A.1. MH-6 Dimensional Data 109
A.2. OH-58 Dimensional Data 113
E.1. Test and Test Conditions (Test Plan) 166
E.2. OH-58 Emergency Procedures (Test Plan) 167

LIST OF ABBREVIATIONS

ADI	Attitude Direction Indicator
ADS	Aeronautical Design Standard
AH	Attack Helicopter
AWR	Airworthiness Release
CH	Cargo Helicopter
CG	Center-of-Gravity
EPS	External Passenger System
ESHP	Engine Shaft Horsepower
$ESHP_{ref}$	Engine Shaft Horsepower referred
FAA	Federal Aviation Administration
FAR	Federal Aviation Regulation
FARP	Forward Area Refuel Point
FLOT	Forward Line of Troops
FSB	Forward Staging Base
FTM	Flight Test Manual
GPS	Global Positioning System
HSI	Horizontal Situation Indicator
ISB	Initial Staging Base
KCAS	Knots Calibrated Airspeed
KIAS	Knots Indicated Airspeed
KTAS	Knots True Airspeed
$KTAS_{ref}$	Knots True Airspeed referred
LDO	Lateral Directional Oscillation
MD	McDonnell Douglas
MH	Multi-Mission Helicopter
MDHC	McDonnell Douglas Helicopter Company
MIL SPEC	Military Specification
MIL STD	Military Standard
MSA	Mine Safety Appliances Company
NOE	Nap of the Earth
NVG	Night Vision Goggle
OBJ	Objective
OH	Observation Helicopter
SHSS	Steady Heading Side Slip
SOAG	Special Operations Aviation Group
SOAR	Special Operations Aviation Regiment
SOF	Special Operations Forces
SOP	Standard Operating Procedure
STC	Supplemental Type Certificate

LIST OF ABBREVIATIONS (continued)

TQ	Engine Torque
UCE	Usable Cue Environment
UH	Utility Helicopter
VC	Velocity Calibrated
VCR	Vibration Cue Rating
VFR	Visual Flight Rules
VI	Velocity Indicated
VMC	Visual Meteorological Conditions
VO	Velocity Observed
VT	Velocity True
VT ref	Velocity True Referred

Chapter 1

INTRODUCTION

Background

After the failure of Operation RICE BOWL, the attempted U.S. hostage rescue in Iran in April 1980, the United States Army began testing and evaluating to develop special operations aviation capabilities. The 101st Airborne Division (Air Assault) at Fort Campbell, Kentucky provided the UH-60s and CH-47s while the Army National Guard initially provided the OH-6 light observation helicopters (figure 1.1). Volunteers were selected from the 101st Aviation Group's C/158 and D/158 (UH-60), A/159th (CH-47), and B/229th (OH-58) to form Task Force 158 and develop tactics, techniques and procedures for aviation in special operations mission profiles.



Figure 1.1. U.S. Army OH-6A Cayuse

The 101st was selected because it had recently fielded the UH-60 Black Hawk helicopter, which was already proven extremely reliable and safe while conducting demanding missions. Additionally, the 101st possessed a large number of CH-47 medium-lift helicopters that could complement the smaller Black Hawks and agile OH-6 (Little Birds). Beginning in June 1980, intensive training was conducted focusing on long-range, low-level, night flying with primitive full-faced AN/PVS-5 night vision goggles (NVGs). The testing and evaluation demonstrated the need to have three different type aircraft, the light helicopter company using OH-6's, the extended range and lift of the UH-60, and the extended range and FARP capable CH-47.

On 1 April 1982, the decision was made to form a standing Army special operations Aviation Task Force known as Task Force 160 consisting of volunteers from Task Force 158. Noteworthy however, the 160th has continued to be referred to as Task Force 160 to this day.

The goals of this new organization were to provide speed, surprise, and violence of action. The mission requirements were to provide quick on-time precision infiltration, extraction and precision attack capabilities in any environment anywhere in the world (± 30 seconds). The landings required placing passengers on building rooftops, flat or pitched, or onto moving vehicles. The OH-6 aircraft, modified to carry 2.75-inch rockets and 7.62-millimeter Gatling guns, were to provide precision gunfire. The mission profile required the 160th to conduct all of these tasks at night with little to no communications to maintain the element of surprise. [9]

Early Contingencies

In October 1983, Task Force 160 received its baptism by fire. The unit received short notice deployment order for Operation Urgent Fury (the invasion of Grenada). The primary mission was to conduct infiltration and exfiltration of special operation forces (SOF) personnel into hostile locations. [9]

In 1987, Operation PRIME CHANCE (1987-1989) was initiated to protect ships passing through the Persian Gulf. The 160th participated through sustained nighttime operations while supporting a joint military task force under very difficult and hazardous conditions. Aircrews of the 160th habitually operated from small deck ships 30 feet above the water at night with very limited visibility using night vision goggles. Instrument flight capability and proficiency were a necessity. Operation PRIME CHANCE resulted in the first successful night combat engagement that neutralized an enemy threat while using aviator night vision goggles and forward looking infrared devices. The 160th presence deterred numerous attacks on international shipping and slowed the mine-laying process. Once again, the 160th proved to be a decisive weapon with international implications. [9]

June 1988, Operation Mount Hope III, the 160th received a directive to recover a Mi-24 Hind attack helicopter from a remote location in Africa. The operation required two MH47 crews to fly 490 miles at night without outside navigational aids extract the Hind and return. [9]

December 1989, the 160th Special Operations Aviation Group (SOAG) was called upon for a spearhead mission for Operation Just Cause, the liberation of Panama. Participating in the first blows to oust a hostile dictator and safeguard American lives, the Nightstalkers participated in the successful pre H-hour airborne and air assaults. Missions in Panama City included the rescue of an American being held captive in Modelo Prison, the insertion of a beacon and combat controllers at Torrijos-Tocumen Airport, and the aerial assault on the Panamanian Defense Headquarters the Commandancia. After the capture of General Noriega, some elements of the 160th remained in Panama for several months in support of Operation Promote Liberty. [9]

December 1990, the 160th Special Operations Aviation Regiment (SOAR) participated in Operations Desert Shield and Desert Storm. The primary missions were the infiltration and exfiltration of SOF personnel deep behind enemy lines. [9]

In the summer of 1993, elements of the 160th deployed as part of Task Force Ranger, on Operation UNOSOM II in support of the United Nations forces in Somalia. Elements of the Regiment conducted operations in a hostile environment. The Regiment lost five dedicated crewmen and two MH-60 aircraft to hostile ground fire during the search for Somali warlord Mohammed Fahra Aideed. [9]

September 1994, the 160th again was called upon for Operation Uphold Democracy. Using a new concept of Adaptive Joint Force packaging, a large portion of the 160th staged on the aircraft carrier USS America [9]

Most recently, the 160th has deployed elements in support of Operation Joint Endeavor in Bosnia and Operation Assured Response in the nation of Liberia. [9]

160th Special Operations Mission Requirements

The 160th must be proficient and capable of deploying worldwide at a moments notice. Additionally, the 160th pilots must be proficient and capable at a variety of special mission tasks. The missions require operations in urban, desert, mountainous, and over-water environments. They are performed primarily at night using night-vision goggles and at extremely high gross weights. Crews are subsequently trained to be proficient in pinpoint-accuracy, low-level terrain navigation, close formation flight, confined area landings, suppressive fire techniques, and small-deck shipboard landings.

A typical 160th mission, if there is one, is depicted in Figure 1.2. These missions can last from just a few minutes to as long as 8-10 hours. Some of these missions are accomplished single-pilot, during the hours of darkness, in a combat environment, at maximum gross weight, all while using NVGs. Normally the aircraft are deployed via United States Air Force transport aircraft to an Initial Staging Base (ISB). While at the ISB, final planning will be conducted for the ongoing mission. When the aircrews and aircraft are ready, they will self-deploy closer to the area of concern to the Forward Staging Base (FSB). At the FSB, the aircrews join all of their SOF personnel. Due to the adverse effects of flying on the outside of the MH-6's, the SOF personnel will normally request an additional landing

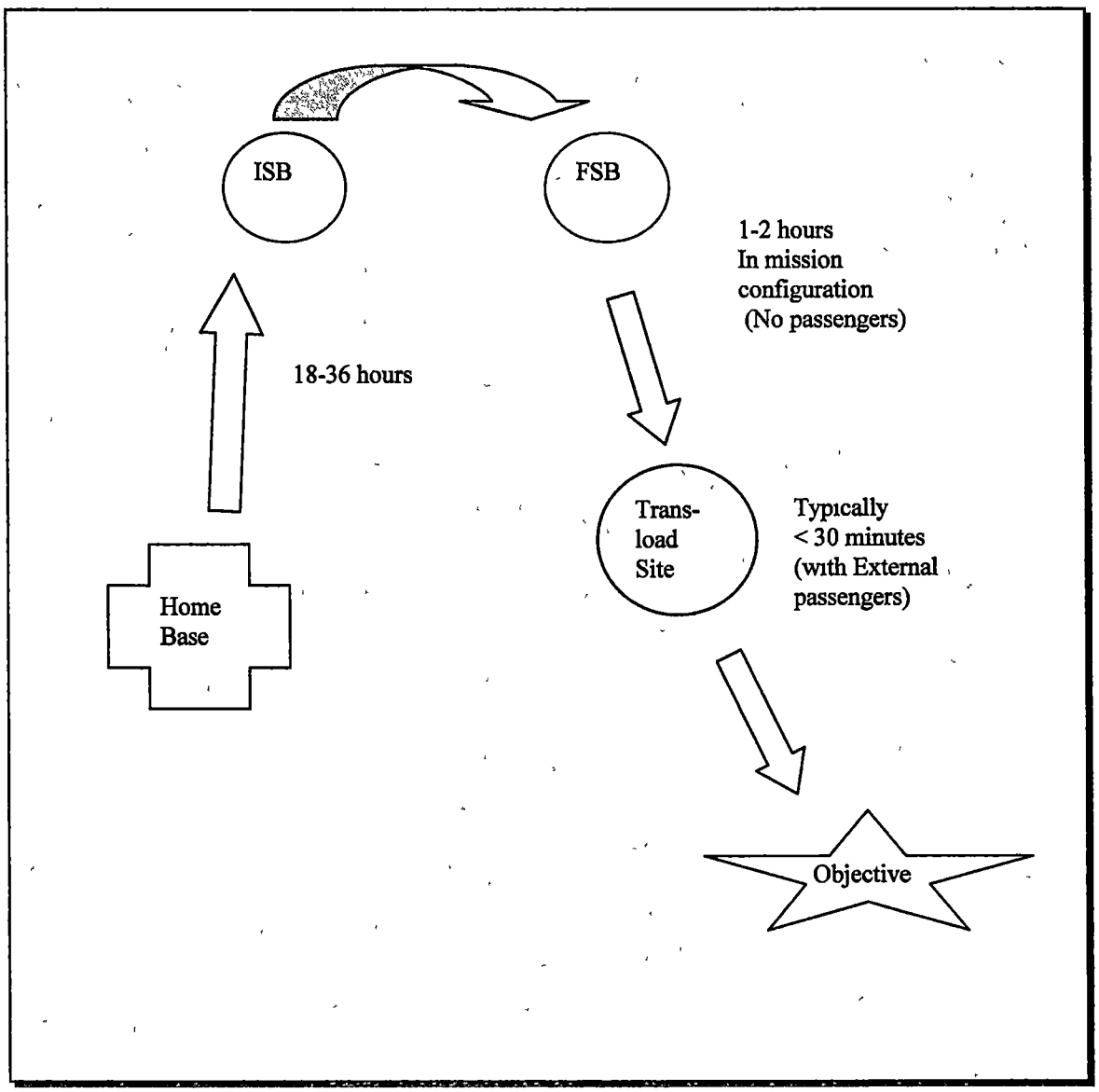


Figure 1.2. Typical 160th Mission Scenario.

area just short of the objective. This last landing area is usually used as a passenger transload site, moving the SOF personnel from the less arduous flight inside the UH-60's or CH-47's, and onto the MH-6's for the short precision flight into the target area. After the ground mission is complete the MH-6's conduct the exfiltration of the SOF personnel and transport them to a safe area and transload them into the waiting UH-60's or CH-47's. Once the transload is completed, the MH-6's self-deploy back to the safety of the FSB and prepare for follow-on missions.

The transload site is of particular interest to the crews of the 160th. One needs only to look back at the ill-fated transload site, Desert One, conducted during Operation Rice Bowl in the desert of Iran in 1979. The ability to eliminate this extra landing site in unfamiliar, austere locations would be an attractive option for the both 160th. If the passengers carried on the outside of the Little Birds were capable of flying longer and farther without increasing their exposure to adverse conditions, the need for this extra transload site could be eliminated. This would reduce the overall mission complexity thus reducing the associated risk levels.

MH-6 Mission Profile

The primary missions of the A/MH-6J helicopters (Figure 1.3) are to support specified missions of the U.S. Joint Special Operations Command. In the execution of these

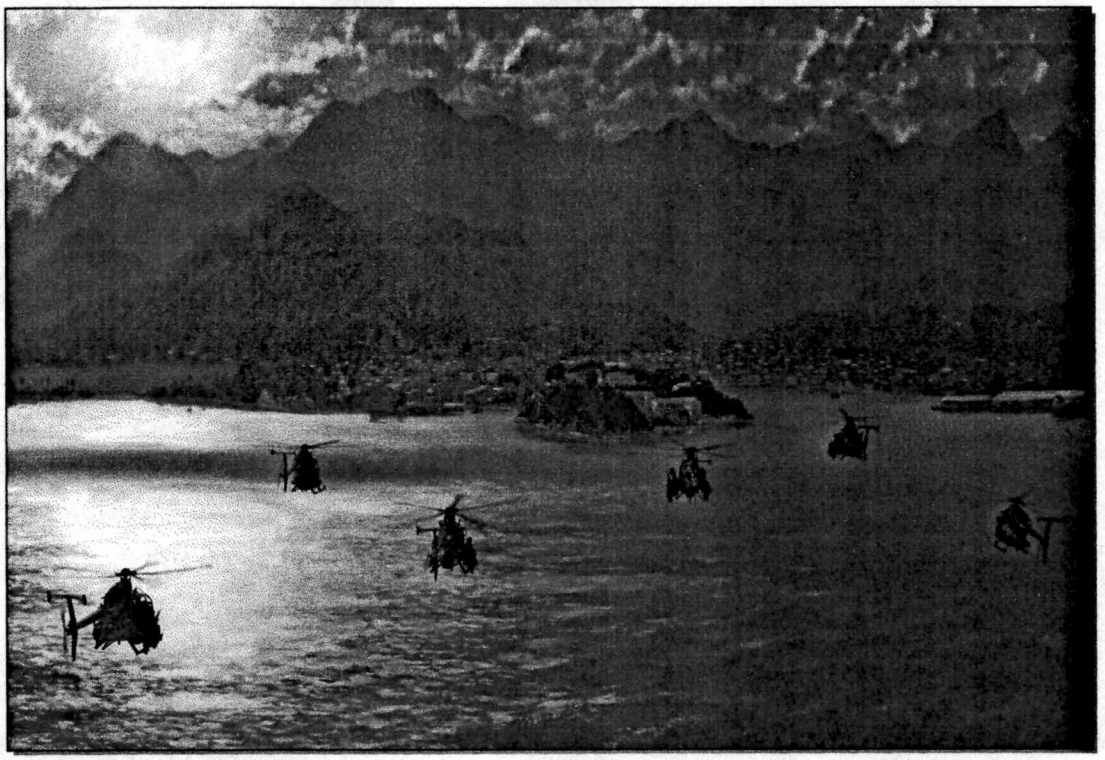


Figure 1.3. MH-6 and AH-6 Special Operations Helicopters.

missions, the aircraft and crew must be capable of both unopposed and opposed low altitude insertion and extraction of SOF personnel. The 160th MH-6 mission dictates that the basic aircraft weights remain as light weight as possible to therefore increase payload all while operating at the maximum allowable gross weight. Each additional pound of equipment installed on the aircraft will therefore require a tradeoff in either fuel or payload.

When flying with the actual mission profile (with external passengers) the MH-6 represents an increase of 16.5 ft^2 equivalent flat plate drag or higher, dependent on equipment installed. This coupled with the passenger fatigue due to the constant 60 to 80 knots of

airflow is detrimental to their mission accomplishment. Using the Drag versus Torque Chart in the MH-6 Operator's Manual, this increase in equivalent flat plate drag is roughly equal to an additional 16 pounds per square inch (PSI) of torque at an airspeed of 80 knots (Sea Level, 30° C). Additionally, the increase of equivalent flat plate drag can be converted to an increase in fuel flow from approximately 232 pounds per hour to approximately 282 pounds per hour at an airspeed of 80 knots.

Taking this analysis one step further, this change in equivalent flat plate drag equates to an approximate reduction in the combat radius from 1 hour 43 minutes (137 nm) to 1 hour 25 minutes (113 nm), based on starting the mission with a full main tank (59.9 gallons useable fuel).

Chapter 2

THEORY OF PERFORMANCE FLIGHT-TESTING

General

The foundation of flight-testing in general, and performance testing in particular, is dependent upon identifying the applicable variables for a given condition based on sound theory with appropriately applied assumptions and simplifications. Educated and efficient test planning and careful observation yield test results that address specific aspects of performance which can be analyzed in the context of the intended mission. [3]

With safety being paramount, the concept of incremental build-up is one of the most important practical philosophical flight-testing lessons. Practically, build-up is the process of proceeding from the known to the unknown in an incremental, methodical pattern. Philosophically, build-up is the manner in which flight testing should be structured; beginning with the best documented, least hazardous data points and proceeding toward the desired end points, always conscious of the aircraft, pilot, and test limits. There should be no surprises in flight-testing. [3]

While specification compliance and handbook performance requirements dictate that quantitative performance data are gathered, qualitative data are gathered also during

performance flight-testing. The educated observations of the flight test crew often provide more insight into the overall suitability of a system for its mission than the quantitative data. During all flight tests, the crew continuously makes and records observations. These observations may be recorded manually or automatically. They may relate directly to the test being performed or they may relate to the general flight environment. Flight test time is expensive and all opportunities to evaluate the helicopter must be taken. [3]

Purpose

In general, performance flight-testing for mission suitability should begin with realistic mission profiles. In what environment will the end user be expected to operate? Is this aircraft expected to operate in conjunction with other aircraft types, and are the airspeeds compatible? In what threat environment is the aircraft expected to operate? Is the combat radius and combat range sufficient to support the mission profile with the expected mission payload? These and other questions must be answered based on the requirements of mission suitability, independent of the requirements of the specification. [3]

The purpose of a helicopter performance flight-testing is to investigate the aircraft performance characteristics in level flight to achieve the following objectives:

How high?

How fast?

How far?

How long?

The main reasons for performance flight-testing are; mission suitability, aircraft performance, and specification compliance.

Mission Suitability

Mission suitability is the capability of the helicopter to fulfill its mission. Each aircraft or weapon system is developed to meet or fulfill a mission requirement. This mission is comprised of many sub-missions and tasks, and they must be performed in many areas of the world under different conditions. Inherent to mission suitability determination is the conclusion whether the aircraft can perform the intended mission safely, whether capability can be substantially improved, or whether a particular characteristic should be avoided in the future. Additionally, during performance evaluations, specific characteristics may be identified that, if appropriately applied in flight technique, may enhance mission capability and should be recommended as standard operating procedure. [3]

Aircraft Performance

To provide operators in the field or fleet with the maximum performance possible from the helicopter, contractually supplied performance data must be verified and sometimes

expanded for inclusion in the flight handbook. Additionally, operating techniques which affect the helicopter's performance must be verified or developed. [3]

Specification Compliance

Each helicopter or weapon system is developed by a manufacturer to meet certain specifications. To insure contract compliance, someone must check the performance parameters of the system against the contractual requirements and specifications. This consideration demands accurate quantitative data derived as the result of flight testing. [3]

Level Flight Performance

The concepts associated with the analysis of level flight power required are better understood when the individual contributions are examined separately. The total power required in forward flight is defined as the summation of the following power requirements:

1. Induced power (P_i): Power required to produce induced flow, affects main and tail rotor, discussed in terms of the momentum theory.
2. Profile power (P_O): Power required to drag the rotor blade through a viscous fluid, affects main and tail rotor, discussed in terms of the blade element theory.
3. Parasite power (P_p): Power required to drag fuselage through a viscous fluid, affected by equivalent flat plate area, discussed in terms of simple aerodynamic theory.

4. Miscellaneous power (P_m): Power required to overcome cooling losses, transmission losses, accessory power (hydraulic and electrical) and tail rotor power required, generally presented in terms of mechanical efficiency η_m, as a function of forward speed.

Typical power usage at a hover is depicted in Figure 2.1. As the helicopter proceeds from hover into forward flight, the total power requirement changes significantly due to the effect of translational velocity on the rotors and due to the variation of parasite drag with forward airspeed. The effect of forward flight on each of the individual power requirements is displayed in figure 2.2.

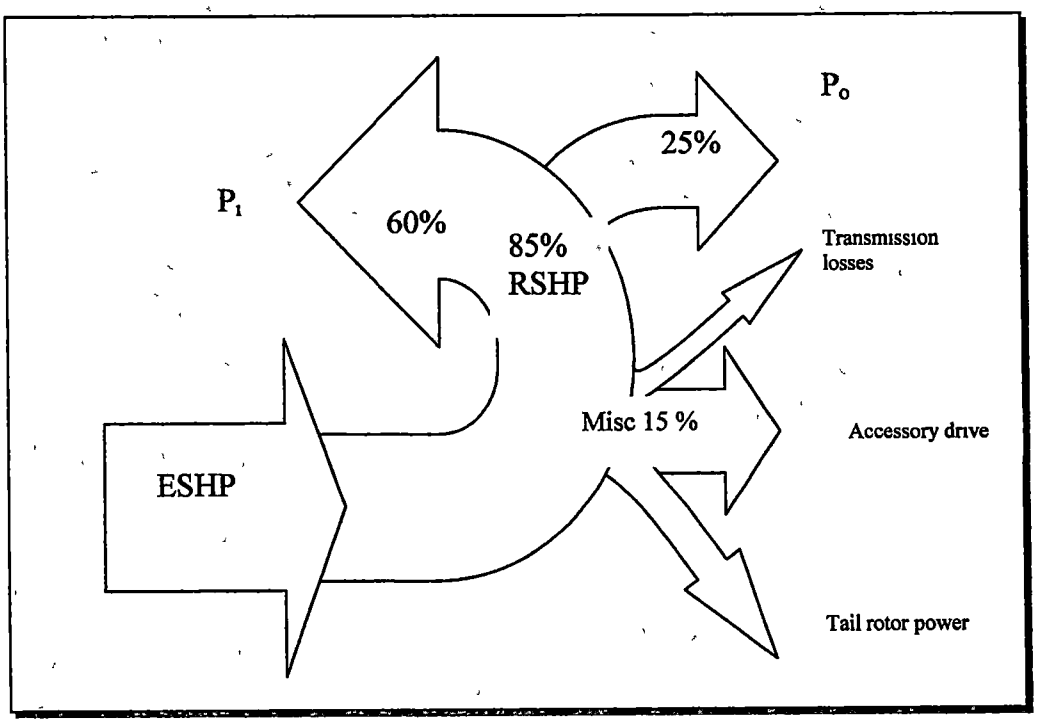


Figure 2.1 Typical Power Usage at a Hover.

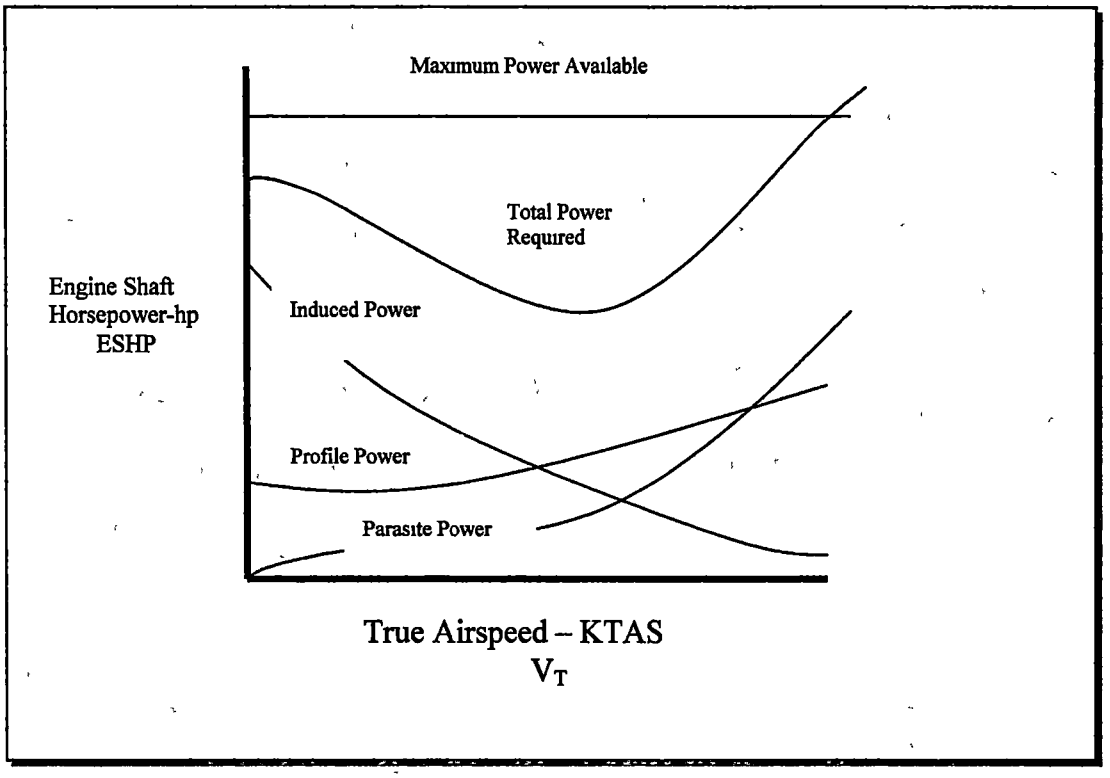


Figure 2.2. Analysis of Power Required in Level Flight.

Induced Power

Predicting the induced power requirements of the main rotor in forward flight becomes a more complicated problem than in hover and no theory exists which enables the exact calculation of the induced velocity distribution over the rotor disc. Induced power in forward flight can be analyzed by the momentum theory to explain an additional increase in mass flow rate through the disc with forward speed. The mass flow rate through the disc is a function of the vectorial sum of the component velocities at the rotor. As forward flight speed increases, the mass flow rate through the rotor increases due to its

translation and the change in velocity required to produce a certain thrust, induced velocity, decreases.

The approximation of induced power in forward flight then becomes:

$$P_{i_f} = \frac{T^2}{2\rho A_D V_R} = \frac{W^2}{2\rho A_D V_f}$$

Where:

P_{if}	-	Induced power in forward flight
T	-	Thrust
ρ	-	Density
A_D	-	Rotor disc area
V_R	-	Resultant velocity
W	-	Weight
V_f	-	Forward flight velocity.

Profile Power

As in hovering flight, the blade element theory is used to analyze the rotor blade profile power in forward flight. Since the profile power is a function of azimuth angle (ψ), it is a cyclic in magnitude. The profile power is generally expressed as an average value. The average profile power for b (number of blades) is obtained by integrating the following equation with respect to radius (dr) and azimuth ($d\psi$).

$$P_o = \frac{b}{2\pi} \iint \frac{1}{2} C_{d_o} \rho (\Omega r + V_f \sin\psi)^3 \, c dr d\psi$$

Where:

Po	-	Profile Power
b	-	Number of Blades
C_{do}	-	Blade element profile drag coefficient
ρ	-	Density
ΩR	-	Blade element rotational velocity
V_f	-	Forward flight velocity
ψ	-	Blade azimuth angle
c	-	Blade chord.

The integration yields:

$$P_o = \frac{1}{8} \sigma_R C_{d_o} \rho A_D (\Omega R)^3 (1 + 4.65\mu^2)$$

Where:

P_o	-	Profile power
σ_R	-	Rotor solidity ratio, bc/πR
C_{do}	-	Average blade element profile drag coefficient
ρ	-	Density
A_D	-	Rotor disc area
ΩR	-	Blade rotational velocity
μ	-	Advance ratio, $V_f/\Omega R$.

Parasite Power

Parasite drag of a fuselage is composed of two elements: streamline drag (primarily skin friction) where the flow closes smoothly behind the body; and bluff body drag (pressure drag) where the flow separates behind the body. The difference in drag between these two types is dramatically illustrated by Figure 2.3. Since the fuselage is seldom a pure symmetrical shape, the components of the fuselage (rotor hubs, landing gear, rotor mast, vertical fin, etc.) are assigned drag coefficients and summed into a total effective drag coefficient or equivalent flat plate area (f).

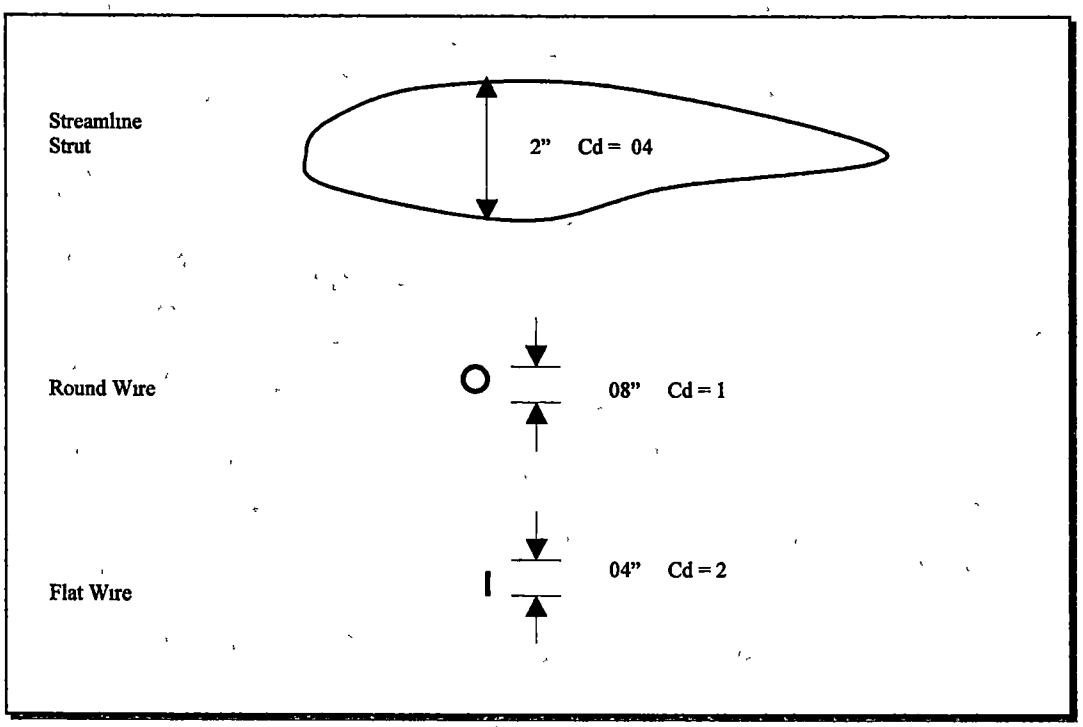


Figure 2.3. Two-Dimensional shapes that have the same drag.

The parasite power in forward flight is a product of drag times velocity:

$$P_p = \frac{1}{2}\rho f V_f^3$$

Where:

P_p	-	Parasite power
ρ	-	Density
V_f	-	Forward flight velocity
ΩR	-	Blade rotational velocity
f	-	Equivalent flat plate area, $C_{Dp} A_f$
μ	-	Advance ratio.

To calculate the change in equivalent flat plate drag the following equation is used:

$$\Delta ESHP_{parasite_{ref}} = \frac{(1)\frac{1}{2}\rho_{ssl} V_{T_{ref}}^3 \Delta f}{550}$$

Then solve for Δf:

$$\Delta f = \frac{(550)\Delta ESHP_{para_{ref}}}{\frac{1}{2}\rho_{ssl} V_{T_{ref}}^3}$$

Miscellaneous Power

Miscellaneous power in forward flight is comprised of all others that are not attributed to P_i, P_o, and P_p. Significant items are transmission losses, accessory power, and tail rotor power. Transmission losses are dependent on rotor speed. Accessory power requirements vary considerably with the number of accessories driven from the main transmission. Tail rotor power is composed of two elements: induced and profile power. If the thrust required by the tail rotor is known, the expressions used for main rotor induced and profile power can be used to determine the tail rotor components.

The thrust required by the tail rotor in equilibrium flight is defined as:

$$T_{TR} = \frac{Q_{MR}}{l_{TR}}$$

Where:

T_{TR} - Tail rotor thrust

Q_{MR} - Main rotor torque

L_{TR} - Tail rotor moment arm.

The tail rotor power required becomes:

$$P_{TR} = \left(\frac{T_{TR}^2}{2\rho A_D V_f} \right)_{TR} + \left[\frac{1}{8} \sigma_R \overline{C}_{d_o} \rho A_D (\Omega R)^3 \left(1 + 4.65\mu^2\right) \right]_{TR}$$

Where:

P_{TR} - Tail rotor power required

T_{TR} - Tail rotor thrust

ρ	-	Density
A_D	-	Rotor disc area
V_f	-	Forward flight velocity
σ_R	-	Rotor solidity ratio
C_{do}	-	Average blade element profile drag coefficient
ΩR	-	Blade rotational velocity
μ	-	Advance ratio.

A modern helicopter has many minor sources of miscellaneous drag, individually small but significant in total. A partial list of these miscellaneous items includes: [10]

Antennas	Windshield wipers
Door handles	External store mounting points
Hinges and latches	Overflow drain tubes
Pitot-static tubes	Abrasive walkways
Temperature probes	Lights
Hand holds	Fueling receptacles
Steps	Ground electrical receptacles
External jacking points	Skin gaps, steps, and mismatches

Total Power Required

The total power required in forward flight is the summation of induced, profile, parasite, and miscellaneous power:

$$P_{Total} = P_i + P_o + P_p + P_m$$

Where:

P_{total}	-	Total power
P_i	-	Induced power
P_o	-	Profile power
P_p	-	Parasite power
P_m	-	Miscellaneous power.

The main rotor power required is:

$$P_{MR} = \left(\frac{W^2}{2\rho A_D V_f} \right)_{MR} + \left[\frac{1}{8} \sigma_R \overline{C}_{d_o} \rho A_D (\Omega R)^3 \left(1 + 4.65\mu^2\right) \right]_{MR} + \left(\frac{1}{2} \rho V_f^3 f \right)$$

Where:

P_{MR}	-	Main rotor power
W	-	Weight
ρ	-	Density
A_D	-	Rotor disc area
V_f	-	Forward flight velocity
σ_R	-	Rotor solidity ratio
C_{do}	-	Average blade element profile drag coefficient
ΩR	-	Blade rotational velocity
μ	-	Advance ratio
f	-	Equivalent flat plate area.

The power required to maintain forward flight is dependent on gross weight, density, forward flight velocity, and rotor speed. The variables in terms of nondimensional coefficients provide a means of evaluating level flight performance. The total power required by the main rotor in nondimensional form becomes:

$$C_p = \frac{C_T^2}{2\mu} + \left[\frac{1}{8}\sigma_R \overline{C}_{d_o}\left(1 + 4.65\mu^2\right)\right] + \left(\frac{1}{2}C_{D_p}\mu^3\right)$$

Where:

C_p	-	Power coefficient
C_T	-	Thrust coefficient
μ	-	Advance ratio
σ_R	-	Rotor solidity ratio
C_{do}	-	Average blade element profile drag coefficient
C_{Dp}	-	Parasite drag coefficient.

The power coefficient (C_p) is a function of the thrust coefficient (C_T) and advance ratio (μ). Therefore, to obtain level flight power required data, μ is varied for constant values of C_T. The expression of C_T is:

$$C_T = \frac{\left(\frac{W}{\sigma_T}\right)}{\rho_{ssl} A_D \left(\Omega R\right)^2}$$

Where:

C_T	-	Thrust coefficient
W	-	Weight
σ_T	-	Test density ratio
ρ_{ssl}	-	Standard sea level air density
A_D	-	Rotor disc area.
ΩR	-	Blade rotational velocity.

The typical values of C_T, C_P, and μ are multiplied by standard values of the nondimensionalizing terms, obtaining the following referred terms:

$$RSHP_{ref} = \frac{C_p \rho_{ssl} A_D (\Omega R)^3}{550} = \left(\frac{RSHP_T}{\sigma_T}\right)\left(\frac{N_{R_S}}{N_{R_T}}\right)^3$$

$$W_{ref} = C_T \rho_{ssl} A_D (\Omega R)^2 = \frac{W_T}{\sigma_T}\left(\frac{N_{R_S}}{N_{R_T}}\right)^2$$

$$V_{T_{ref}} = \mu(\Omega R) = V_T\left(\frac{N_{R_S}}{N_{R_T}}\right)$$

Where:

$RSHP_{ref}$	-	Rotor shaft horsepower
$RSHP_T$	-	Test rotor shaft horsepower
C_P	-	Power coefficient
P_{ssl}	-	Standard sea level air density
A_D	-	Rotor disc area
ΩR_S	-	Standard blade rotational velocity
ΩR_T	-	Test blade rotational velocity
σ_T	-	Test density ratio
W_{ref}	-	Referred weight
W_T	-	Test weight
C_T	-	Thrust coefficient
N_{RS}	-	Standard main rotor speed
N_{RT}	-	Test main rotor speed
V_{Tref}	-	Referred true airspeed
V_T	-	True airspeed
μ	-	Advance ratio.

Referred power may be either RSHP or ESHP, the level flight performance evaluation will be based on ESHP. The expression for the referred engine horsepower is:

$$ESHP_{ref} = \frac{ESHP_T}{\sigma_T}\left(\frac{N_{R_S}}{N_{R_T}}\right)^3$$

Where:

$ESHP_{ref}$	-	Referred engine shaft horsepower
$ESHP_T$	-	Test engine shaft horsepower
σ_T	-	Test density ratio
N_{RS}	-	Standard main rotor speed
N_{RT}	-	Test main rotor speed.

Test Methods

Neglecting the effects of compressibility on the advancing blade, there are two methods of maintaining a constant thrust coefficient (C_T).

1. Maintain (ΩR) constant and vary W and ρ to keep W/σ constant.
2. Maintain ρ constant and vary W and (ΩR) to keep $W/(\Omega R)^2$ constant.

The easiest and most efficient method to obtain a constant C_T is to maintain a constant rotor speed and vary the density ratio as fuel is consumed to maintain a constant W/σ. The W/σ ratio is held constant and airspeed is varied to obtain the level flight power required data. By repeating the test for various values or W/σ, a complete level flight airspeed-altitude envelope can be constructed. [3]

Since a direct reading of density ratio, pressure ratio, and temperature ratio are not available to the pilot, a considerable amount of preflight planning is required to determine a pressure altitude that corresponds to the desired density ratio. Using a known engine start gross weight, a curve is constructed to show the variation of density ratio or pressure ratio with fuel consumed for a constant test referred weight (W/σ or W/δ). [3]

Tests are typically conducted at specification and mission representative center of gravity (CG) and aircraft configuration. When establishing the pressure altitude for each data point, the aircraft is stabilized at a constant airspeed before determining the existing outside air temperature (OAT). The normal test procedure is for the pilot to have a target near the target airspeed rather than an exact airspeed for each data point. Data are recorded in a wings level, ball-centered, level (no vertical velocity), unaccelerated flight. To ensure the conditions are stabilized, one minute of stabilized flight is required before recording data. The collective is fixed during data recording. Cyclic and directional control inputs are minimized during data recording. The pilot or flight test engineer (FTE) must calculate or be furnished the new altitude for the next data point to maintain a constant W/σ or W/δ ratio. [3]

Observed level flight performance data are reduced to nondimensional and referred level flight performance data. These data are analyzed to determine level flight performance, endurance performance, and range performance. [3]

Test results reflect the performance capabilities of the aircraft, while mission suitability is determined from a combination of the flying qualities and performance characteristics as they relate to specific mission tasks.

Chapter 3

AIRCRAFT DESCRIPTION

MH-6 Development History

The McDonnell Douglas MD 500 and A/MH-6 series helicopter have a history that dates back to the early 1960's. Originally designed and built by the Aircraft Division of Hughes Tool Company, the "Hughes 500" appeared as the result of a 1961 United States Army design competition for a light observation helicopter. Hughes' entry into this competition was a single-engine, turbine-powered helicopter called the OH-6A Cayuse. (Figure 3.1) Specific design features of the Cayuse included a fully-articulated four-blade rotor system, two-blade tail rotor, 317 shaft horsepower Allison 250-C18A turbine engine and an empennage that utilized a vertical fin, short ventral fin, and upwardly canted horizontal stabilizer opposite the port-mounted tail rotor. [12]



Figure 3.1. US Army OH-6A Cayuse.

Between 1968 and 1982, further improvements and modifications to the Hughes 500 helicopter led to the 500C and 500D versions. The first new version, the Hughes 500C, was produced through 1978 and came with an upgraded engine (the 400-shp Allison 250-C20) and improved hot-and-high performance. Its appearance, though, was virtually unchanged from the original Hughes 500. Remodeling the helicopter did occur, however, in 1975 with the introduction of the Hughes 500D. Obvious changes included a T-tail empennage with endplate fins for improved forward flight stability and a five-blade main rotor. The 500D package also included a more powerful 420-shp Allison-C20B engine and numerous performance improvements. [12]

In late 1982, the Hughes 500D was replaced by the 500E as the basic U.S. production version. Boasting a more streamlined nose, new endplate fins for the horizontal stabilizer, new "T" grouping of flight instruments, and a number of interior refinements including increased passenger leg and head room, the Hughes 500E represented a significant improvement over its predecessors. In 1985, Hughes Helicopters was renamed to McDonnell Douglas Helicopter Company (MDHC) and the Hughes 500E adopted its current "MD-500E" designation. [12]

The MD-530FF Lifter, first sold in 1984, is a specialized derivative of the MD-500E designed to operate at high altitudes and temperatures with the capability to carry external loads of up to 2000 pounds. On the military side, derivatives of both the MD-500E and 530FF existed as the 500MG Defender and 530MG Defender, respectively. [8]

Nearly all versions of the MD-500 have been used by the U.S. Army specifically, the 160th Special Operation Aviation Regiment. The versions include converted OH-6As to AH-6C and MH-6B followed later by more converted OH-6A to AH-6C MH-6C. Eventually the U.S. Army purchased new-built MH-6E and AH-6F and AH-6G that were converted MD-500Ds. Other models include the MH-6H and the AH-6J (Figure 3.2.). The models in operation today are the MH-6J and the AH-6J.



Figure 3.2. 160th SOAR MH-6H Helicopters.

Description of the A/MH-6

The MH-6J (Figure 3.3.) is a multipurpose, turbine-powered light helicopter with a maximum cruise speed of 121 knots and service ceiling of 16,000 feet MSL. The MH-6 is capable of seating up to seven persons (six externally). In the US military versions of the A/MH-6J, the right front seat is the pilot's seat. The rear seats have been removed and the back of the cabin used as a cargo area. Four doors (two on each side of the fuselage) allow for entry and egress of crew and cargo, and are normally removed for missions. Transparent acrylic panels make up the cockpit windscreen and windows for the doors, allowing for a generous field-of-view. Forward of the seats and on the centerline of the aircraft is a T-shaped instrument panel. The horizontal portion of the panel houses various flight instruments, engine instruments, and warning indicators while the vertical portion of the panel is available for radios and circuit breakers. Additional avionics are located in the



Figure 3.3. U.S Army MH-6J Helicopter.

compartment space located beneath the floorboard of the pilot and front passenger positions. The A/MH-6J fuselage is a semi-monocoque structure constructed primarily of aluminum alloy. It has a central framework consisting of a center beam, two bulkheads (one between the front seats, the cargo compartment, and one between the cargo compartment and the engine), and a mast support structure. The mast supports the rotor hub and absorbs the associated lifting loads. Similar to the fuselage, the tailboom is a monocoque structure of aluminum alloy frames and skin. It supports the stabilizers, tail rotor assembly, and tail rotor transmission. As a whole, the fuselage plus tailboom airframe rests on a non-retractable skid-type landing gear that is attached to the fuselage at twelve points (three attachments at each of four strut locations).

Housed at the juncture of the fuselage and tailboom is a 650 shaft horsepower Allison 250-C30 turbine engine. Clamshell doors forming the lower aft end of the fuselage allow access to the engine compartment. Fuel for the power system is drawn from two interconnected bladder fuel cells, one on either side of the aircraft centerline beneath the rear-seat floorboards, with a total capacity of 64 U.S. gallons. The engine transmits power to the rotors through an overrunning clutch (to allow for autorotation), drive shafts and two transmissions. The main transmission, located above the cargo compartment, distributes engine power to the main and tail rotors. The main rotor receives power directly from the main transmission by way of the main rotor driveshaft. The tail rotor, however, receives power from the main transmission through a tail rotor drive shaft and separate tail rotor

transmission. Located at the aft end of the tailboom, the tail rotor transmission directly feeds the tail rotor assembly.

The two primary lifting and control mechanisms of the MH-6 helicopter are the main rotor and tail rotor assemblies. The main rotor group consists of five main rotor blades attached to a fully articulated rotor hub with offset flapping hinges. A scissors assembly, swashplate and associated mixer control mechanisms complete the arrangement. Rotation of the main rotor is counterclockwise as seen from above. The pilot's cyclic and collective controls provide authority over main rotor tilt and pitch, respectively, allowing for pitch, roll, horizontal and vertical velocity control over the aircraft. Somewhat more straightforward is the tail rotor group which consists of two variable-pitch blades attached semi-rigidly to a short output shaft from to the tail rotor transmission. Rotation of the tail rotor is forward blade up. The pilot's tail rotor control pedals, or anti-torque pedals, provide authority over tail rotor pitch, which provides directional control over the aircraft. Together, the main rotor and tail rotor assemblies provide the helicopter with six-degree-of-freedom motion capabilities and allow the pilot full control over the aircraft in all axes.

As briefly noted above, the pilot's controls consist of a conventional arrangement including cyclic control stick, anti-torque pedals, and collective control stick. The cyclic stick and anti-torque pedals are located directly in front of the pilot's seat, while the collective control is located to the left of the pilot's seat. The entire control system is a solid mechanically linked type that uses tubular push-pull rods throughout. Hence, the control system is reversible (i.e. rotor moments are fed back to the pilot via controls). Hydraulic boost is not

incorporated by any of the systems. However, the cyclic control stick, which provides lateral and longitudinal control over the main rotor, does employ a hydraulic one-way lock device on its longitudinal component. The lock device resists un-commanded aft movement of the cyclic stick (i.e. feedback from the main rotor) for positions aft of trim. The anti-torque and collective systems receive partial control assistance through the use of bungee springs. In the anti-torque system, a bungee spring resists right pedal movement to assist in anti-torque control and is set to provide zero pedal force in balanced cruise flight. In the collective system, the bungee spring is set to assist in movement of the collective away from the center or mid-pitch position.

As an aid to the pilot in forward flight, electric force trim has been incorporated into the cyclic control system. Two trim actuators are utilized for this purpose: one for the lateral cyclic control linkage and one for the longitudinal cyclic control linkage. The actuators employ pre-loaded springs to provide direct force feedback to the stick. Therefore, the cyclic stick moves in response to trim input. Control of either trim actuator is accomplished through a five-position thumb switch located atop the cyclic control grip. Spring loaded to the off position (center), the switch allows movement fore and aft for pitch trim, and left and right for roll trim. With this system, lateral and longitudinal control forces can be trimmed to zero (absolute centering) throughout the speed range of the aircraft.

An important part of the MH-6 design is the horizontal and vertical stabilizing surfaces of the T-tail empennage section. Although immovable and hence uncontrollable by the pilot, the surfaces provide increased stability in forward flight. Directional stability is enhanced

by the flat-sided, constant-thickness airfoil of the vertical stabilizer section that extends above and below the tailboom. The lower half of the vertical stabilizer serves to lower the center of pressure of the section for lateral-directional stability and serves as a mount for the tail skid. Both the upper and lower portions of the stabilizer form an oblique angle with the tailboom that provides for increased effectiveness in climbing and descending flight. Attached to the top of the vertical stabilizer is the horizontal stabilizer section. Comprised of an inverted NACA 6518 airfoil, the horizontal stabilizer is designed to enhance the longitudinal stability characteristics of the helicopter. End plates on the horizontal stabilizer serve to increase the effective aspect ratio of the surface by a factor of approximately 1.4. Additionally, the center of the horizontal stabilizer is offset to the right of the aircraft centerline due to the mounting of the vertical stabilizer on the starboard side of the tailboom. This, too, serves an advantage since it places more of the horizontal stabilizer in the higher dynamic pressure flow field of the advancing rotor. [10]

Description of the OH-58A+

The OH-58A+ helicopter is a single-engine, single main rotor, observation-type helicopter with the capability to carry four people with a maximum gross weight of 3200 pounds. The aircraft is equipped with an Allison T63-A-720 gas turbine engine rated at 420 shaft horsepower (uninstalled sea level, standard day conditions). The main transmission is rated at 317 shaft horsepower maximum. The tailboom is a monocoque structure that supports

the horizontal stabilizer, vertical stabilizer, and tail rotor assembly. The main rotor assembly is a two-bladed, semi-rigid rotor mounted on an under-slung feathering axis hub. The main rotor is 35 feet, 4 inches in diameter and rotates at 354 RPM (100%). The main rotor airfoil section is a 11.2% modified "droop snoot" with an average drag coefficient ($\overline{C}_{d_o}$) of 0.00123 and an average chord ($\overline{c}$) of 13.0 inches. The equivalent flat plate drag area of the OH-58 helicopter is 12.0 square feet. The test aircraft will be tested with the doors removed adding an additional 1.6 square feet for a total of 13.6 square feet of equivalent flat plate drag. Cockpit instruments include: an engine oil pressure driven torquemeter gauge (%Q), a self-generating, electrically-driven Turbine Outlet Temperature (TOT) gauge (°C), a gas producer (N_1) tachometer (%RPM), and an engine (N_2) and rotor (N_R) dual-tachometer gauge (%RPM). A *Trimble Flightmate Pro* handheld Global Positioning System (GPS) was temporarily installed in the test aircraft. An external GPS antenna was mounted on the inside of the test aircraft above the left front seat. The test aircraft is depicted in Figure 3.4.



Figure 3.4. OH-58A+ (Test Aircraft - N88UT)

Main Rotor Hub and Blade Assembly

The main rotor assembly is a tow-bladed, semi-rigid, seesaw type rotor with under slung mounting (figure 3.5). The blades are mounted in the hub assembly grips with through bolts, which have hollow shanks for installation of weights to balance the hub. After balancing, the bolts must be kept with their respective rotor hub grips. Blade alignment is accomplished by adjustment of blade latches, which engage the root end of the blade. The blade grips are retained on the hub yoke by means of tension-torsion strap assemblies. Changes in blade pitch angle are made by rotating the grips on the yoke journals; each grip has two pitch change bearings.

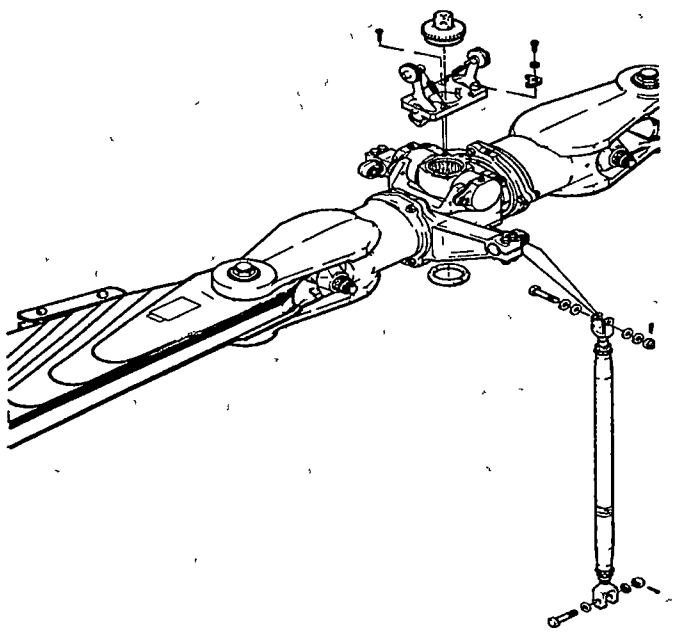


Figure 3.5. Main Rotor Hub Assembly.

Oil reservoirs, with sight gages, are provided for pitch change bearing in the tow grips and for the tow pillow block bearing utilized with the flapping axis trunnion. The rotor blades are all metal, five piece assemblies consisting of an extruded aluminum alloy nose block, aluminum alloy trailing edge, and aluminum honeycomb filler. A flap restraint mechanism is installed on the main rotor hub. The flap restrain assembly serves to prevent excessive flapping of the main rotor during starting and shut down.

Tail Rotor Hub and Blade Assembly

The tail rotor hub and blade assembly conceits of an aluminum alloy forged yoke with stainless steel blades (figure 3.6.).

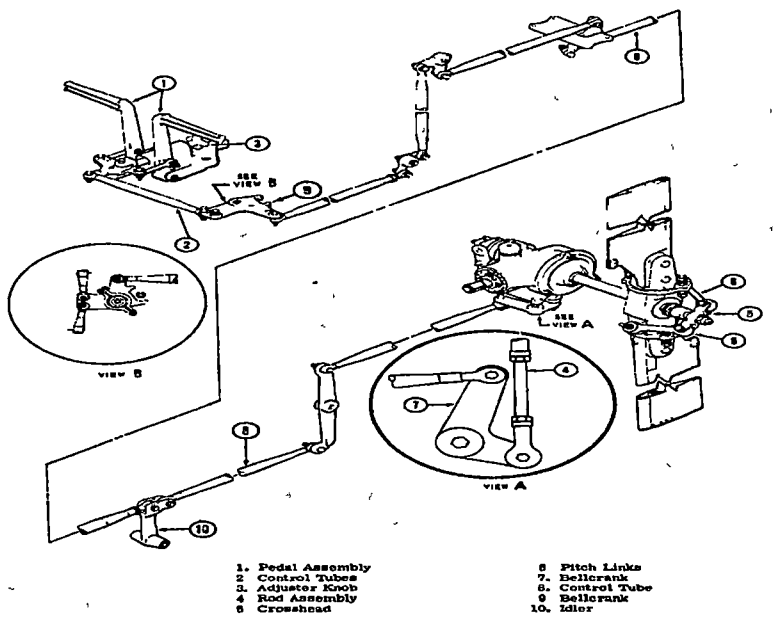


Figure 3.6. Tail Rotor Assembly

The blades are mounted in the yoke by means of spherical bearing, which are mounted in the grip plates on the pitch change axis. The spherical bearings provide for pitch change of the blades. The yoke and blade assembly is mounted on the 90-degree gearbox shaft by means of a splined trunnion, mounted in bearings in the yoke, to provide a flapping axis for the assembly. At time of assembly, spanwise balance is accomplished by use of washers on the blade retention bolts at the yoke, and chordwise balance is attained by washers and/or weights on the trunnion bearing housing retention bolts

Flight Control Hydraulic System

The primary unit of the hydraulic system is a combined pump and reservoir assembly located on the left forward side of the transmission (Figure 3.7.).

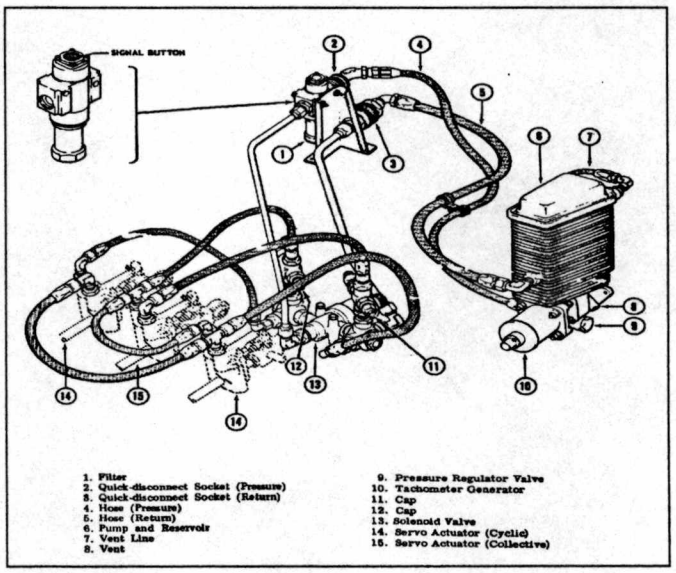


Figure 3.7. OH-58A+ Hydraulic System.

The reservoir filler opening is located on the top of the reservoir. Fluid level may be observed through a transparent plastic sight glass in the side of the reservoir. A valve assembly, located on the right-hand side of the system just above the work deck incorporated a solenoid by-pass valve and filter element assembly, which incorporates a filter condition red button. The hydraulic system is serviced with oil, Specification MIL-H-6506. Reservoir capacity is one pint. The main hydraulic system contains one power pack, three servo actuators with three irreversible valves. The system operates at 600 PSI and adjustment is provided at the relief valve and pressure regulator. The power pack is a self-contained unit located on the forward face of the transmission and driven by the transmission oil pump shaft. The transmission driven hydraulic pump provides for fully boosted flight controls being available during autorotative flight. The complete unit is removable from the pylon without disrupting the hydraulic system. The irreversible valves isolate the servo system from the flight controls in the case of hydraulic malfunction and permit extended periods of flying without excessive feedback from the controls.

FLIGHT CONTROLS

The flight control system consists of push-pull control tubes and bellcranks actuated by conventional helicopter cyclic, collective, and directional controls (figure 3.8.). The controls are routed beneath the pilot's seats aft of the center of the helicopter and up to the cabin roof through the control column, which also serves as a primary cabin structure.

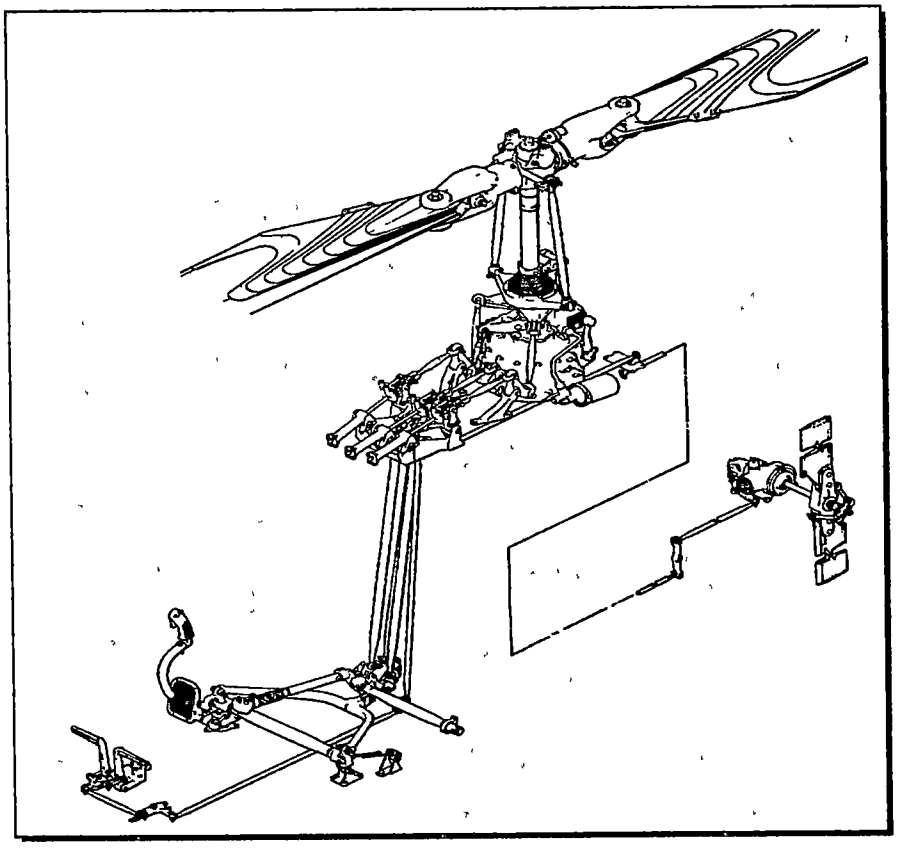


Figure 3.8. OH-58A+ Flight Control System.

Access doors located on the aft side of the control column and removable seats are provided for control inspection and maintenance accessibility. Cyclic and collective controls are routed to the main rotor blades through the swashplate. The directional controls are routed through the tail boom to the tail rotor. Fixed length control tubes and a minimum of adjustable tubes simplify rigging. All self-aligning bearings and rod ends are spherical bearings and require no lubrication. The cyclic and collective control systems incorporate hydraulic servo actuators that utilize irreversible valves to minimize control force feedback.

Differences Between the OH-58A+ and the MH-6

Airframe

The OH-58A+ helicopter's forward transmission fairing is one of the most significant differences between the OH-58 and the MH-6 helicopter effecting this investigation. On the OH-58A+ helicopter the forward transmission fairing begins at approximately station 60, which is well forward of the rear door opening as depicted in Figure 3.9.

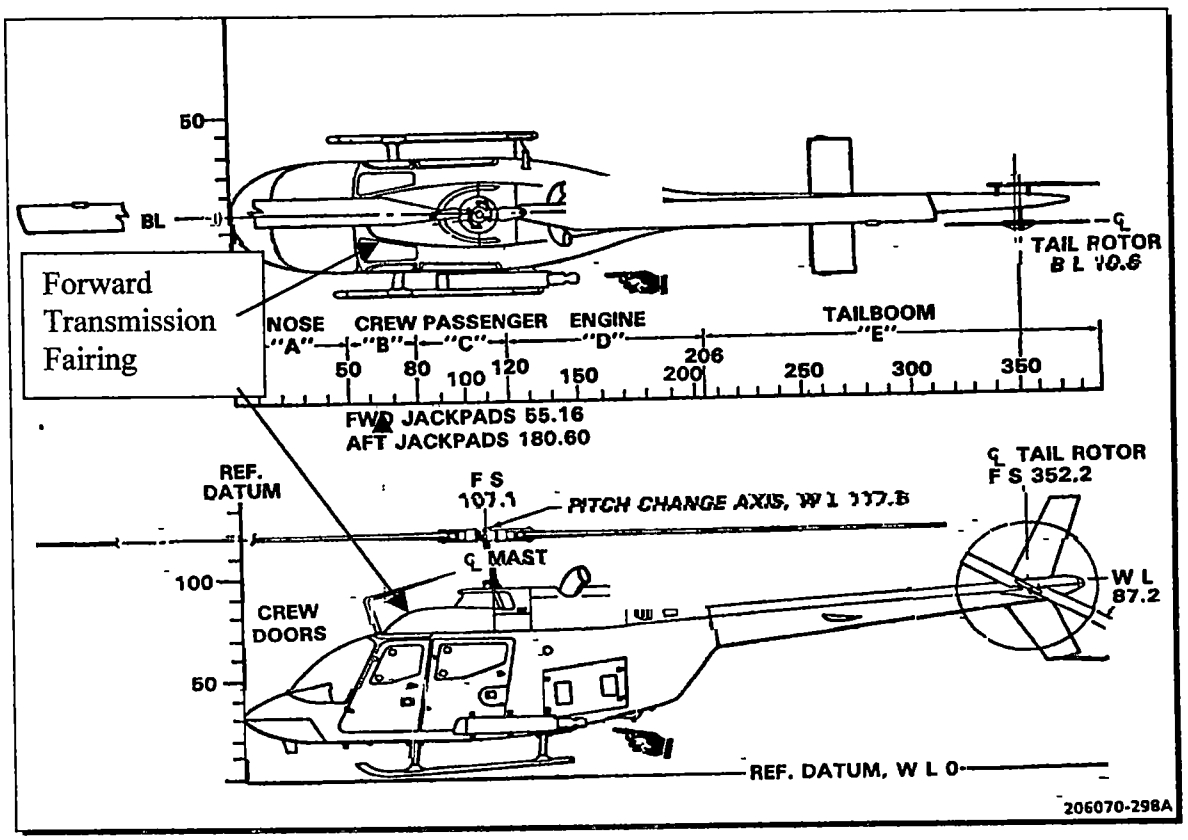


Figure 3.9. OH-58A+ Station Diagram

Specifically, this forward fairing on the OH-58 contributes to the downward flow of air that enters the passenger compartment when the aircraft is flown with its doors removed. Additionally, the shape of the rear door appears to contribute to the increased airflow into the passenger cabin area during nose down attitudes associated with forward flight. The demonstrated airflow along the forward transmission fairing of the OH-58A+ helicopter is depicted in Figure 3.10.

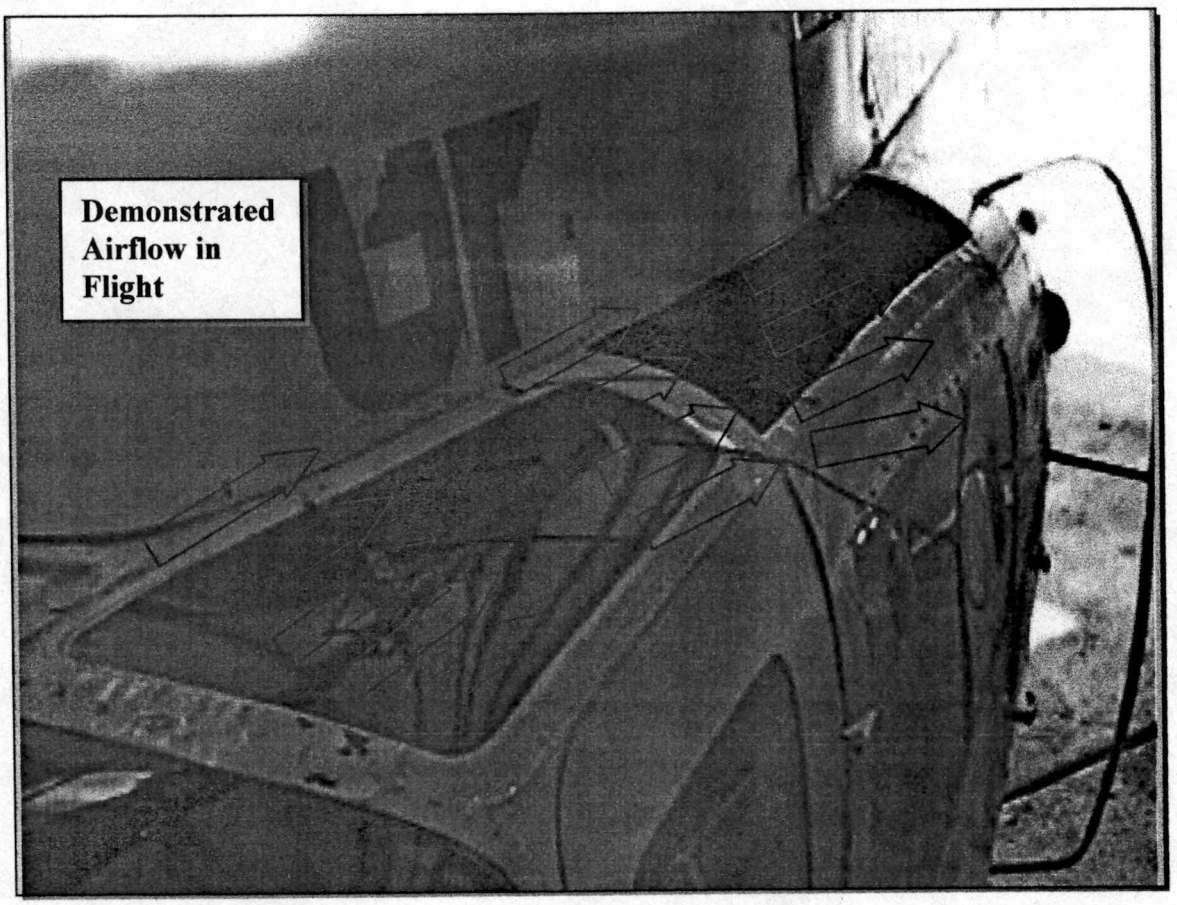


Figure 3.10. OH-58A+ Forward Transmission Fairing and Resulting Airflow.

A study of the MH-6 helicopter's fuselage shows that it does not have a forward transmission fairing. The fairing that surrounds the transmission (commonly referred to as the doghouse) starts at approximately station 95 as depicted in Figures 3.11. This design may result in contrary findings and help insure that the airflow deflected by the Flow Diverters will not be directed down into the passenger compartment. The shape of the rear door is tapered down at the back top corner on the MH-6. This taper design helps minimize the airflow into the rear cabin area during the nose down attitudes associated with forward flight. Additionally, the current placement of antennas on the MH-6J helicopter act as a fence, helping the airflow to remain parallel to the doghouse.

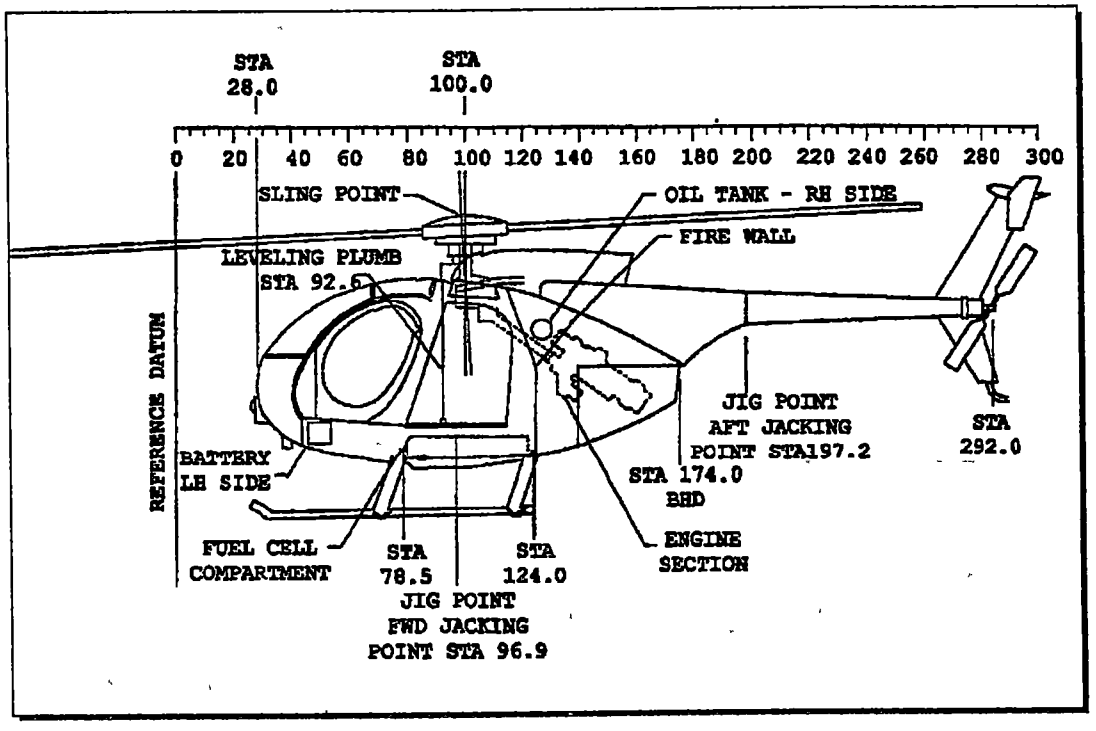


Figure 3.11. MH-6 Station Diagram

The profile view of each aircraft (Figures 3.12 and 3.13) depicts the differences between the forward transmission fairing on the OH-58 and the beginning of the fairing on the MH-6.

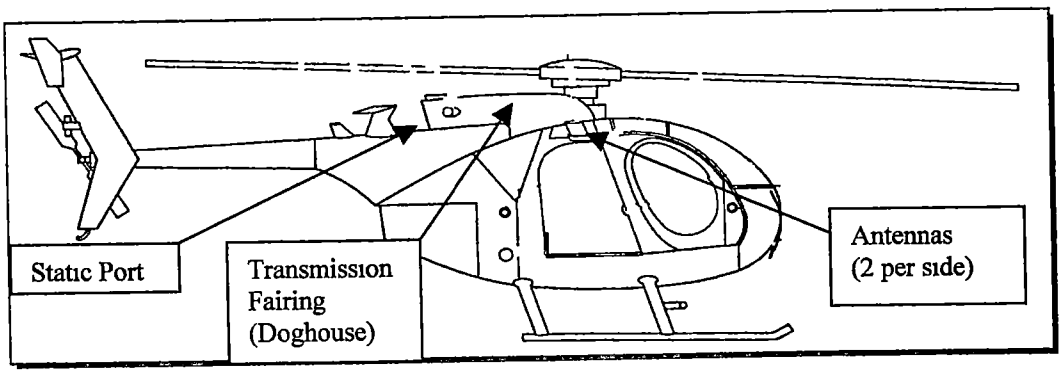


Figure 3.12. MH-6 Profile View.

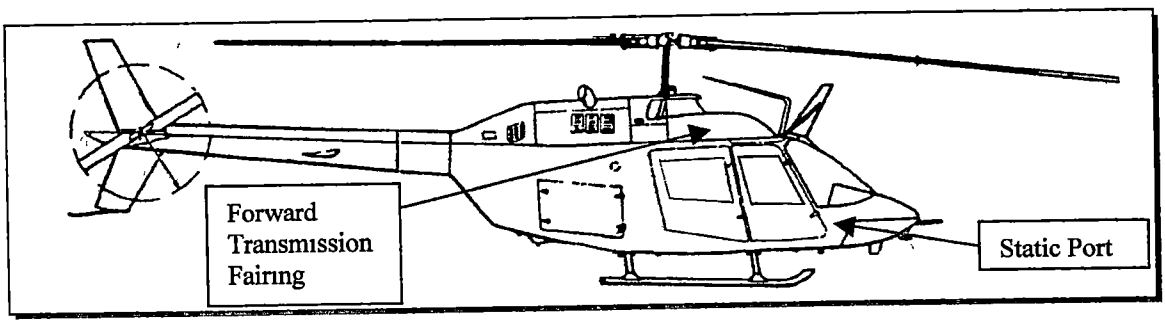


Figure 3.13. OH-58A+ Profile View.

Pitot Static Systems

Position errors, or "installation errors", are the result of other than free stream pressures at the pressure sensor, or errors in the local pressure at the source resulting from the shape, location, or orientation of the sensor. The total pressure position errors result from the location of the pitot tube in the rotor downwash and the changing incidence of the probe. The static pressure position errors result from the complete flow around the airframe.

The main difference in the pitot static systems between the OH-58 and the MH-6 are the locations of the static ports. The static port on the OH-58 is located just forward of the pilot and copilot cabin doors as depicted in Figure 3.14. This location makes the OH-58 susceptible to static pressure errors with the Flow Diverters installed.

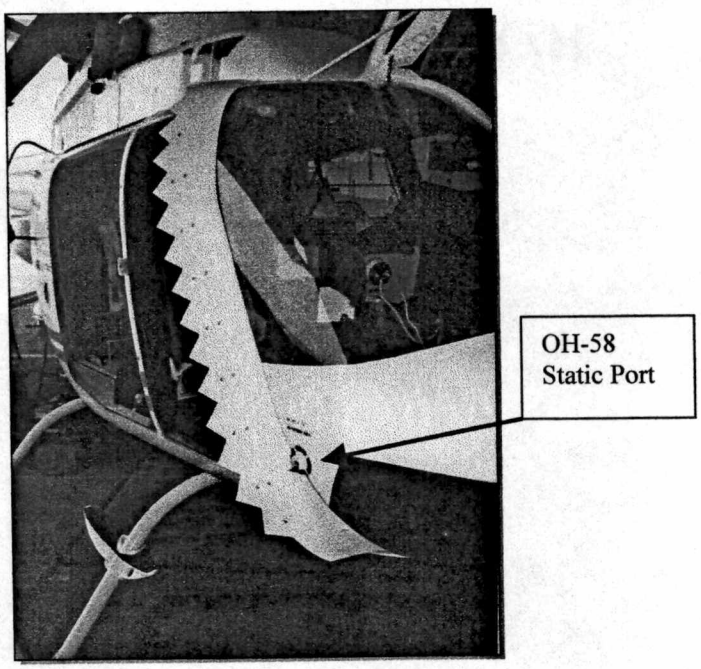


Figure 3.14. Test Aircraft static port position.

The location of the static port on the MH-6 is up behind the engine air inlet fairing "doghouse", well away from the influence of the Flow Diverters as depicted in Figure 3.15.

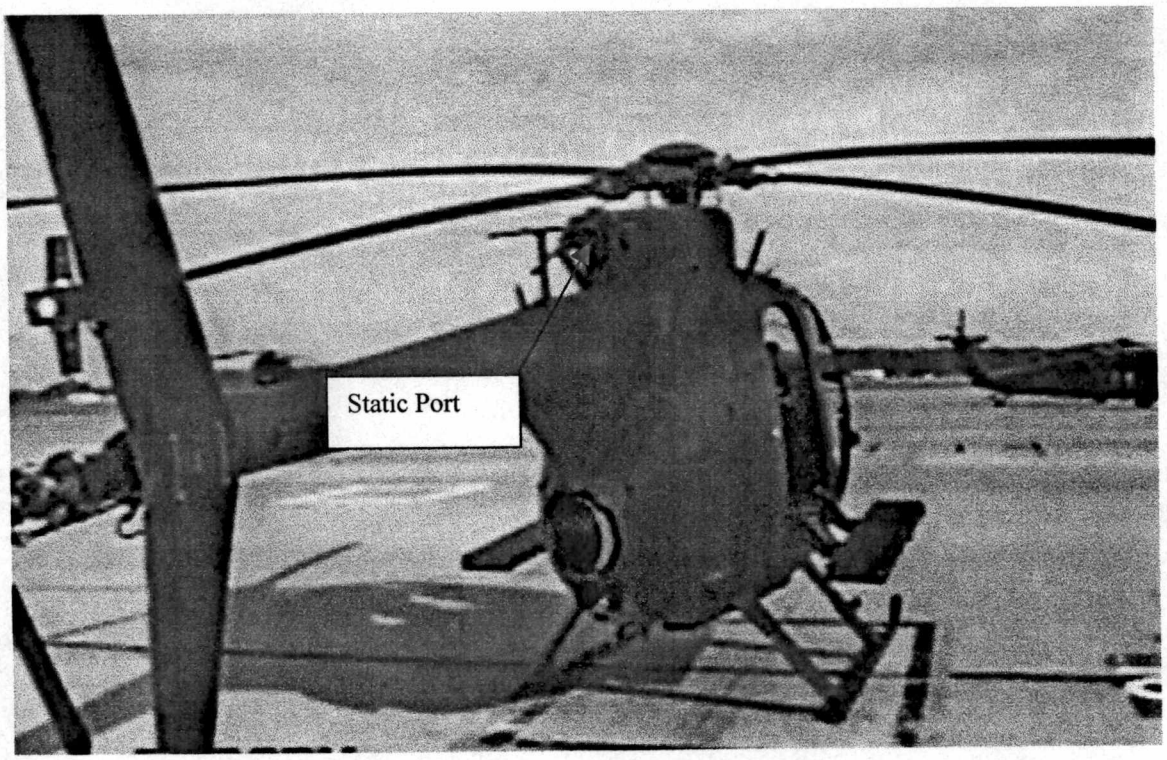


Figure 3.15. MH-6 static port position.

Chapter 4

DESIGNING OF THE FLOW DIVERTERS

Research Motivation

For most aircraft in use today, there is a constant pursuit to go further, faster, and more efficiently without compromising safety. The 160th SOAR is no exception to this pursuit, while their need to accomplish this goal can have direct impact on whether or not a mission of national interest is successful. The 160th MH-6's, commonly referred to as the Little Birds, are of particular concern due to the passengers riding on the outside of the aircraft (Figure 4.1), thus increasing passenger fatigue and reducing the aircraft performance.

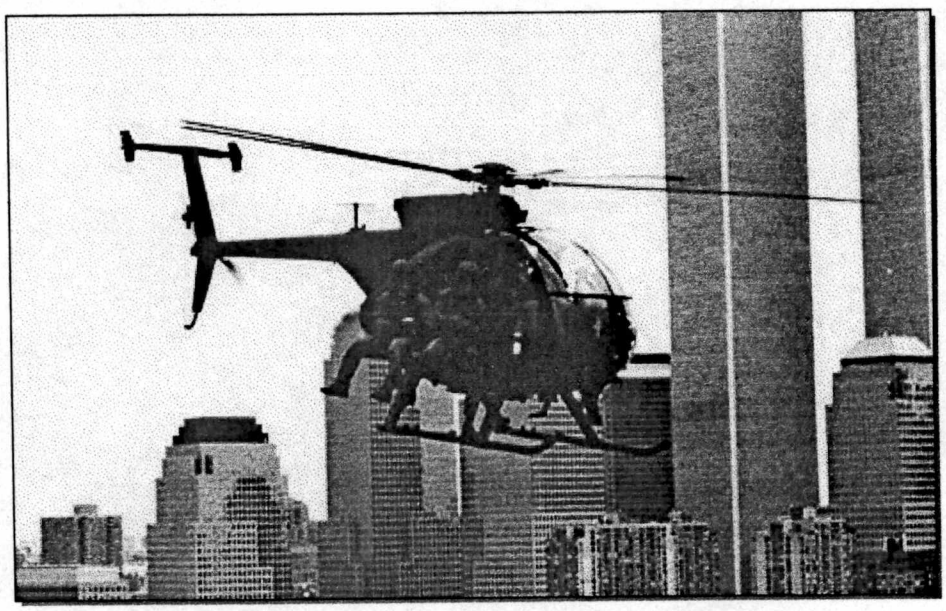


Figure 4.1. MH-6 (Little Bird) with external passengers.

In 1997 an experiment was conducted to investigate the flow fields generated around the fuselage of the current MH-6 Helicopter at the University of Tennessee Space Institute. Water Tunnel testing results showed using a 6 inch sawtooth flow diverting device mounted just forward of both pilot and copilot doors that the flow of air entering the rear passenger compartment could be significantly reduced. From this experimental study the following recommendations were made:

- *Flight tests should be conducted with the actual helicopter modified with the sawtooth flow-diverting device to quantify the data from the test model.*
- *Flight tests should be conducted to determine the amount of noise and cabin pressure created by the application of these flow diverting devices.*
- *Future test should be conducted to determine the impact on the drag created by the flow diverting devices.*
- *Precisely measured flow diverting devices should be utilized to increase the merit of the data collected.*
- *Further testing on the impact of the downstream flow to the tail rotor should be investigated utilizing the actual helicopter.* [6]

As part of the continued efforts of the University of Tennessee Space Institute's (UTSI) Flight Research Department a preliminary design of a flow diverters were made based on

the earlier water tunnel testing. Additionally, this experiment attempted to identify changes to passenger comfort and if other (simpler) flow diverting device designs would accomplish the same results. These flow diverters were installed concurrently with the flight test Data Acquisition (DAQ) pallet installation in UTSI's Bell OH-58A+ (N88UT) operated by the Flight Research Department. To complete the preliminary design of the OH-58A+ flow diverters a systems engineering process was utilized.

Systems Engineering Process

The systems engineering process is a disciplined approach to problem-solving using functional decomposition to break down the components of the system into identifiable pieces that can be managed at a subsystem level. The process is designed to optimize the system's components, attributes, and relationships to maximize the efficiency of the entire system, instead of optimizing the system's individual elements, which may sacrifice overall system efficiency. In the case of the Flow Diverters, the system consists of the aircraft (Hardware), Flow Diverters (Hardware), the airflow (Environment), the personnel (Live ware) on the external passenger system (EPS), and flight crew. The system difficulties lie mainly in the relationship between the aircraft and the Flow Diverters, representing the Hardware to Hardware (H-H) interface, between the aircrew and the Flow Diverters representing the Hardware to Live ware (L-H) interface, and the Flow Diverters and the airflow representing the Hardware to Environment (H-E) in the SHEL model (Figure 4.2).

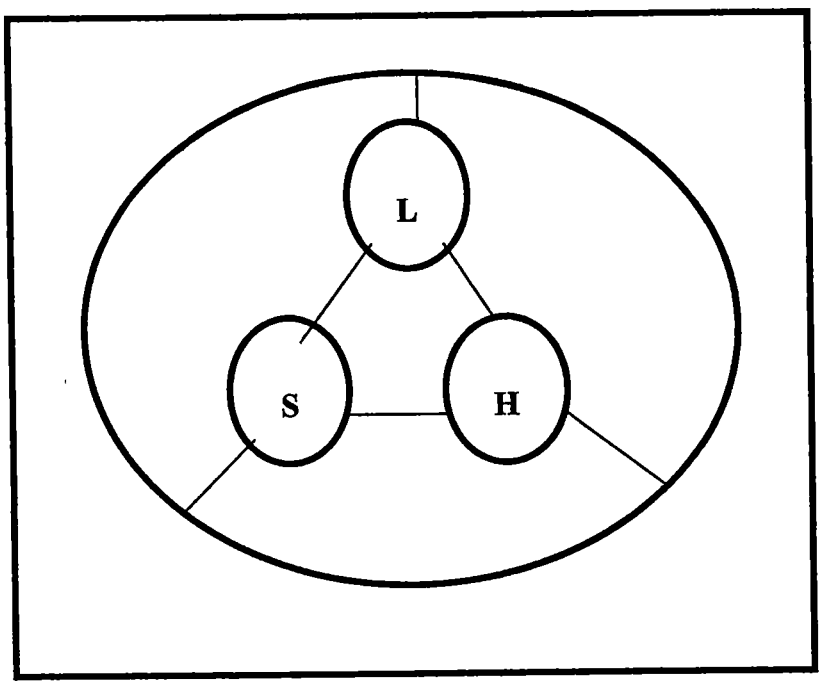


Figure 4.2. The SHEL Model. [1]

The SHEL Model

Systems are composed of three major resources: Hardware, Software and Live ware. Hardware is the components and materials used to make up the physical portion of the system. Software is the procedures, rules, practices and habits that govern the system's operation. Live ware is the human beings within the system, often the system operator. In any system, each of the above exists in a surrounding environment, over which the system designer has no control. These four elements make up a construct known as the SHEL model.

While each of the components is critical in the system, equally critical are the interfaces between each of the components. As well, none of these resources interact in a vacuum. In reality, all of these resources will operate in the context of an environment made up of physical, economic, political, and social factors. [1]

The author applied the concepts of the SHEL model and used a seven-step process to develop a solution to the problem. The process consisted of the following steps: problem definition, alternatives generation, alternatives and constraints analysis, system selection, and system testing, and identification of the solution's impact on other portions of the overall system (mission suitability).

Problem Definition

Clearly defining the problem is first step of the approach to obtaining an engineering solution. It is crucial that the scope of the problem be sufficiently narrowed such that solutions can be generated with the appropriate level of specificity to be effective. In the case of the MH-6 the author began with the typical mission profile and the need to reduce passenger fatigue and reduce the effective drag of the aircraft while in a mission profile. Narrowing the scope further, exposes the fact that not only was there a need to design the Flow Diverters but an aircraft was needed for flight-testing. The problem of interest in this thesis therefore is the flight-testing of the Flow Diverters installed on a test helicopter.

Alternatives Generation

Alternatives generation and constraints analysis is the phase when potential solutions to the problem are conceptually developed. A free-thinking approach is used throwing none of the potential solutions out, until the system constraints are applied. The system constraints eliminate the impractical alternatives and reduce the scope of those alternatives that remain practical but need a reduction in scope to fit within the constraints of the system. The system constraints may be any of a wide variety from economic to physical structures preventing progress in a particular direction. Due to the following issues when using an MH-6 helicopter, a similar aircraft, an OH-58A+, was chosen as the specific alternative solutions to the MH-6:

1. Scheduling conflicts in arranging the use of an MH-6 helicopter.
2. Airworthiness Release (AWR) issues when installing experimental equipment.
3. The UTSI aircraft is installed with calibrated instruments
4. The ease of prototype flow diverter installation on Public Category aircraft is simplified, not requiring design approval by U.S. Army.
5. Initial components could be fabricated utilizing spare OH-58s stored at UTSI Flight Research Hanger as templates.

System Selection

The system selection phase further narrows the range of choices by selecting the solutions that offer the most promise to be effective, then preparing them for testing. After choosing the aircraft, an acceptable Flow Diverter design was chosen and made. The chosen system is the 6" Sawtooth Flow Diverter system, depicted in Figure 4.3. This original design concept comes from the previous water tunnel study at UTSI. Matt Mulnik developed the initial design in a study at UTSI.

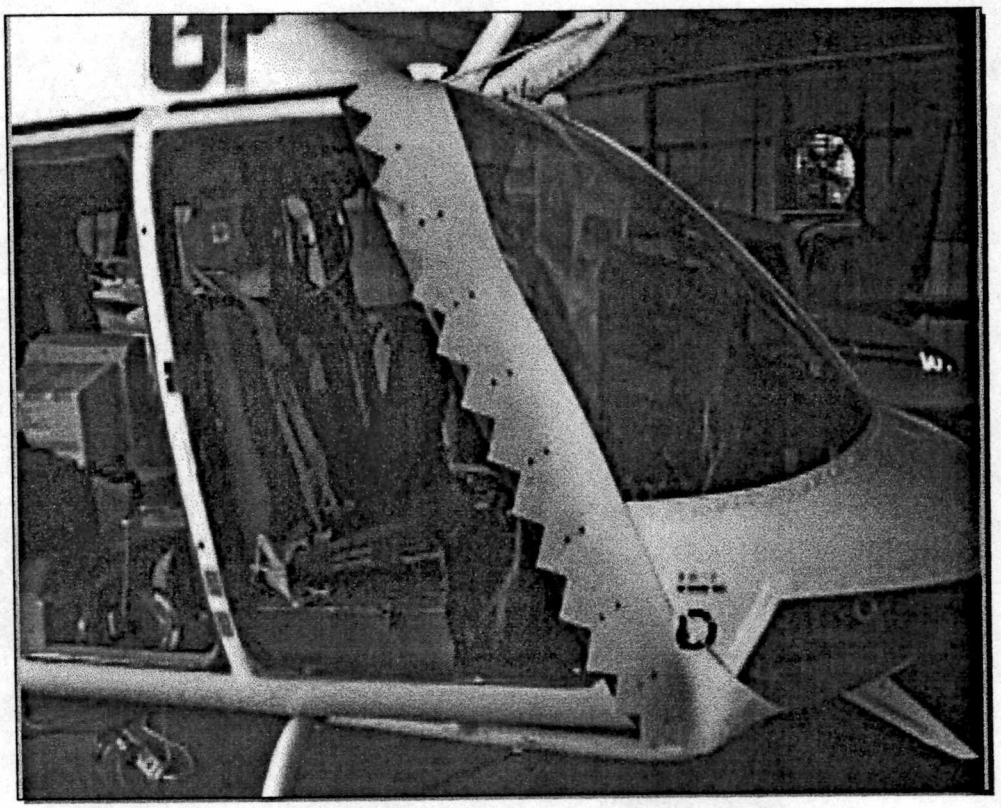


Figure 4.3. Initial Design of the 6" Sawtooth Flow Diverters.

System Testing

System testing is conducted to ensure the solution(s) operate within the constraints of the system and accomplish their assigned mission. Testing may be conducted by simple analysis, mock-ups, and in the latter stages, flight test. During the flight testing of the 6" Sawtooth Flow Diverters it was discovered that there was a need for a simpler and safer design. Specifically, a design that offered no sharp edges and yet maintained or improved on the original designs performance. It was at this point during this testing that several iterations of the systems engineering process were run. The next design was the 6" Flat Plate (with Vortex Generators), depicted in Figure 4.4. In the continued pursuit of a more effective design, the final design was the 8" Flat Plate (with Vortex Generators), depicted in Figure 4.5.



Figure 4.4. 6" Flat Plate (with Vortex Generators) Flow Diverter.

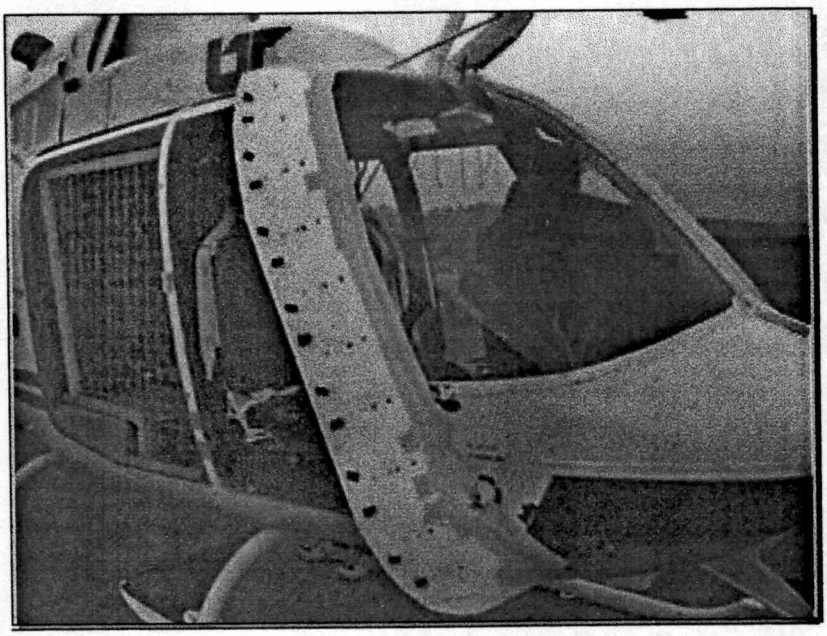


Figure 4.5. 8" Flat Plate (with Vortex Generators) Flow Diverter.

Systems Effect on the Overall System

Solutions to problems in a system may impact other parts of the system or other systems altogether. When solving one problem it is imperative that the designer identify the potential side effects of incorporating the solution and determine if the solution warrants implementation.

One potential side effect of the Flow Diverter system is its impact on the flight crew's field of view (FOV). A rectilinear graph from the design eye position is presented in Appendix C, Figure C.26. Another important issue is the increase in weight that the Flow would have when installed. This initial set of Flow diverters has a total weight of 12 pounds. Due to the uncertainty of this experiment, the initial set of Flow Diverters were

built out of materials that would get the job done without regard to weight. It is quite possible that future designs would weigh less than 10 pounds.

Flow Visualization System

In order to conduct a thorough testing of the above systems, a Flow Visualization System had to be designed. Each of the sub-systems was run through the systems engineering process stated above. The Flow Visualization System includes; tufted windscreens, tufted interior, tufted screen, tufted rod, deflected flow distance measuring device, and a smoke generating system. Each of these systems are pictured in Appendix E.

Noise Evaluation

To sample cabin noise a dosimeter was used instead of the common decibel meter to record an average reading as opposed to instantaneous noise levels. The meter chosen for this test is the MSA Noise Dosimeter Model 80, as depicted in Figure 4.6. This dosimeter meets ANSI specifications S1.4-1971 (R1976) for type 2 Sound Level Meters and ANSI S1.25 for Personal Noise Dosimeters. The meter is "A" weighted as required by OSHA. "A" weighted dosimeters apply a weighted scale to the received noise determined by the frequency's interpretation by the human ear. The dosimeter was mounted to the center control rod housing, with microphone taped to the headliner within two feet of the rear passenger's ear.

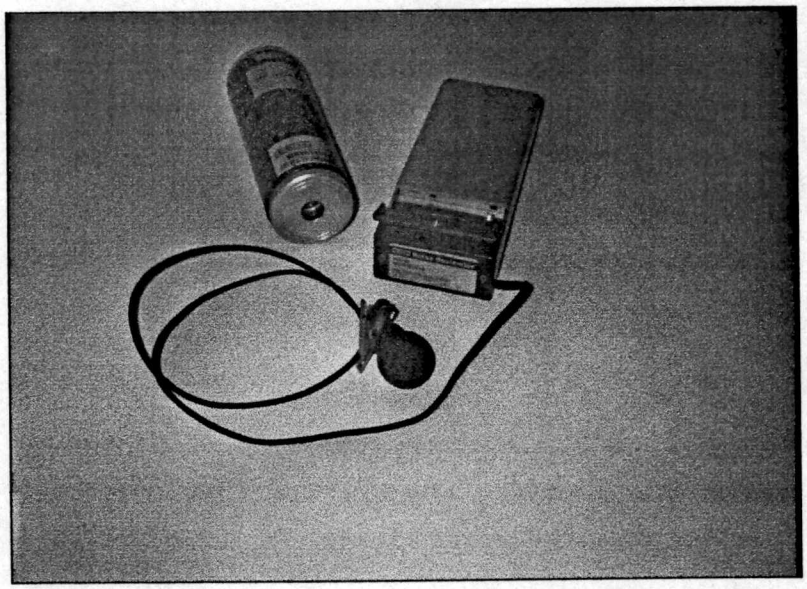


Figure 4.6. MSA Model 80 Noise Dosimeter.

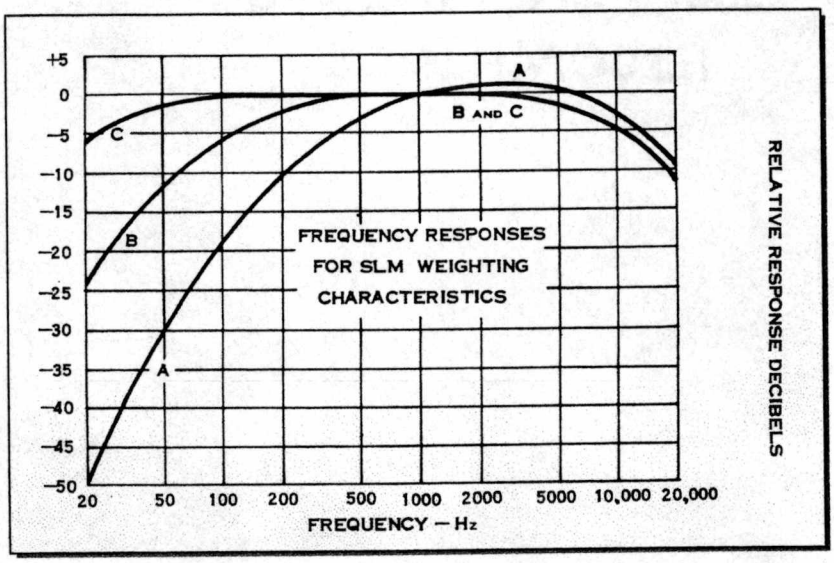


Figure 4.7. Noise Dosimeter "A" Weighted Scale.

Chapter 5

FLIGHT TEST RESULTS AND DATA ANALYSIS

Purpose

The purpose of this test was to evaluate the Flow Diverting Devices on the test helicopter with the doors removed for:

- Reduction in Passenger fatigue
- Performance improvements
- Differences in handling qualities
- Validation of the concepts of the water tunnel tests
- Validation of the approach for investigating the Flow Diverters

General

This study investigated the use of Flow Diverting Devices to reduce passenger fatigue and parasite drag (specifically equivalent flat plate drag) for the 160th Special Operations Aviation Regiment MH-6 Helicopters. Due to cost, scheduling, and airworthiness release

(AWR's) issues this study focused on the actual flight test data of a similar helicopter, the OH-58A+.

The flight-testing investigated the level flight performance, and handling qualities with doors removed, with and without the Flow Diverters installed. Consideration was also given in the design to discover ways of minimizing the airflow on the external passengers (amount of deflection), of minimizing noise level, and of minimizing restrictions to the field of view measured from the cockpit.

The baseline aircraft (with doors removed) was tested with three different types of Flow Diverting Devices (6 inch Sawtooth, 6-inch Flat Plate with Vortex Generators, and 8-inch Flat Plate with Vortex Generators installed). The flight tests conducted are listed in the Table 5.1. After the baseline testing, the flow diverting tests started with the 6-inch Sawtooth Level Flight Performance, as per the previous water tunnel study. Next, the test investigated a simpler design the 6-inch Flat Plate with Vortex Generators. During the flight testing it was determined that to achieve the same flow as the water tunnel test, the Flow Diverters would need to be approximately 8-inches wide. Additionally, the Sawtooth Flow Diverter design had multiple sharp points at the trailing edge, which might have compromised the safety of the crew upon egress from the aircraft. Therefore, a solution was achieved with the 8-inch Flat Plate (with Vortex Generators) Flow Diverters. The 8-inch Flow Diverter allowed for an increase in mass flow and the retained safety aspects of minimal reduction to the pilot field of view as well as no sharp edges.

Instrumentation and Data Acquisition

Experimental sensitive instrumentation and data recording equipment were installed onboard the test aircraft. Cockpit instrumentation were used to acquire pertinent parameters. Fuel flow data were extracted from the Operator's Manual. The external equipment required to collect the desired test data were: A programmable calculator, Stopwatch, GPS, Two Video Recorders, Portable Voice Recorder, and a noise dosimeter. Data from the Data Acquisition System (DAQ) were recorded on a laptop computer, and the manually recorded data were taken on kneeboard cards by the FTE's. The data were analyzed, using data reduction displayed on an Excel spreadsheet and presented in Appendix C. The primary means for performance data collection was the hand recording of cockpit data. This was due to unreliable data collected by the newly installed DAQ system.

The primary data was collected and evaluated in four categories:

1. Performance:
    a. What drag increase/decrease.
    b. Deflection – Reduced direct airflow on the passengers, thus reducing fatigue.
2. Visual - What the flow was doing.
3. Acoustics - Dosimeter.
4. Handling Qualities.

Table 5.1.

Test and Test Conditions

Hours Flown	Event #	Description	Crew	Weight Referred (W/σ)	Pressure Altitude (ft)
1.5	1	Pitot Static Calibration	1 pilot, 2 FTE's	3600	995 - 6430
	2	Baseline testing & Handling Qualities (LDO)	1 pilot, 2 FTE's	3600	5240 - 6430
1.5	3	Best Angle Testing	1 pilot, 2 FTE's	3600	3920 - 5510
1.0	4	Flow Diverting Device Testing & Handling Qualities (LDO)	1 pilot, 2 FTE's	3600	3830 - 4665
1.0	5	Modified Flow Diverting Device Handling Qualities (LDO)	1 pilot, 2 FTE's	3600	3890 - 5160
0.5	6	Back Doors Installed Baseline	1 pilot, 2 FTE's	3600	3810 - 4075
1.0	7	8 inch Modified 40 Deg Level Flight	1 pilot, 2 FTE's	3600	4230 - 4935
1.0	7B	8 inch Modified Best angle & Level Flight	1 pilot, 2 FTE's	3600	3790 - 6030
0.5	8	Formation Training Flight	**Test Acft** 1 pilot, 1 FTE **Chase Acft** 1 pilot, 2FTE's	3320	1000 - 2000
1.5	9	Flow Visualization	**Test Acft** 1 pilot, 1 FTE **Chase Acft** 1 pilot, 2 FTE's	3275	1000 - 2000
0.4	10	Flat Plate (without VGs) Noise Test	1 Pilot, 1 FTE	N/A	1500

Pitot Static System Calibration *(Event 1)*

General

The standard aircraft and boom pitot static systems were bench tested using a water manometer and a mercury barometer with a vacuum pump. The test methods used for the calibration of the pitot and static systems were the Measured Course method outlined in FTM 106 and the Global Positioning System (GPS) outlined in lecture notes by Dr. Ralph Kimberlin. The pitot static systems were evaluated during a single flight of 0.9 hours. Helicopter loading was a single pilot at the pilot station, one Flight Test Engineer (FTE) at the co-pilot station, and one FTE in the passenger compartment. The average center of gravity (CG) was 109.7 inches (mid-range), at an average gross weight (GW) of 3032 pounds.

Data Analysis

The Standard Aircraft Instrument Calibrations, Boom Instrument Calibrations, Instrument corrected airspeed vs. Calibrated Airspeed, and the Position Error Corrections are depicted in Appendix B, Figures B.1. thru B.6. It was predicted that the test aircraft's static port position relative to the Flow Diverter (Figure 5.1) would be prone to error. This error was verified through later testing thus, the boom pitot static system was used for all testing. With the Flow Diverters installed the ship airspeed system had an error range from –5 to – 15 knots relative to the boom system.

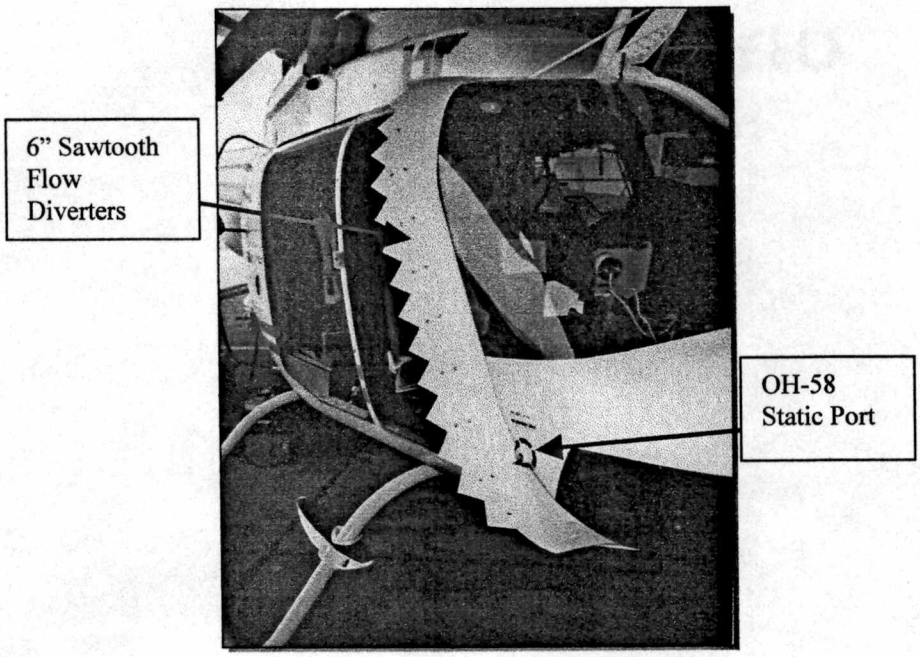


Figure 5.1. Test Aircraft static port position

Baseline Level Flight Performance Test *(Event2)*

General

Level flight performance was conducted as outlined in FTM 106. All flight tests were evaluated at one (1) W_{ref} 3600 lbs. maintaining 100% Nr. The Baseline Level Flight Test was evaluated during a single flight of 0.6 hours. The baseline aircraft test configuration was as depicted in Figure 5.2. The pressure altitude range was 5240 to 6420 feet. The pressure altitude was varied as necessary to maintain the desired W_{ref}. Helicopter loading was a single pilot at the pilot station, one FTE at the co-pilot station, and one FTE in the passenger compartment, The average CG was 109.7 inches, at an average gross weight (GW) of 2997 pounds.



Figure 5.2. OH-58 A+ Test Aircraft in Baseline Configuration.

Data Analysis

Data are presented in Appendix C, Figure C.1. The airflow throughout the cabin is depicted in Figures 5.3. Generally, the strongest airflow would enter the rear cabin doors and then curl inward toward the center. At this point the airflow would continue up toward the cockpit area directly over the back of the pilot and copilot's seats. Qualitatively, it was difficult for the FTE in the passenger compartment to conduct basic tasks such as holding down personal equipment and performing routine communications.

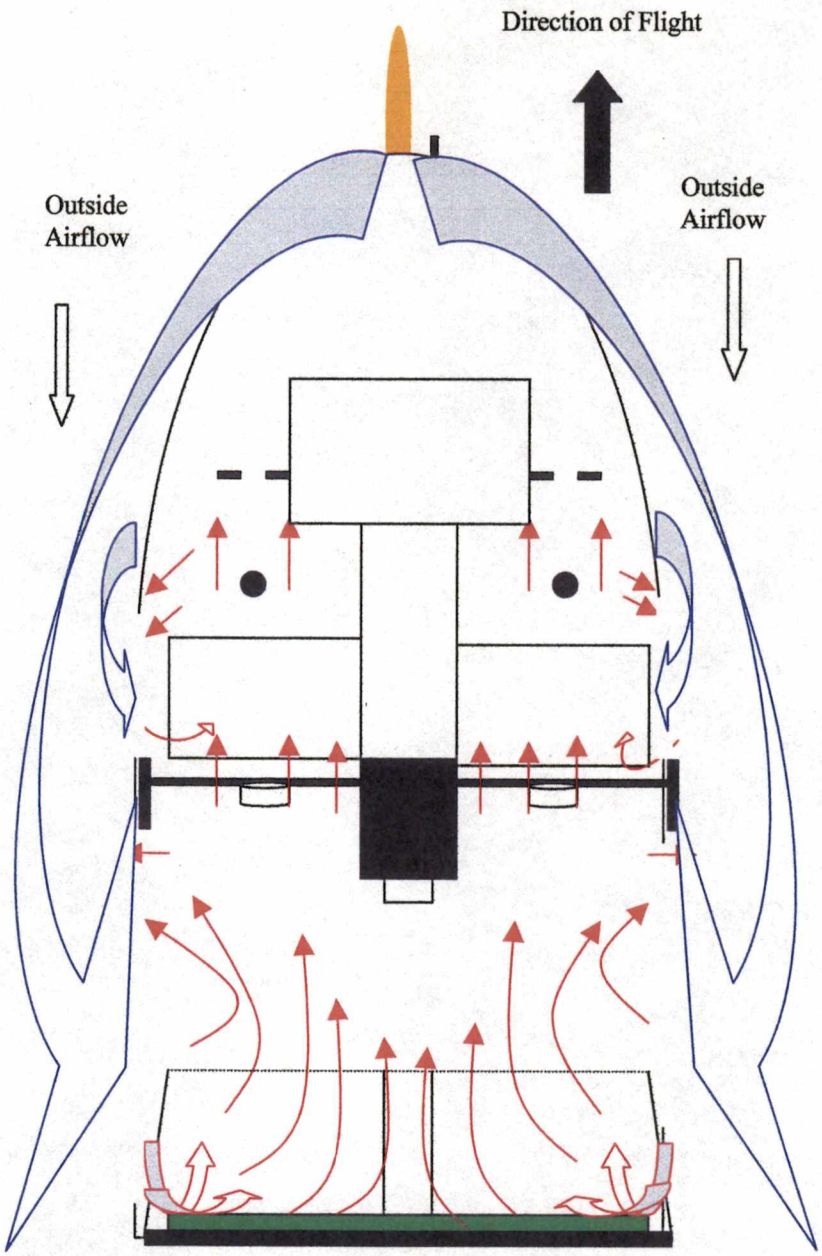


Figure 5.3. OH-58A+ Baseline Airflow Diagram.

Best Angle Test *(Event 3)*

General

The best angle test was evaluated during three flights totaling 1.5 hours. The 6" Sawtooth Flow Diverters were installed for this test. The distance the airflow was deflected determined the best deflection angle. This measurement was taken with a tufted measurement device mounted in the passenger compartment behind the pilot seat at station 85, as depicted below in Figure 5.4. Helicopter loading was a single pilot at the pilot station, one FTE at the co-pilot station, and one FTE in the passenger compartment. The average center of gravity (CG) was 109.7 inches, at an average gross weight (GW) of 3032 pounds. The FTE in the passenger compartment operated the tufted measuring device and recorded the distances that the airflow was deflected due to the Flow Diverter angle variation.

Data Analysis

Data are presented in Appendix C, Figures C.5 thru C.8. During this test it was discovered that the Flow Diverters would provide the best results with an angle between 40° and 50°. This best angle corresponded closely to the previous water tunnel testing. Tufts inside and outside the cabin were added to qualitatively analyze the projected airflow throughout the test aircraft cabin.

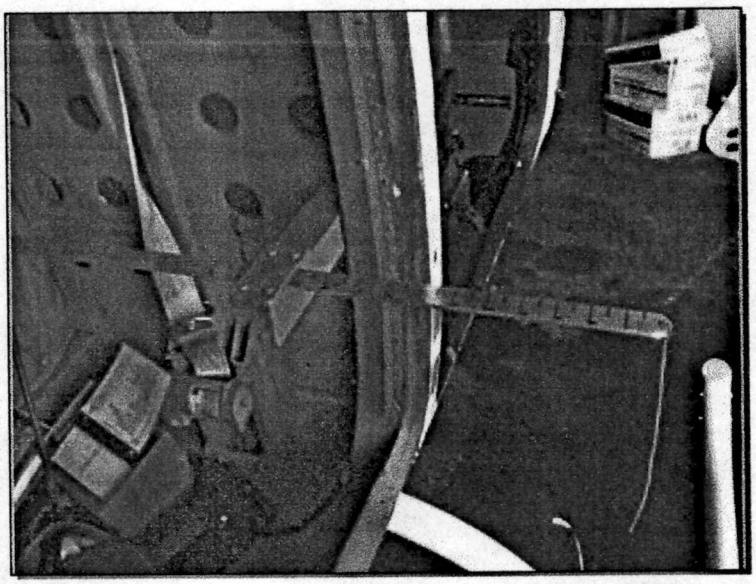


Figure 5.4. Best Angle Tufted Measuring Device.

Level Flight Test with 6" Sawtooth Flow Diverters Installed *(Event 4)*

General

Level flight performance with the 6" Sawtooth Flow Diverters was conducted as outlined in FTM 106. The flight test was evaluated at one (1) W_{ref} (3600 lbs.) maintaining 100% Nr. The Level Flight Test was evaluated during one flight totaling 1.0 hour. The Flow Diverters were set at an angle of 40°. The pressure altitude range was 3900 to 4665 feet. The pressure altitude was varied as necessary to maintain the desired W_{ref}. Helicopter loading was a single pilot at the pilot station, one FTE at the co-pilot station, and one FTE in the passenger compartment. The average center of gravity (CG) was 109.7 inches, at an average gross weight (GW) of 3016 pounds.

Data Analysis

$ESHP_{ref}$ versus True Velocity, $ESHP_{ref}$ versus Inches Deflected, True Velocity versus Inches Deflected, and Equivalent Flat Plate Drag versus Velocity True are depicted graphically in Appendix C, Figures C.2 thru C.5. The 6 inch Sawtooth Flow Diverters, set at a 40°, demonstrated a deflection of the airflow approximately 6 inches at 60 Knots and 7 inches at 80 Knots. Using the following equation:

$$\Delta f = \frac{(550)\Delta ESHP_{ref}}{\frac{1}{2}\rho_{ssl} V_{T_{ref}}^3}$$

These deflections were achieved with an average increase of 6.5-ft^2 equivalent flat plate drag as shown in Table 5.2.

Table 5.2.
6" Sawtooth
Equivalent Flat Plate Drag Calculations.

Knots	Ft/sec	Baseline ESHP	ESHP	δ ESHP	δ Flat Plate Drag	Average
60	101.4	170.0	195.0	25.0	11.1	6.5
70	118.3	188.3	215.0	26 7	7.5	
80	135 2	219 5	245.0	25.5	4.8	
90	152.1	255.9	277 0	21.1	2 8	

During this flight-test, there was a noticeable reduction of airflow into the front cabin area. Generally, the Flow Diverters deflected most of the air to or just past the back of the passenger compartment door. However, some of the airflow was going above the Flow Diverters and then angled in at approximately 45° into the top rear corner of the rear doors. This deflection was caused by two separate factors. The main transmission forward fairing and a negative pressure area inside the cabin due to the effectiveness of the Flow Diverters. The projected airflow in and around the cabin of the test aircraft is depicted in Appendix C, Figures C.24 and C.25.

Level Flight Test with 6" Flat Plate Flow Diverters Installed *(Event 5 & 6)*

General

Level flight performance with the 6" Flat Plate (with Vortex Generators) Flow Diverters were evaluated at one (1) W_{ref} (3600 lbs.) maintaining 100% Nr. The Level Flight Test was evaluated during one flight of totaling 1.0 hours. The Flow Diverters were set at a 40° angle. The pressure altitude range was 3890 to 5160 feet. The pressure altitude was varied as necessary to maintain the desired W/σ. Helicopter loading was a single pilot at the pilot station, one FTE at the co-pilot station, and one FTE in the passenger compartment. The average center of gravity (CG) was 109.7 inches, at an average gross weight (GW) of 3023 pounds.

Data Analysis

$ESHP_{ref}$ versus True Velocity, $ESHP_{ref}$ versus Inches Deflected, True Velocity versus Inches Deflected, and Equivalent Flat Plate Drag versus Velocity True are depicted graphically in Figures C.9 thru C.12. The 6 inch Flat Plate (with Vortex Generators) Flow Diverters, set at a 40° angle, demonstrated a deflection of the airflow approximately 10 inches at 60 Knots and 8.75 inches at 80 Knots. These deflections were achieved with an average increase of 7.3 ft^2 equivalent flat plate drag, as shown in Table 5.3.

Table 5.3.
6" Flat Plate with Vortex Generators
Equivalent Flat Plate Drag Calculations.

Knots	Ft/sec	Baseline ESHP	ESHP	δ ESHP	δ Flat Plate Drag	Average
60	101.4	170.0	198.0	28 0	12.4	7.3
70	118.3	188 3	215 0	26.7	7.5	
80	135.2	219 5	250.0	30 5	5.7	
90	152 1	255 9	282 2	26 3	3.5	

Level Flight Test with 6" Flat Plate Flow Diverters, Back Doors Installed *(Event 6)*

General

Level flight performance with the 6" Flat Plate (with Vortex Generators) Flow Diverters with rear doors installed were evaluated at one (1) W_{ref} (3600 lbs.) maintaining 100% Nr. The Level Flight Test was evaluated during one flight of totaling 0.5 hours. The Flow Diverters were set at a 40° angle. The pressure altitude range was 3810 to 4065 feet. The pressure altitude was varied as necessary to maintain the desired W/σ. Helicopter loading was a single pilot at the pilot station, one FTE at the co-pilot station, and one FTE in the passenger compartment. The average center of gravity (CG) was 110.0 inches, at an average gross weight (GW) of 3060 pounds.

Data Analysis

During this flight-test, the back doors were installed to investigate the blockage of the inflow of air in the upper corner of the rear doors. As the crew conducted flight testing at slow to faster airspeeds, the test was terminated before reaching 80 KIAS. As the airspeed was increased from 70 to 80 KIAS an audible and observed moderate vibration at the rear door window was noticed. Audibly, the crew heard a moderate rumble above the sound of normal aircraft and engine noises. Visually, upon inspection it was noticed that both rear windows were vibrating moderately with the tendency to increase with airspeed. This vibration increased as airspeed increased and was assigned a pilot vibration rating of 6 at 80 KIAS based on the vibration rating scale outlined in FTM 107.

Level Flight Test with 8" Flat Plate (with Vortex Generators) Flow Diverters *(Event 7)*

General

Level flight performance with the 8" Flat Plate (with Vortex Generators) Flow Diverters were evaluated at one (1) W_{ref} (3600 lbs.) maintaining 100% Nr. The Level Flight Test was evaluated during a single flight of 1.0 hour. The Flow Diverters were set at a 40° angle. The pressure altitude range was 4230 to 4935 feet. The pressure altitude was varied as necessary to maintain the desired W/σ. Helicopter loading was a single pilot at the pilot station, one FTE at the co-pilot station, and one FTE in the passenger compartment. The average center of gravity (CG) was 109.7 inches, at an average gross weight (GW) of 3015 pounds.

Data Analysis

$ESHP_{ref}$ versus True Velocity, $ESHP_{ref}$ versus Inches Deflected, True Velocity versus Inches Deflected, and Equivalent Flat Plate Drag versus Velocity True are depicted graphically in Figures C.13 thru C.16. The eight inch Flat Plate (with Vortex Generators) Flow Diverters, set at a 40° angle, demonstrated a deflection of the airflow approximately 15.5 inches at 60 Knots and 12.5 inches at 80 Knots. A qualitative evaluation in flight confirmed that there was a reduction in airflow into the passenger compartment. Additionally, this test determined that the amount of deflection on either side of the test Aircraft was highly sensitive to aircraft trim condition (ball-centered) as depicted in Figure

C.17. These deflections were achieved with an average increase of 4.0 ft^2 (equivalent flat plate drag) as shown in Table 5.4.

Table 5.4.
8" Flat Plate with Vortex Generators
Equivalent Flat Plate Drag Calculations.

Knots	Ft/sec	Baseline ESHP	ESHP	δ ESHP	δ Flat Plate Drag	Average
60	101.4	170	182.0	12 0	5.3	
70	118 3	188 3	202 0	13.7	3.8	4 0
80	135.2	219.5	235.0	15 5	2.9	
90	152.1	255.9	285 0	29 1	3.8	

8" Flat Plate (no Vortex Generators) Flow Diverters Installed *(Event 10)*

General

Level flight performance with the 8" Flat Plate (no Vortex Generators) Flow Diverters were evaluated at one (1) W_{ref} (3600 lbs.) maintaining 100% Nr. The 8" Flat Plate (no Vortex Generators) Flow Diverters were evaluated for the effectiveness of the Vortex Generators. The Level Flight Test was evaluated during a single flight of 0.4 hours. The pressure altitude was varied as necessary to maintain the desired W/σ. The Flow Diverters were set at a 40° angle. Helicopter loading was a single pilot at the pilot station, and one FTE at the

co-pilot station. The average center of gravity (CG) was 109.7 inches, at an average gross weight (GW) of 2937 pounds.

Data Analysis

A qualitative evaluation was conducted to determine the effectiveness of the 8" Flat Plate without the Vortex Generators. During this test there were occasional lateral directional oscillations and abrupt lateral accelerations of the airframe at all airspeeds. These motions were most likely caused by the disruption of the normal airflow around the fuselage back to the vertical stabilizer. This test was conducted in nearly identical parameters to the level flight test with the 8" Flat Plate (with Vortex Generators) with the exception of the removal of the vortex generators. The absence of the vortex generators seemed to produce a disruptive airflow around the fuselage that interacted adversely with the vertical stabilizer. This disruptive airflow was also audible to the crew as a low frequency, pulsating, rumble. Employment of the Flow Diverters without vortex generators is not advisable.

Flow Visualization Test *(Events 8 & 9)*

General

Flow visualization was used on all flight tests by flying with a tufted screen, tufted rod, tufted windscreen, and tufts installed throughout the crew cabin. Specific Flow visualization flight-testing was conducted during three flights totaling 2.0 flight hours.

Helicopter loading for the test aircraft was a single pilot at the pilot station, and one FTE at the co-pilot station. The average center of gravity (CG) was 110.4 inches, at an average gross weight (GW) of 2711 pounds. The loading for the chase aircraft was a single pilot at the pilot station, and one FTE (safety pilot) at the co-pilot station. This test required the chase aircraft to be installed with video recording capability. The tufted screen was installed as depicted in Figure 5.5.

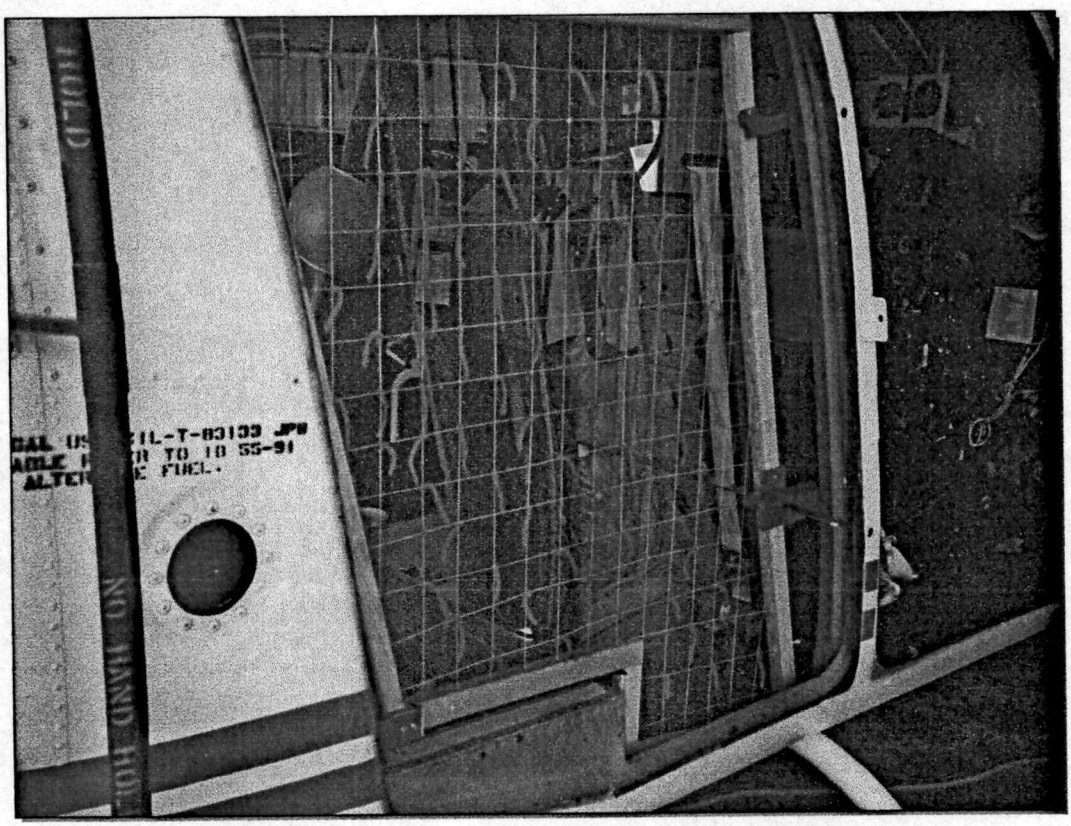


Figure 5.5. Test Aircraft Tufted Screen Installation.

Data Analysis

Before conducting smoke flow visualization flight-testing, a build-up approach was taken. The Smoke Generator System was tested independently on the ground (Appendix G, Figure G.8.) and while attached to an automobile (Appendix G, Figures G.9 and G.10). These tests were conducted to verify the safety and validity of the system. Specific Flow visualization flight tests involved the installation of experimental equipment (Smoke Generator System) mounted on the test aircraft as depicted below in Figures 5.6. and 5.7. This equipment was used to verify visually the precise flow pattern induced by the Flow Diverter. As an added safety measure, all doors were reinstalled and a representative 18" section of the Flow Diverter was installed on the right side of the aircraft (Figure 5.6.). These additional safety steps were taken as a precaution to ensure that no smoke would enter the cockpit during flight and endanger the crew.

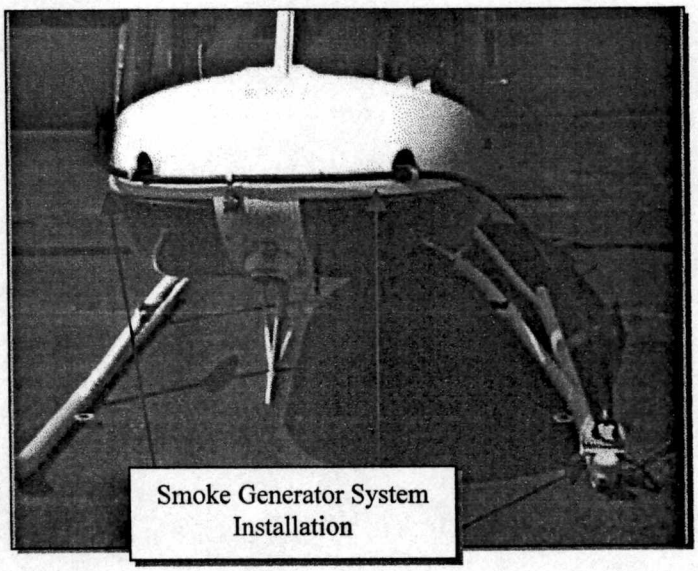


Figure 5.6. Experimental Smoke Generator System.

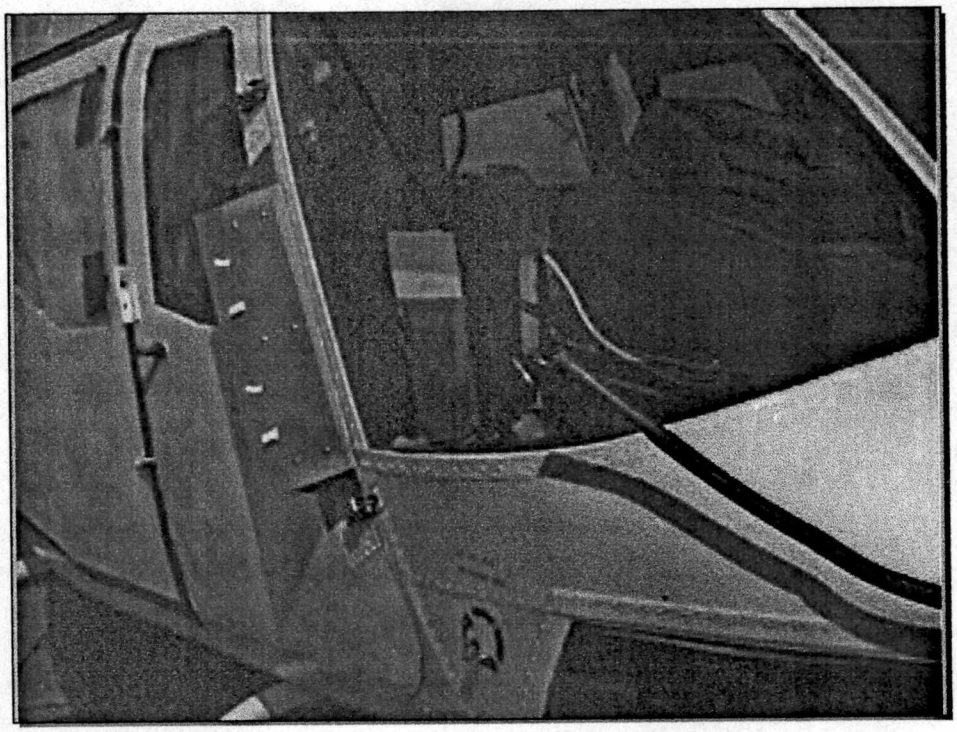


Figure 5.7. Representative 18" Section of Flat Plate Flow Diverter

The smoke visualization technique worked exceptionally well. However, the smoke provided by the standard M-18 military smoke canisters (Figure 5.8.) did not provide enough smoke volume to assess flow characterization from the video. Additionally, the recording of this data was difficult. This technique required a chase aircraft with stabilized video. This requirement was due to difficulty in attaining quality video from a ground video source, of the test aircraft in flight at the precise moment the smoke generator system was operating.

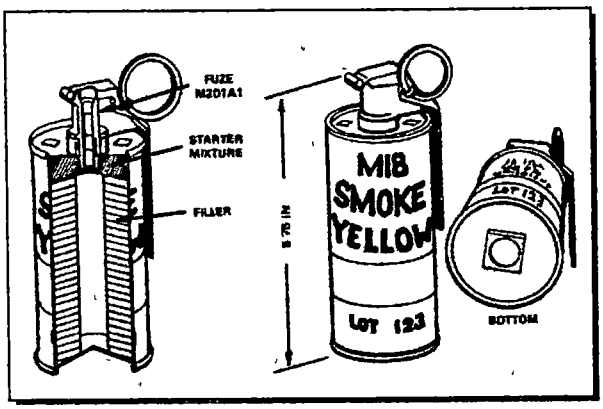


Figure 5.8. M18 Smoke Canister

Airflow Testing with Flow Diverters Installed *(Events 2 – 7B)*

General

Airflow evaluations were conducted during all of the flight tests. Tufts inside and outside the cabin were used to qualitatively analyze the projected airflow around the test aircraft cabin.

Data Analysis

Generally, the Flow Diverters deflected most of the air to, or just past, the back of the passenger compartment door. However, some of the airflow was going above the Flow Diverters and then angled in at approximately 45° into the top rear corner of the rear doors. This rear door inflow most likely was caused by two separate factors. First, the main transmission forward fairing was inducing flow downward from the helicopter roof. Second, the negative pressure area inside the cabin due to the effectiveness of the Flow Diverters.

Additionally, there was some air going under the Flow Diverters and wrapping around the aircraft and entering the lower portion of the rear doors. This deflection was most likely caused by the air seeking the lower pressure area. The projected airflow in and around the cabin of the test aircraft is depicted in Figures C.24 and C.25.

Noise Level Testing *(Events 1 – 7B)*

General

In addition to assessing the physical passenger comfort the noise level in the cabin was monitored for low and high pitch aerodynamic sounds due to the vortex generator and reduced wind velocities entering the cabin. To sample cabin noise a Mine Safety Appliances Model 80 Noise Dosimeter (Figure 5.9.) was used. The model 80 Noise Dosimeter was used to record an average reading as opposed to instantaneous noise levels. The meter is "A" weighted as required by OSHA. "A" weighted dosimeters apply a weighted scale to received noise determined by the frequency's interpretation by the human ear.

Data Analysis

During all of the flight tests there were no significant differences in the recorded noise level (Table 5.5). The average noise level reading during all flight tests was 101.3 decibels (db). The maximum noise level recorded was 103.5 db. The minimum noise level recorded was 100.0 db.

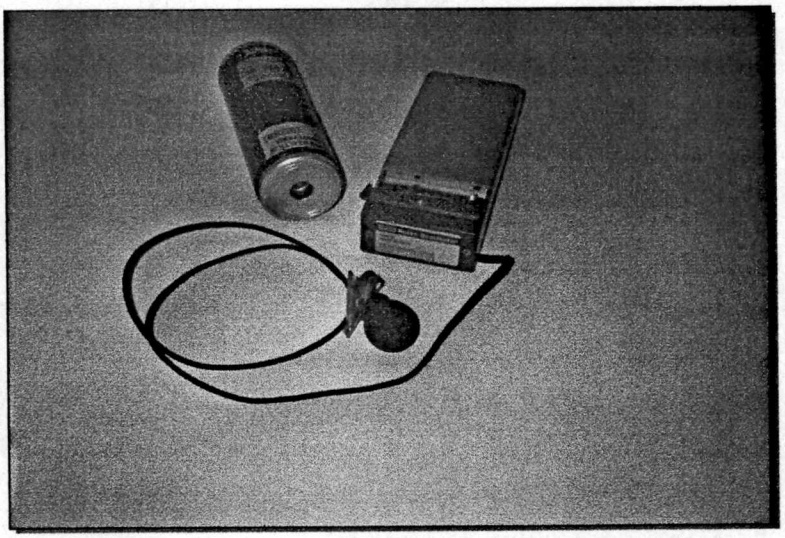


Figure 5.9. MSA Model 80 "A" Weighted Noise Dosimeter.

Table 5.5. Flight Test Noise Level Readings

Event [1]	Duration (hours)	Percentage Dosage	Average Decibels (dbA)
1 & 2 (Baseline Aircraft)	1.3	100	103.5
3 (6" Sawtooth)	1.2	65	100.5
4	0.8	60	102.5
5	1.0	50	100
7	0.9	50	100.5
7B	0.9	55	101

Notes: *1. Event numbers taken from Table 5.1.*

Handling Qualities *(Events 2 & 7)*

General

The lateral-directional oscillation (LDO) characteristics were documented for the test aircraft in the baseline and 8" Flat Plate (with Vortex Generator) configurations. These tests were conducted at a trim airspeed of 80 KIAS using release from Steady Heading Sideslip (SHSS). The newly installed Data Acquisition (DAQ) system was unable to gather any meaningful data so the cockpit data were used to record the needed parameters.

Data Analysis

The test aircraft LDO Root Locus Plots are presented in Appendix C, Figure C.18. The LDO for baseline aircraft configuration was moderately damped in the yaw axis with a sideslip (β) damping ratio of 0.5. The sideslip oscillation had a period of 2.8 seconds, corresponding to an observed frequency (ω_d) of 2.2 rad/sec. The max roll (ϕ) attained from the LDO was 2° and max sideslip (β) was 11° providing a 0.18 ϕ/β ratio. The aircraft was moderately damped in the roll axis. For this test the LDO characteristics of the OH-58A+ helicopter were satisfactory. The LDO for the 8" Flow Diverter configuration showed no noticeable changes from the baseline aircraft.

COMPARATIVE DATA ANALYSIS

Flow Diverters

General

For direct comparison analysis, Appendix C, Figures C.18 thru C. 23 compare the flight-test data from one configuration to another.

Data Analysis

The performance of the 6" Flat Plate Flow Diverters was improved significantly over the 6" Sawtooth version. Comparative data between the 6" Sawtooth and the 6" Flat Plate Flow Diverters is depicted in Appendix C, Figure C.19. This data shows that there was very little difference between these two Flow Diverters in terms of increased parasite drag. However, the 6" Flat Plate Flow Diverters had an increase deflection of 25% at 80 KTAS, as depicted in Appendix C, Figures. It could not be determined if the increase in deflection was due to the vortex generators or to an increase in mass flow from the flat plate design.

The 8" Flat Plate and the 6" Flat Plate Flow Diverters are compared in Figure C.16 thru Figure C.19. Although the problem with the airflow over the top of the Flow Diverters could not be eliminated, there was a significant improvement in the performance and deflection of the airflow over both the 6" Sawtooth and the 6" Flat Plate Flow Diverters. The increase in deflection was approximately 79% above the 6" Sawtooth deflection and an

average of 43% over the 6" Flat Plate version. This significant increase combined with the decrease in equivalent flat plate drag was attributed to the increase in mass flow rate generated by the larger Flow Diverter.

The test results of the full scale Flow Diverters did not correspond exactly to the results of the water tunnel testing. These differences highlight the fact that scaled model testing in a water tunnel can give proof of concepts. However, the water tunnel tests do not necessarily correspond exactly to full scale flight testing. Some of these differences were due to using a similar aircraft instead of the actual full scale aircraft that was tested in the water tunnel. The similar aircraft flight testing was successful at proof of concept on a full scale aircraft. However, the airflow around the similar aircraft fuselage was different from that of the MH-6. This validates the need to conduct the further flight testing on the actual MH-6 helicopter.

Chapter 6

DATA REDUCTION

Data Reduction

Data from each of the flight tests were recorded manually and automatically using the cockpit instrumentation and the DAQ. Data reduction were conducted manually in accordance with the USNTPS FTM 106. The following equations were used in the manual data reduction:

$$H_{p_c} = H_{p_o} + \Delta H_{p_{ic}} + \Delta H_{pos}$$

Where:

H_{pc}	-	Calibrated pressure altitude
H_{po}	-	Observed pressure altitude
ΔH_{pic}	-	Altimeter instrument correction
ΔH_{pos}	-	Altimeter position error.

$$T_a = T_o + \Delta T_{ic}$$

Where:

T_a	-	Ambient temperature
T_o	-	Observed temperature
ΔT_{ic}	-	Temperature instrument correction.

$$T_a(^\circ K) = T_a(^\circ C) + 273.15$$

Where:

Ta (°K)	-	Ambient temperature, °K
Ta (°C)	-	Ambient temperature, °C.

$$\sigma_T = \frac{\delta}{\theta} = \frac{\delta}{\left(\frac{T_a}{T_{ssl}}\right)}$$

Where:

σ_T	-	Test density ratio
δ	-	Pressure ratio
θ	-	Temperature ratio
T_a	-	Ambient temperature, °K
T_{ssl}	-	Standard sea level temperature, 288.15 °K.

$$ESHP_T = K_Q(Q)(N_{R_T})$$

Where:

$ESHP_T$	-	Test engine shaft horsepower
K_Q	-	Engine torque constant
Q	-	Engine torque
N_{RT}	-	Test main rotor speed.

$$ESHP_{ref} = \frac{ESHP_T}{\sigma_T}\left(\frac{N_{R_S}}{N_{R_T}}\right)^3$$

Where:

$ESHP_{ref}$	-	Referred engine shaft horsepower
$ESHP_T$	-	Test engine shaft horsepower
σ_T	-	Test density ratio
N_{RS}	-	Standard main rotor speed
N_{RT}	-	Test main rotor speed.

$$W_T = ESGW - FU$$

Where:

W_T	-	Test weight
ESGW	-	Engine start gross weight
FU	-	Fuel used.

$$W_{ref} = \frac{W_T}{\sigma_T}\left(\frac{N_{R_S}}{N_{R_T}}\right)^2$$

Where:

W_{ref}	-	Referred weight
W_T	-	Test weight
σ_T	-	Test density ratio
N_{RS}	-	Standard main rotor speed
N_{RT}	-	Test main rotor speed.

$$\Omega R = K_{GR}\left(N_{R_T}\right)\left(\frac{2\pi}{60}\right)(R)$$

Where:

ΩR	-	Rotational velocity
K_{GR}	-	Gear ratio
N_{RT}	-	Test main rotor speed
R	-	Rotor radius.

$$C_P = \frac{P}{\rho_a\left(A_D\right)(\Omega R)^3}$$

Where:

C_p	-	Power coefficient
P	-	Power
ρa	-	Ambient density
A_D	-	Rotor disc area
ΩR	-	Rotational velocity.

$$C_T = \frac{T}{\rho_a\left(A_D\right)(\Omega R)^2}$$

Where:

C_T	-	Thrust coefficient
T	-	Thrust
ρa	-	Ambient density
A_D	-	Rotor disc area
ΩR	-	Rotational velocity.

$$V_c = V_o + \Delta V_{ic} + \Delta Vpos$$

Where:

V_c	-	Calibrated airspeed
V_o	-	Observed airspeed
ΔV_{ic}	-	Airspeed instrument correction
ΔV_{pos}	-	Airspeed position error.

$$V_T = \frac{V_c}{\sqrt{\sigma}}$$

Where:

V_T	-	True airspeed
V_c	-	Calibrated airspeed
σ	-	Density ratio.

$$V_T = V_T\left(\frac{N_{R_S}}{N_{R_T}}\right)$$

Where:

V_{Tref}	-	Referred true airspeed
V_T	-	True airspeed
N_{RS}	-	Standard main rotor speed
N_{RT}	-	Test main rotor speed.

$$\mu = 1.69\left(\frac{V_T}{\Omega R}\right)$$

Where:

μ	-	Advance ratio
V_T	-	True airspeed

ΩR	-	Blade rotational velocity.

$$a = 38.967\sqrt{T_a\left(^{\circ}K\right)}$$

Where:

a	-	Speed of sound
T_a	-	Ambient temperature.

$$V_{tip} = \left(\frac{\Omega R}{1.69}\right) + V_T$$

Where:

V_{tip}	-	Blade tip velocity
ΩR	-	Blade rotational velocity
a	-	Speed of sound.

$$M_{tip} = \frac{V_{tip}}{a}$$

Where:

M_{tip}	-	Blade tip Mach number
V_{tip}	-	Blade tip velocity
V_T	-	True airspeed.

$$\varpi_d = \frac{2\pi}{P}$$

Where:

P	-	Period
Π	-	Mathematical constant
Ω_d	-	Damped frequency

$$\varpi_n = \frac{\varpi_d}{\sqrt{1-\zeta^2}} = \frac{\frac{2\pi}{P}}{\sqrt{1-\zeta^2}}$$

Where:

P	-	Period
π	-	Mathematical constant
ω_d	-	Damped frequency
ω_n	-	Natural frequency
ζ	-	Damping ratio

Noise Evaluation Data Reduction

The data parameters were required for each flight; Duration of exposure and Percent Dosage. Both of these parameters were read directly from the MSA model 80 Noise Dosimeter. These parameters were then entered on the Nomograph depicted in Figure 6.1. The average decibels were determined by the intersection of the two parameters.

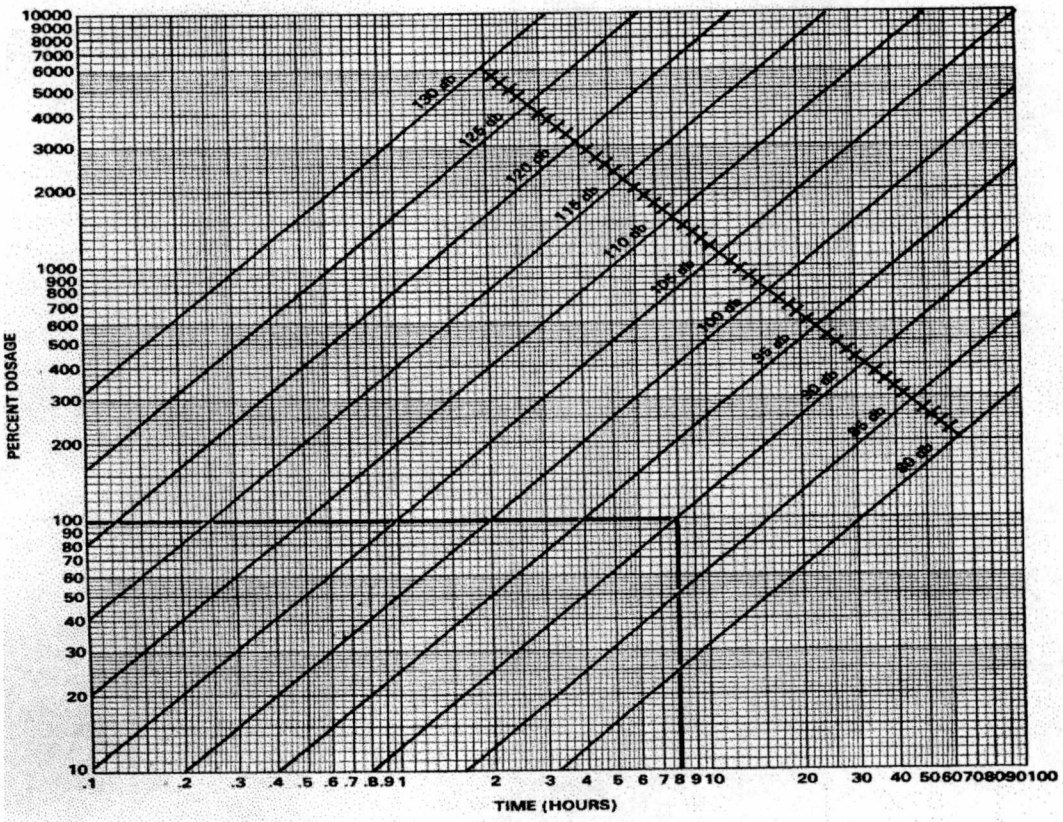


Figure 6.1. Equivalent Sound-Level Nomograph

Chapter 7

CONCLUSIONS

After one year of research, 3 months of designing, and 10 flight test hours, the author concluded:

1. The concept of rapid prototyping flight-testing of the Flow Diverters installed on a similar aircraft is valid.

2. A potential solution for the MH-6 and its high mission effective drag configuration is possible using the 8" Flat Plate (with Vortex Generators) Flow Diverters.

3. With a setting of 40°, the Flow Diverters were capable of deflecting the airflow approximately 15 inches (Table 7.1). The largest deflection was achieved using the 8" Flat Plate (with Vortex Generator).

Table 7.1.

Flow Deflection

Flow Diverter	60 KTAS	80 KTAS	Average
6" Sawtooth	5 inches	7 inches	6 inches
6" Flat Plate	10 inches	8.5 inches	9.25 inches
8" Flat Plate	15 inches	13.25 inches	14.125 inches

4. The 8" Flat Plate (with Vortex Generators) Flow Diverters were the most effective. The increase in deflection averaged approximately 79% over the 6" Sawtooth and an average of 43% over the 6" Flat Plate version. An analysis from the test data showed that an angle between 40° - 50° was the optimum for the maximum deflection.

5. It is possible that an MH-6 with Flow Diverters installed will reduce its Effective Drag (D_{eff}) when flying in a high drag mission configuration with external passengers. This reduced D_{eff} would increase the MH-6's range and loiter time.

Table 7.2.
Mission Scenario Configuration Comparisons.

Configuration	**Δf** (From Baseline Aircraft)	**Fuel**	**Fuel Flow**	**Time** (at 80 kts)	**Radius**
MH-6 Baseline (EPS, No Doors)	0	Full Main	232	1 hr 43 min	137 nm
MH-6 (EPS, No Doors, and External Pax)	16.5	Full Main	285	1 hr 25 min	113 nm
MH-6 (EPS, No Doors, External Pax, and 8" Flow Diverters)	4.0 (Approximately)	Full Main	255	1 hr 35 min	127 nm

6. Although the test aircraft showed an increase in Parasite Power (P_p) from the baseline configuration, this comparison is not operationally representative. The actual mission profile for the MH-6 represents an increase in equivalent flat plate drag of 16.5 square feet or greater from its baseline configuration. The OH-58 has an increase of 1.6 square feet from its baseline configuration. Further, some of the OH-58's increase in Parasite Power may also be due to the design, specifically the forward transmission fairing appeared to be forcing the airflow down to the upper rear corner of each of the rear door areas (Figures C.18 and C.19.). A study of the MH-6 aircraft design indicates that this may not exist problem due to differences in fuselage shape.

7. The handling qualities of the test aircraft with Flow Diverters installed did not change from the baseline aircraft. However, when the Vortex Generators were removed from the 8" Flat Plate Flow Diverters, the flow field was such that it caused random yaw oscillations and yaw accelerations in the test aircraft.

8. Although there was some loss in Field of view with the 8" Flow Diverters installed, it was not significant enough to have a detrimental effect on the mission suitability.

9. Although no video data useful for determining detailed flow characteristics was captured while using the Smoke Generator System, the design and concept of the system was safe and effective. If a greater volume of smoke can be safely attained, this system should work as designed.

160th Mission Requirements

The 160th MH-6 mission dictates that the basic aircraft weights remain as light weight as possible to therefore increase payload all while operating at the maximum allowable gross weight. Each additional pound of equipment installed on the aircraft will therefore requires a tradeoff in either fuel or payload. The total cost in weight of the Flow Diverters would be approximately 10 pounds. Additionally, the typical MH-6 mission profile requires the aircraft to fly with an effective drag increase of 16.5 Ft^2 or higher, dependent upon the mission equipment installed. This coupled with the fatigue brought on to the passengers due to the constant 60 to 80 knots of airflow they experience is detrimental to their mission accomplishment.

The author believes that it is possible to reduce the MH-6 mission effective drag and significantly reduce the airflow off the external passengers. This is important for two reasons:

1. Minimizing the airflow on the passengers.

2. This can lead to an expanded mission envelope for flying with external passengers. This mission envelope expansion would include the ability to fly in colder temperatures as well as making it more feasible to fly in precipitation. Additionally, it may be possible to maintain greater enroute speeds without adding to the fatigue of the passengers.

Chapter 8

RECOMMENDATIONS

Based upon proof of principle in a rapid prototyping flight test evaluation of full scale Flow Diverters, the author made the following recommendations:

1. Develop a set of flow diverters specifically for the MH-6.
    a. 8" Flat Plate with Vortex Generators.
    b. The angle should be between 40° and 50°.
2. Conduct Flight Tests with an OH-6 or MH-6 in its typical mission configuration.
    a. These tests should include flights with and without external ballast.
    b. At least two of the flight tests should be with an external passenger. For a qualitative comparison evaluation one flight test should be with no deflection and the other with maximum deflection.
3. Recommend that all doors are removed at all times with Flow Diverters installed.

4. Recommend the use of the Smoke Generator System with a greater volume of smoke. This can be done by either a specialized smoke canister or with a portable smoke generator.

WORKS CONSULTED

REFERENCES

1. Carterette, Edward C. and Friedman, Morton P. "*Human Factors in Aviation*," Academic Press, 1988.

2. Flight Test Manual, "*Rotary Wing Performance*" Naval Air Test Center, USNTPS-FTM-No. 106, 31 December 1996.

3. Flight Test Manual, "*Rotary Wing Stability and Control.*" Naval Air Test Center, USNTPS-FTM-No. 107, 31 December 1995.

4. Headquarters, Department of the Army, "*Operator's Manual for the Mission/Modified A/MH-6J Special Operations Aircraft*," 15 December 1998.

5. Headquarters, Department of the Army, "*Operator's Manual Army Model OH-58A/C Helicopter*," 17 January 1989.

6. Hicks, Eric G. "Experimental Study of Alternative Flow Diverting Devices for the Modified MH-6J Helicopter." The University of Tennessee Space Institute, Tullahoma, Tennessee, November 1997.

7. Kimberlin, Ralph D., "*Performance Flight Testing Lecture Notes,*" The University of Tennessee Space Institute, Tullahoma, Tennessee, March 2000.

8. Lambert, Mark, ed. "*Jane's, All the World's Aircraft*," 1992 – 1993. Great Britain: Butler and Tanner, 1993.

9. Nightstalkers, *160th SOAR Home Page*, 14 August 2000. Available at http://www.goarmy.com/job/branch/sorc/soar/history.htm.

10. Prouty, Raymond W. *Helicopter Performance, Stability, and Control*. Malabar, FL: Krieger, 1990.

11. Taylor, John W. R., and Kenneth Munson. *History of Aviation*. New York: Crown, 1972.

12. Taylor, John W.R. "*Jane's, All the World's Aircraft*," 1977 – 1978. Great Britain: Butler and Tanner, 1993.

13. White, Frank M. "*Fluid Mechanics*." New York: McGraw-Hill, 1986.

BIBLIOGRAPHY

Asanuma, Tsuyoshi, "*Flow Visualization.*" Proceedings of the International Symposium on Flow Visualization, October 12-14, 1977, Tokyo, Japan. Washington: Hemisphere, 1979.

Brown, Dennis, "*Reynold's Number Comparison,*" Derby Tech, June 1985. Available at http://207.242.75.40/derbtech/reynolds.

Carterette, Edward C. and Friedman, Morton P. "*Human Factors in Aviation,*" Academic Press, 1988.

CCI, "Pre-molded vortex generators," June 2000. Available at http://www.mywebco.com/cci/index.html.

Cowley, S. J., Stewart, P.A., "*High-Reynolds-Number Flow,*" 15 June 2000. Available at http://www.damtp.cam.ac.uk/brouchure/1995/.

Defense Technical Information Center, AVSCOM Technical Report 76-9, Vol 1. 31 Dec. 1973.

Defense Technical Information Center, USAAEFA Project No. 76-11-1, March 1978.

Defense Technical Information Center, USAAEFA Project No. 81-07, October 1981.

Defense Technical Information Center, USAAEFA Project No. 81-01-4, August 1982.

Defense Technical Information Center, USARTL TR-79-20, November 1979.

Defense Technical Information Center, USAAEFA Project No. 76-11-2, April 1979.

Flight Test Manual, "*Rotary Wing Performance*" Naval Air Test Center, USNTPS-FTM-No. 106, 31 December 1996.

Flight Test Manual, "*Rotary Wing Stability and Control.*" Naval Air Test Center, USNTPS-FTM-No. 107, 31 December 1995.

Headquarters Department of the Army, Airworthiness Release Supplemental for AH/MH-6J. Washington: GPO, 1995.

Headquarters, Department of the Army, "*Operator's Manual for the Mission/Modified A/MH-6J Special Operations Aircraft,*" 15 December 1998.

Headquarters, Department of the Army, "*Operator's Manual Army Model OH-58A/C Helicopter,*" 17 January 1989.

"*Introduction to Boundary Layer Concepts*," 17 June 2000. Available at http://www.mech.port.ac.

Jackson, Paul. "*Jane's, All the World's Aircraft*," 1998-1999. London: Butler and Tanner Limited 1998.

Jackson, Paul. "*Jane's, All the World's Aircraft*," 1999-2000. London: Butler and Tanner Limited 1999.

Kimberlin, Ralph D., "*Performance Flight Testing Lecture Notes*," The University of Tennessee Space Institute, Tullahoma, Tennessee, March 2000.

Kimberlin, Ralph D., "*Course Notebook Flight Testing*", The University of Tennessee Space Institute, Tullahoma, Tennessee, as revised.

Lambert, Mark, ed. "*Jane's, All the World's Aircraft*," London: Butler and Tanner, 1993.

McCormick, Barnes W. "*Aerodynamics, Aeronautics, and Flight Mechanics*," 2nd edition John Wiley and Sons, Inc. 1995

Mine Safety Appliances Company, "*Noise Dosimeter Model 80 Instruction Manual*", Pittsburgh, Pennsylvania,.

Nightstalkers, *160th SOAR Home Page*, 14 August 2000. Available at http://www.goarmy.com/job/branch/sorc/soar/history.htm.

Prouty, Raymond W. *Helicopter Aerodynamics*. Phillips Publishing, Inc., 1985.

Prouty, Raymond W. *More Helicopter Aerodynamics*. PJS Publications Inc., 1988.

Prouty, Raymond W. *Even More Helicopter Aerodynamics*. Phillips Business Information Inc., 1993.

Prouty, Raymond W. *Helicopter Performance, Stability, and Control*. Malabar, FL: Krieger, 1990.

Richards R. B. "Principles of Helicopter Performance." Naval Air Test Center, Patuxent River, Maryland, October 1994.

Richwine, David M. "*A Smoke Generator System for Aerodynamic Flight Research.*" NASA Technical Memorandum 4137, September 1989

Roberts, Sean C. *Aircraft Performance Flight Testing of Light Aircraft*. Flight Research Inc., 9 July 1982.

Robertson, Greta A., and Keith E. Arthur. "*Measuring the Benefits of a Complex System: The Rotorcraft Pilot's Associate Evaluation Program.*" American Helicopter Society 51st Annual Forum, Ft. Worth, TX, May 9-11, 1995.

Taylor, John W. R., and Kenneth Munson. *History of Aviation*. New York: Crown, 1972.

United States Army Aviation Engineering Flight Activity. "Airworthiness and Flight Characteristics Evaluation of the MDHC 530FF Helicopter." AEFA Project No. 86-15, Edwards AFB, CA:, May 1989.

United States Army Aviation and Troop Command. " Aeronautical Design Standard, Handling qualities Requirements for Military Rotorcraft." ADS-33, St. Louis, MO., July 1994.

U.S. Department of Transportation Regulations, Federal Aviation Regulations (FAR) 23.49 and 23.201, as revised.

Ward, Donald T. "*Preliminary Design of an Intermittent Smoke Flow Visualization System.*" NASA Contractor Report 186027, 1993.

White, Frank M. "*Fluid Mechanics.*" New York: McGraw-Hill, 1986.

APPENDICES

APPENDIX A

MH-6 and OH-58A+ Physical Data.

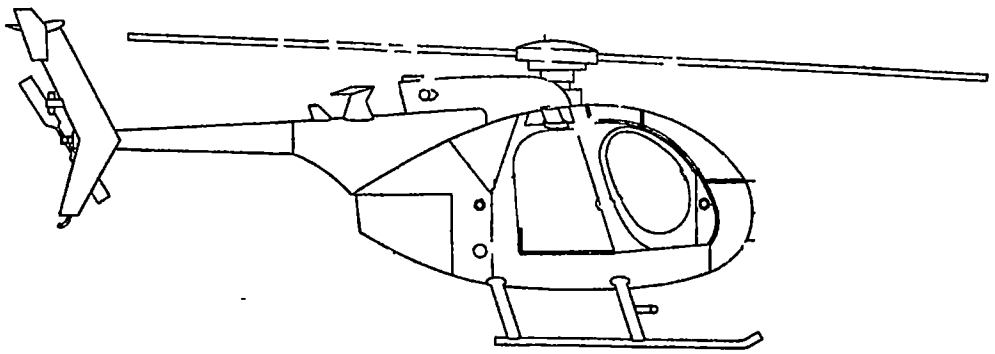


Figure A.1. MH-6

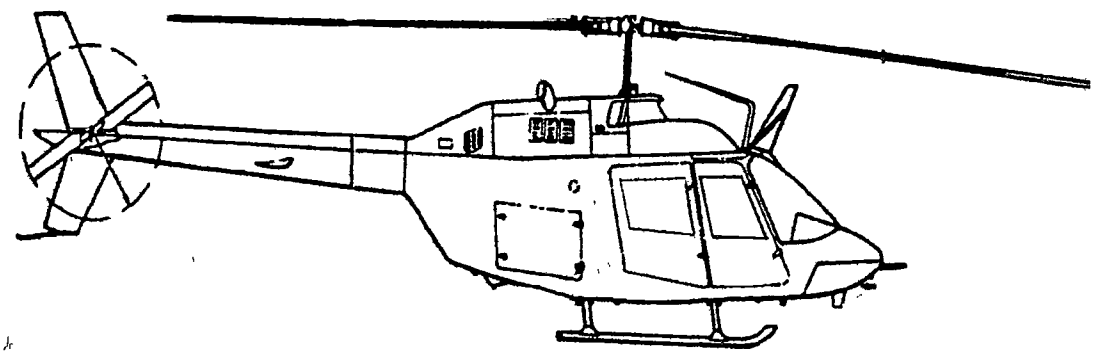


Figure A.2. OH-58A

Table A.1. MH-6 Dimensional Data

Rotor Characteristics

	Main	Tail
Number of Blades	5	2
Rotor Diameter (ft)	27.35	4 75
Rotor Disc Area (ft^2)	587.5	17.72
Blade Chord (constant) (inches)	6.75	5 33
Blade Twist (deg)	9.5 washout	9.5 washout
Total Blade Area (ft^2)	38.46	2.10
Solidity (thrust weighted)	0.0653	0.1150
Airfoil Section, NACA	0015	63-415
Delta 3 (ft^2)	0	30
Droop Stop Flapping (deg)	-6	10 soft, 15 hard
Droop Stop Coning (deg)	0 static,	-2 rotating
Built-in Collective Pitch at 3/4 radius (straps untwisted, deg)	7.75	4.03
Flap Hinge Offset (inches)	6	-

Rotor Speed Limits

	MAIN ROTOR		TAIL ROTOR	
	(rpm)	(ft/sec)	(rpm)	(ft/sec)
Maximum Pwr Off				
Design	533	763	3182	791
Redline	508	727	3033	754
Minimum Pwr Off				
Design	390	559	2328	579
Redline	410	587	2448	609
Maximum Pwr On	477	684	2848	708
Minimum Pwr On	473	677	2824	702

Stabilizer Data

Horizontal Stabilizer P/N SKD-421-087-511

Span (ft)	5.33
Tip Chord (ft)	1.22
Root Chord (ft)	1.90
Area (ft^2)	8 18
Airfoil Root	NACA 6518 Inverted
Airfoil Tip	NACA 6515 Inverted

Table A.1. MH-6 Dimensional Data (Continued).

Weights (lb)		Engines	
Empty	1,455	Type	Allison 250-C20B
Maximum takeoff	3,000	Number	1
Fuel capacity	416	Max T.O rating	420 shp
		Max usable power	375 shp

Rotor Parameters		Main Rotor	Tail Rotor
Radius (ft)	R	13.2	2.3
Chord (ft)	c	.56	0.44
Solidity	σ	068	.119
No of blades	b	5	2
Tip speed (ft/sec)	ΩR	680	704
Twist (deg)	θ_1	-9	-8.6
Hinge offset ratio	e/R	032	- - -
Airfoil		NACA 0015	NACA 63-415
Collective range (deg)		0 to 14.3	-13 to 27
Longitudinal cyclic range (deg)		-7 to 17	- - -
Lateral cyclic range (deg)		-8 5 to 5 5	- - -
Polar Moment of Inertia (slug ft^2)	J	263	23

Stabilizer Parameters	Horizontal	Upper Vertical	Lower Vertical
Span (ft)	5 33	3 54	2.29
Tip Chord (ft)	1 22	0.94	0 59
Root Chord (ft)	1 90	1 27	1.27
Area (ft^2)	8 18	3 91	2.14
Airfoil Root	NACA 6518 Inverted	13 4% thick*	13 4% thick*
Airfoil Tip	NACA 6515 Inverted	18 3% thick*	28.0% thick*
Incidence	9° relative to hub plane	- - -	- - -
End Plates	(2) four-sided polygons	- - -	- - -
End Plate Total Area (ft^2)	2.38	- - -	- - -

*Vertical stabilizer is flat sided, constant thickness (2.06 inch) section

Table A.1. MH-6 Dimensional Data

(continued).

Incidence (deg) (relative to hub plane)	8 92–9 42
Total Area of End Plates, (ft^2)	1 42 each

Upper Vertical Stabilizer – Portion above Centerline of Boom

Span (ft)	3 45
Tip Chord (ft)	0.94
Root Chord (ft)	1.27
Area (ft^2)	3.91
Airfoil Root	13 4 % thick– modified section*
Airfoil Tip	18.3 % thick– modified section*

Lower Vertical Stabilizer – Portion Below Centerline of Boom

Span (ft)	2.29
Tip Chord (ft)	0.59
Root Chord (ft)	1 27
Area (ft^2)	2.14
Airfoil Root	13 4 % thick– modified section*
Airfoil Tip	28 0 % thick– modified section*

* Vertical Stabilizer is flat sided, constant thickness (2.06 inches) section

CONTROL RIGGING, DESIGN

Main Rotor

Collective Pitch, Full Travel, min	14.25 deg (up to down)
Collective Pitch at Down Stop	0 to 3 deg (ground adjustable)
	0 to 3 deg (gnd adjustable)
Range of Cyclic Pitch Blade Angles from Neutral Rigging Position, minimum	Forward 17 deg
	Aft 7 deg
	Left 7 deg
	Right 5 5 deg

Tail Rotor

Range of Blade Pitch Angles at 3/4 radius (deg)	13 (right thrust)
	27 (left thrust)

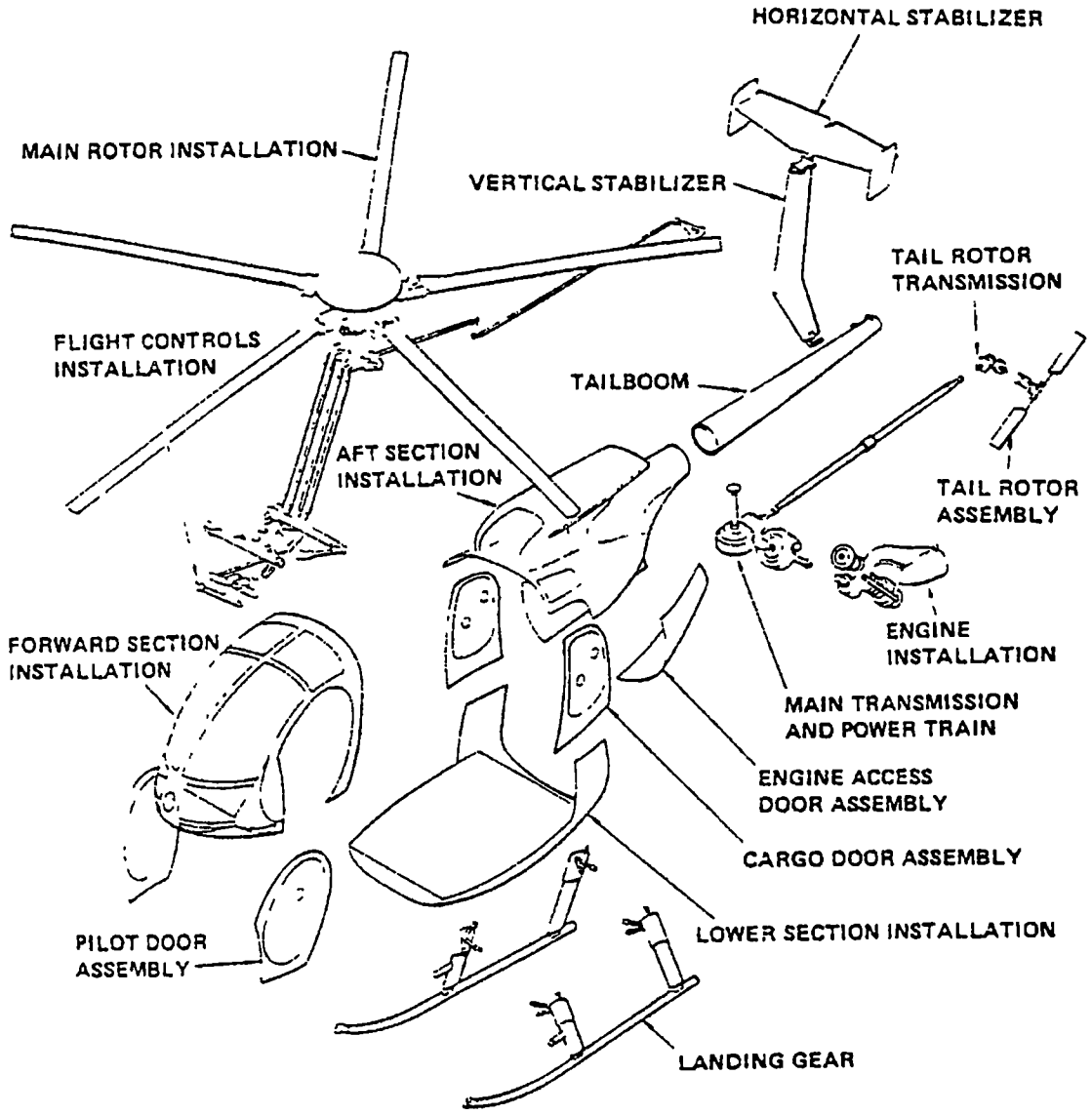


Figure A.3. MH-6 Major Components.

Table A.2. OH-58A+ Dimensional Data

	Standard Landing Gear	High Landing Gear
Forward Tip of Main Rotor (Static position) to ground with droop	9 ft. 6.0 in	10 ft. 0.0 in
Forward Tip of Main Rotor to Ground (Tie Down)	12 ft. 0.0 in.	12 ft. 6.0 in.
Forward Tip of Main Rotor to Ground (Forward Down)	6 ft. 8.0 in.	7 ft. 2.0 in.
Ground to Top of Main Rotor Reservoirs	9 ft. 7.0 in.	10 ft. 9.0 in.
Bottom of Cabin	13.0 in.	27.0 in.
Top of Vertical Stabilizer	8 ft. 1.5 in.	10 ft. 1.5 in.
Tail Skid to Ground	1 ft. 4.4 in.	3 ft. 4.4 in.
Lower Cutter to Ground	12.0 in.	2 ft. 2.0 in.
Skid Gear Width	6 ft. 5.4 in.	7 ft 3.0 in.
Horizontal Stabilizer Width	6 ft. 5.2 in.	No Change
Main Rotor Diameter	35 ft. 4.0 in.	No Change
Tail Rotor Diameter	5 ft. 2.0 in.	No Change
Overall (Main Rotor Fore and Aft) to Aft End of Tail Skid	40 ft. 11.8 in.	No Change
Nose of Cabin to Aft End of Tail Skid	32 ft. 2.0 in.	No Change
Nose of Cabin to Center Line of Main Rotor	8 ft. 10.1 in.	No Change
Skid Gear	8 ft. 1.3 in.	10 ft. 4.2 in.
Nose of Cabin to Center Line of Forward Cross Tube	6 ft. 0.0 in.	5 ft. 9.4 in.
Nose of Cabin to Center Line of Aft Cross Tube	10 ft. 9.0 in.	10 ft. 6.3 in.
Pitot Tube	6.8 in.	No Change

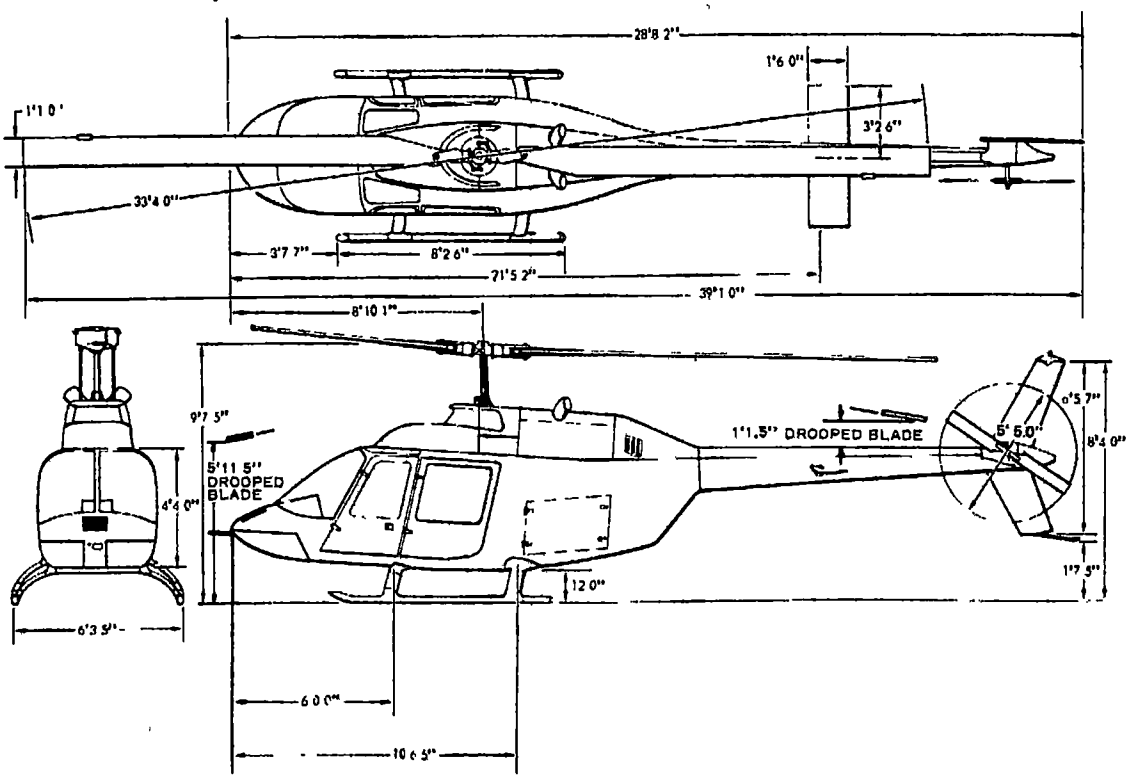


Figure A.4. OH-58A+ Physical Dimensions

Appendix B

TEST AIRCRAFT PITOT STATICS

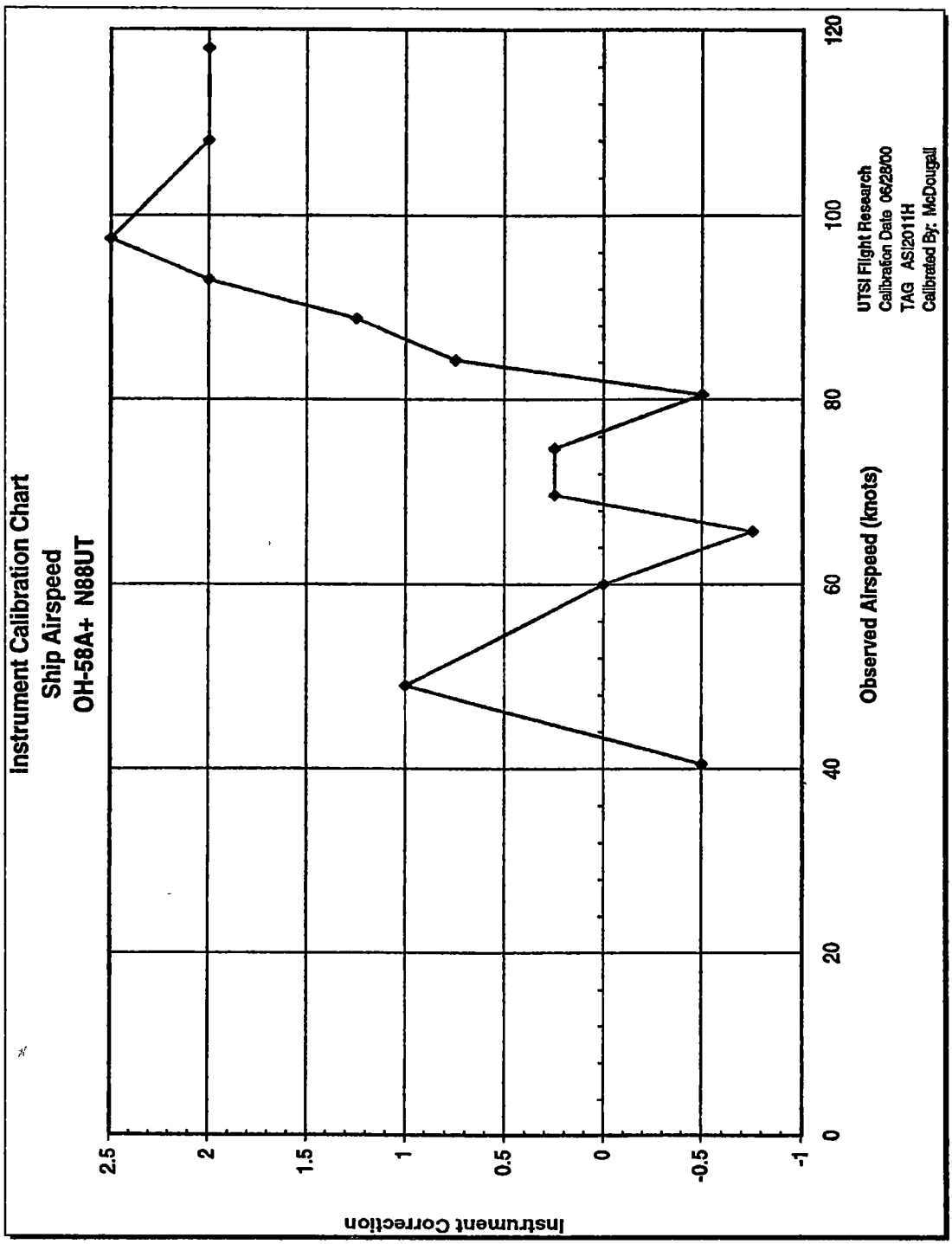


Figure B.1. N88UT Ship Airspeed Indicator Calibration Chart.

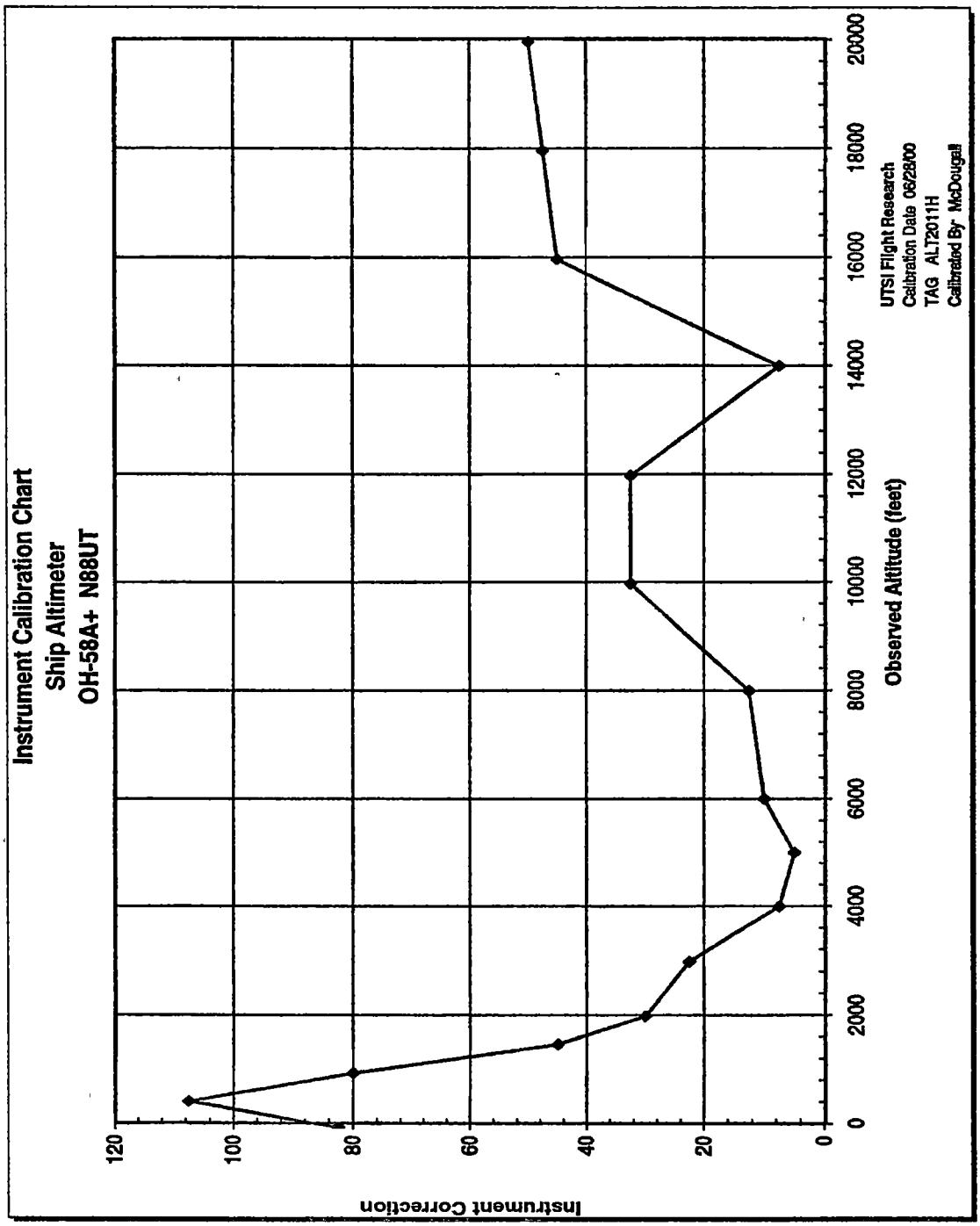


Figure B.2. N88UT Ship Altimeter Calibration Chart.

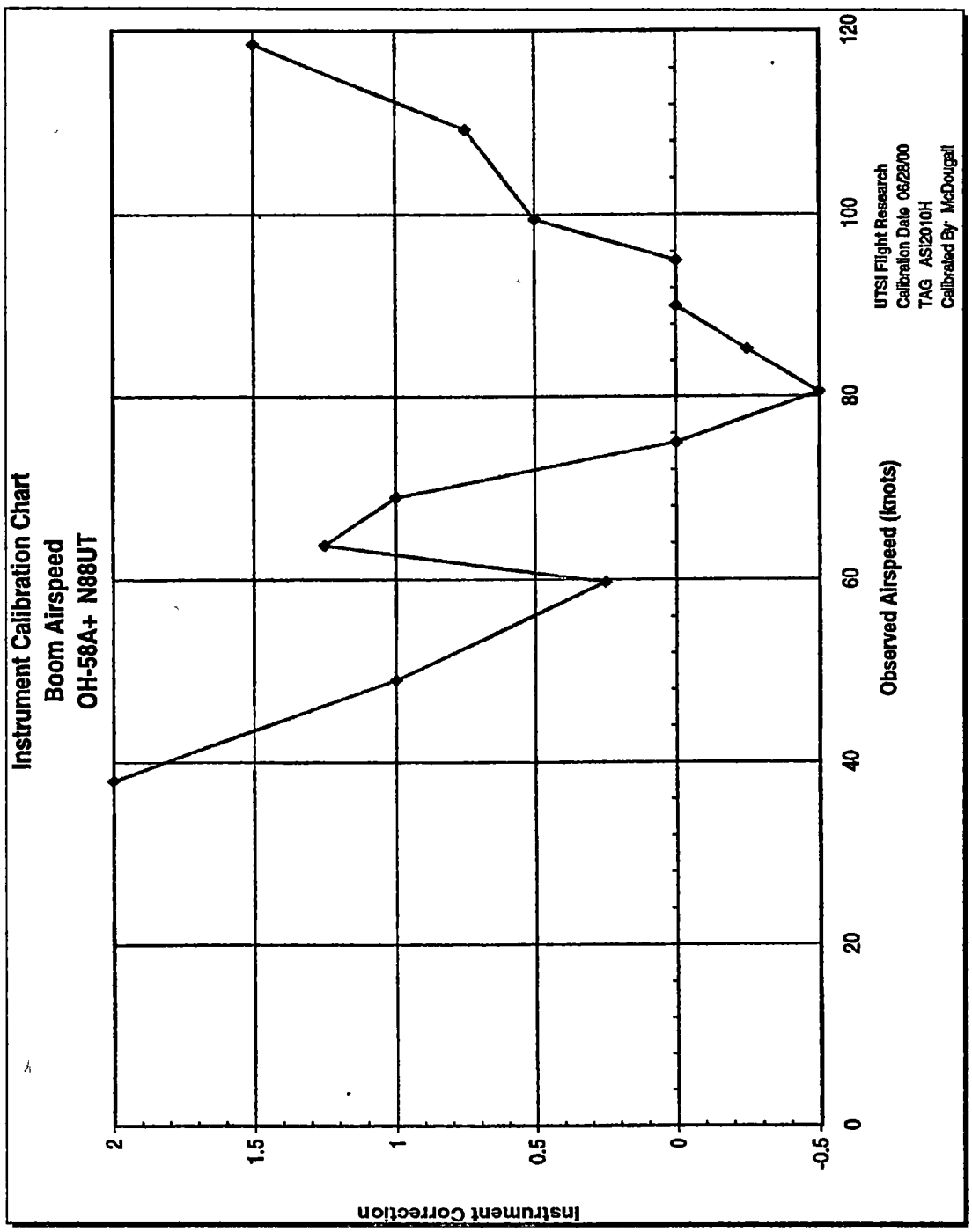


Figure B.3. N88UT Boom Airspeed Indicator Calibration Chart.

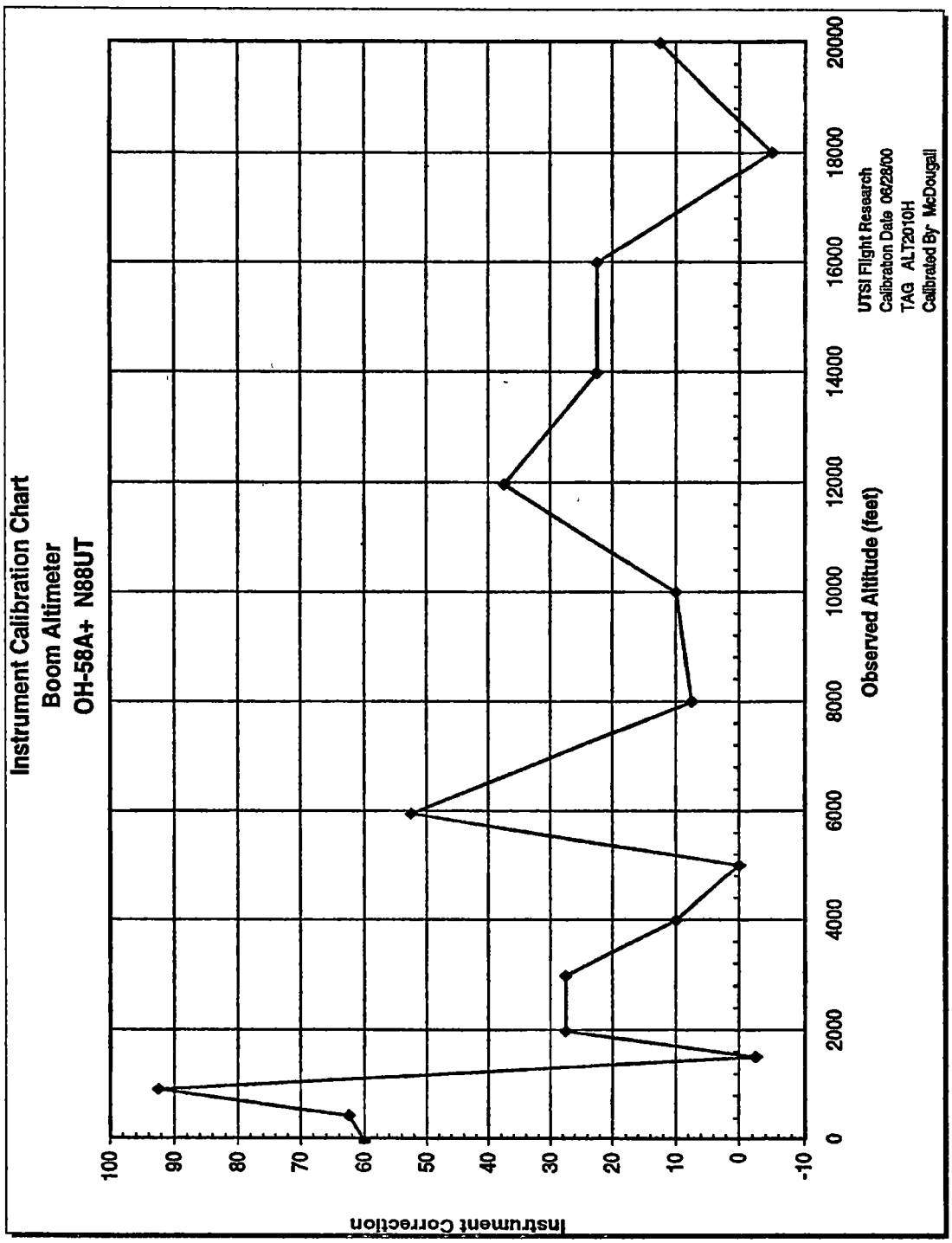


Figure B.4. N88UT Boom Altimeter Calibration Chart.

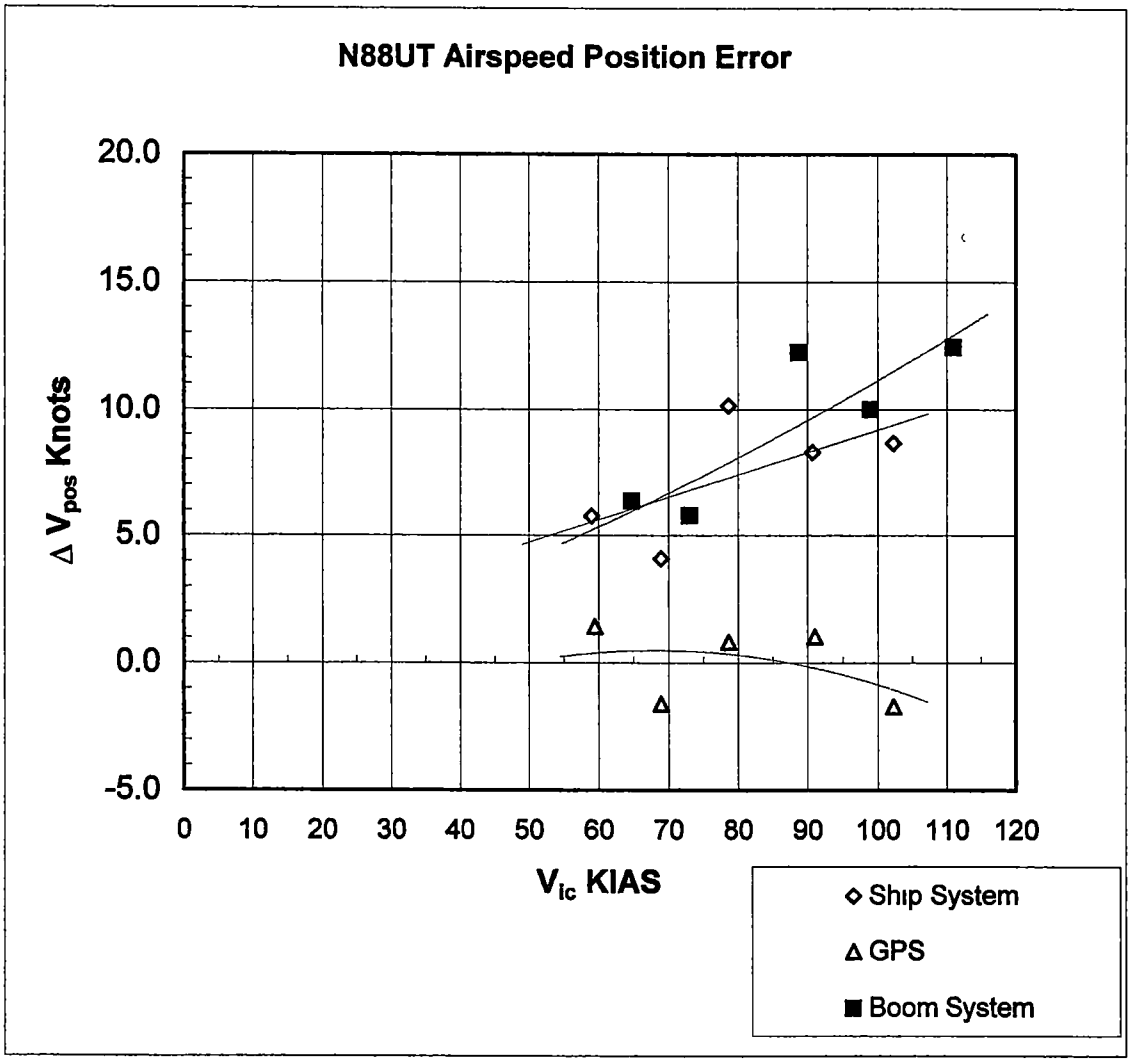


Figure B.5. N88UT Position Error Chart.

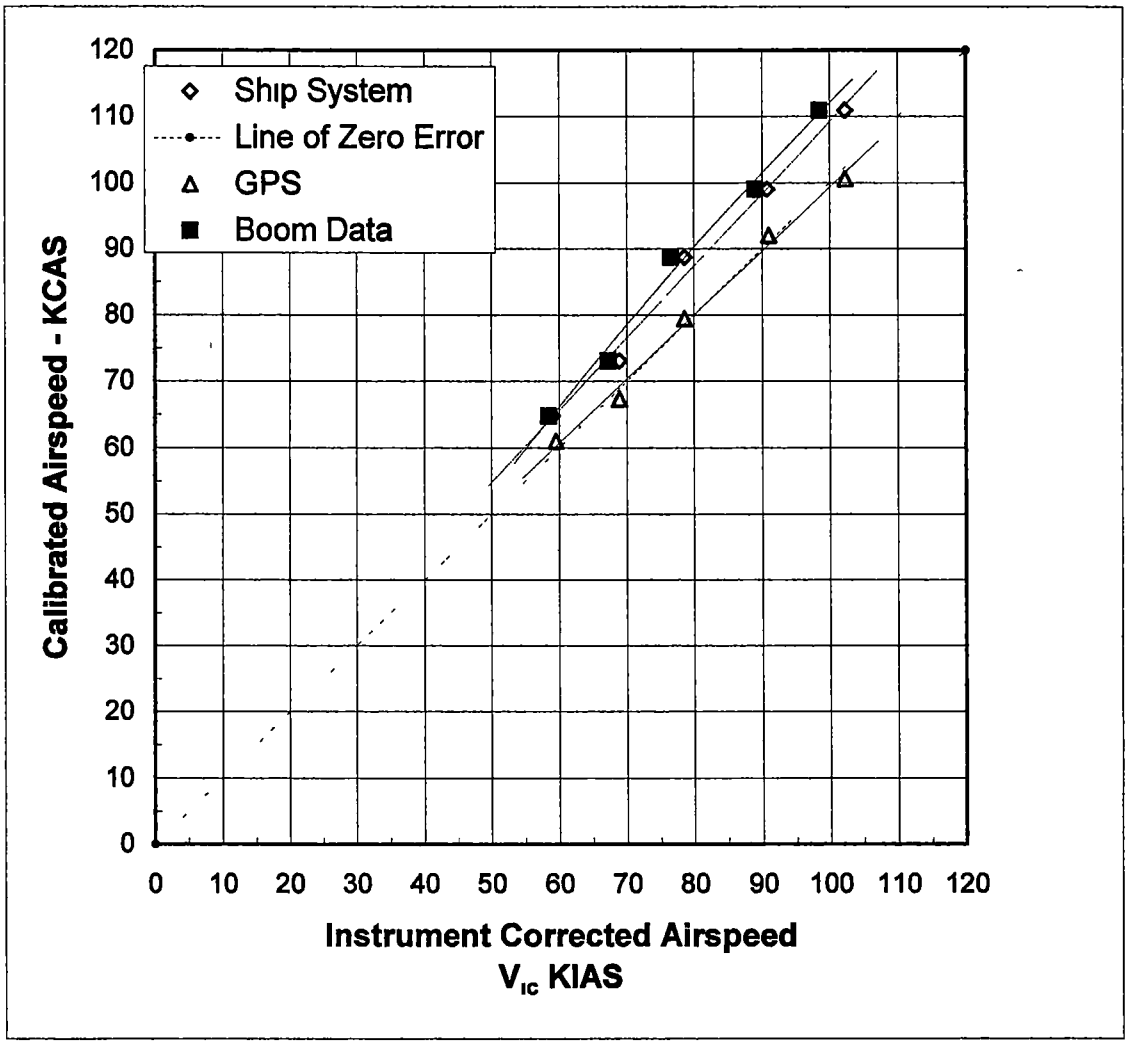


Figure B.6. N88UT Instrument Corrected vs. Calibrated Airspeed Chart.

APPENDIX C

FLIGHT TEST DATA

Aircraft:	OH-58A+	**Date:**	2 – 4 August 2000
Pilot:	Lewis	**FTE's:**	McDougall, Mulnik
Test:	6" Sawtooth Flow Diverters	**C_T:**	.0036

Configuration: High skid gear installed, Pitot static probe installed, All doors removed, W/σ 3600 lbs., Average CG 109.7.

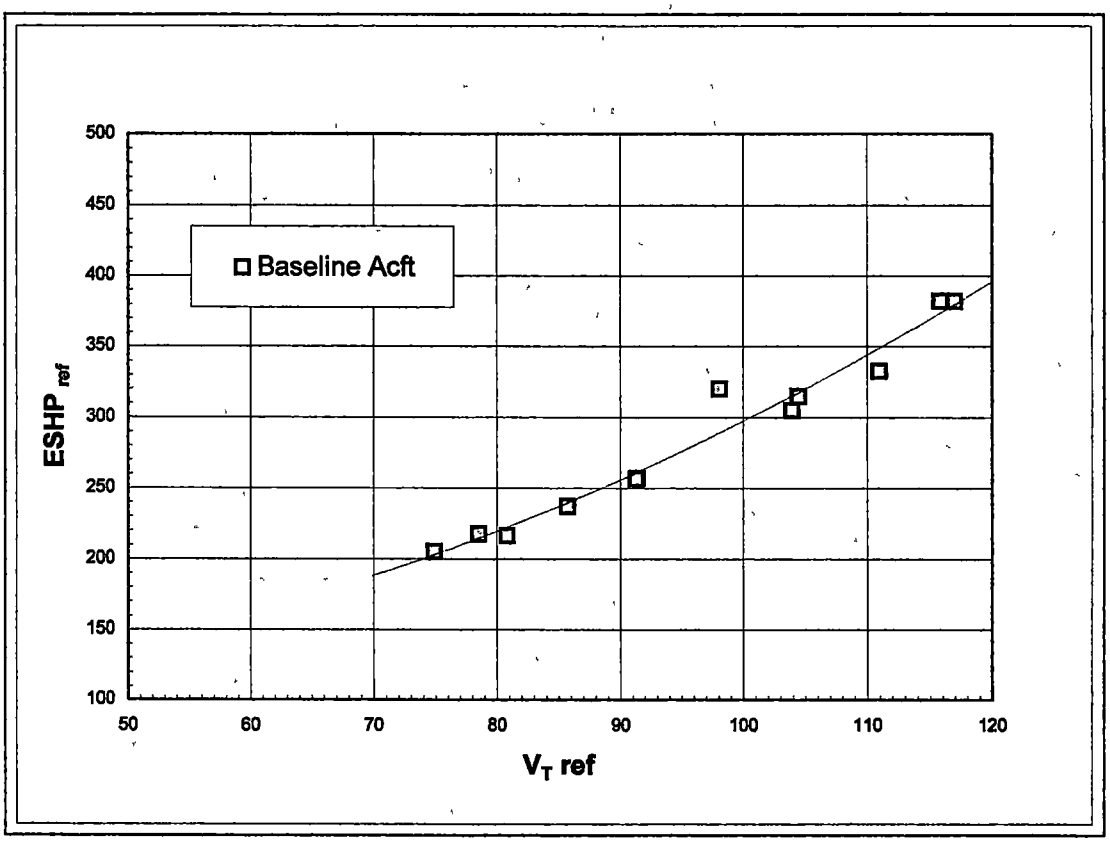


Figure C.1. Referred Level Flight Performance, Baseline Aircraft.

Aircraft:	OH-58A+	**Date:**	2 – 4 August 2000
Pilot:	Lewis	**FTE's:**	McDougall, Mulnik
Test:	6" Sawtooth Flow Diverters	**C_T:**	.0036

Configuration: High skid gear installed, Pitot static probe installed, All doors removed, W/σ 3600 lbs, Average CG 109.7.

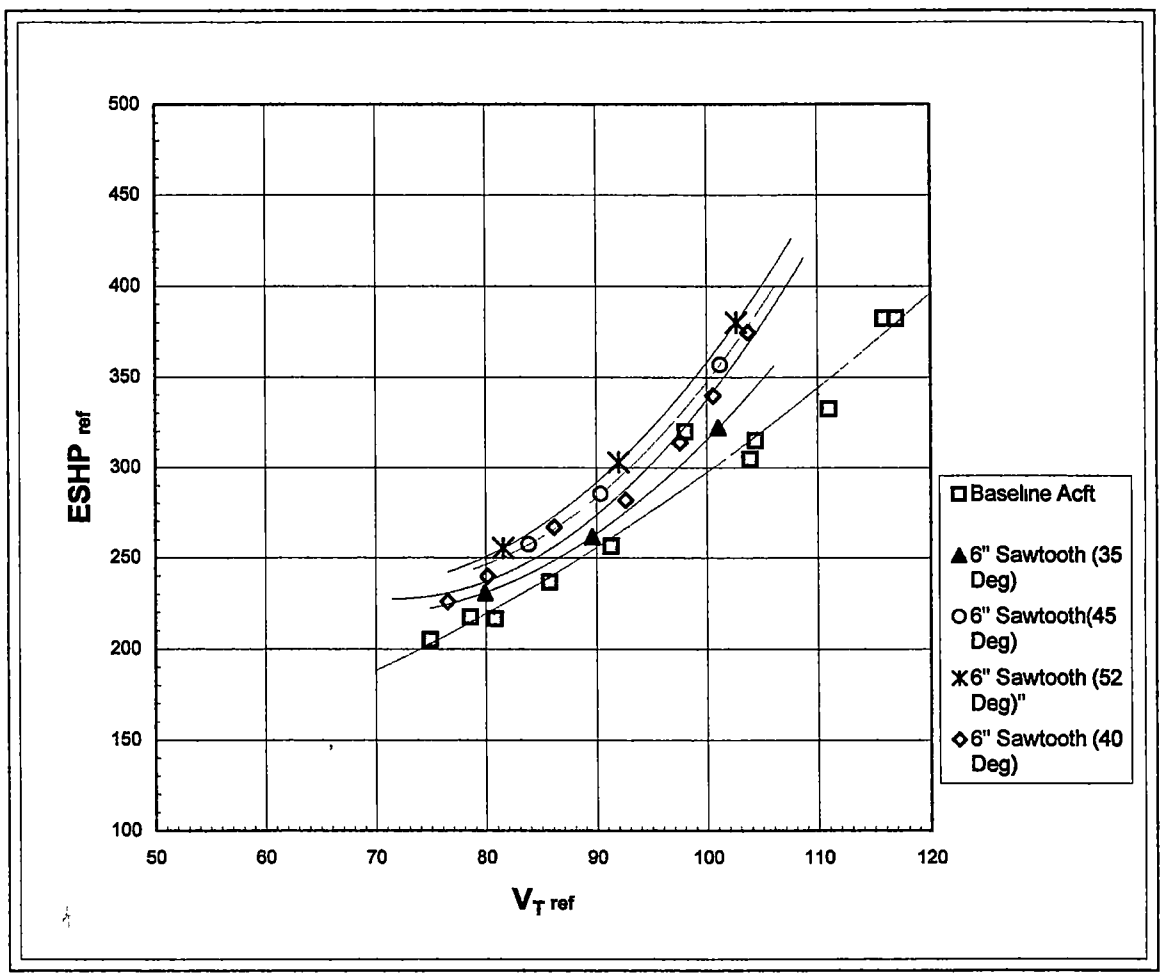


Figure C.2. Referred Level Flight Performance, 6" Sawtooth Flow Diverters, set at 35°, 45°, and 52°.

Aircraft:	OH-58A+	**Date:**	2 – 4 August 2000
Pilot:	Lewis	**FTE's:**	McDougall, Mulnik
Test:	6" Sawtooth Flow Diverters	**C_T:**	.0036

Configuration: High skid gear installed, Pitot static probe installed, All doors removed, W/σ 3600 lbs., Average CG 109 7.

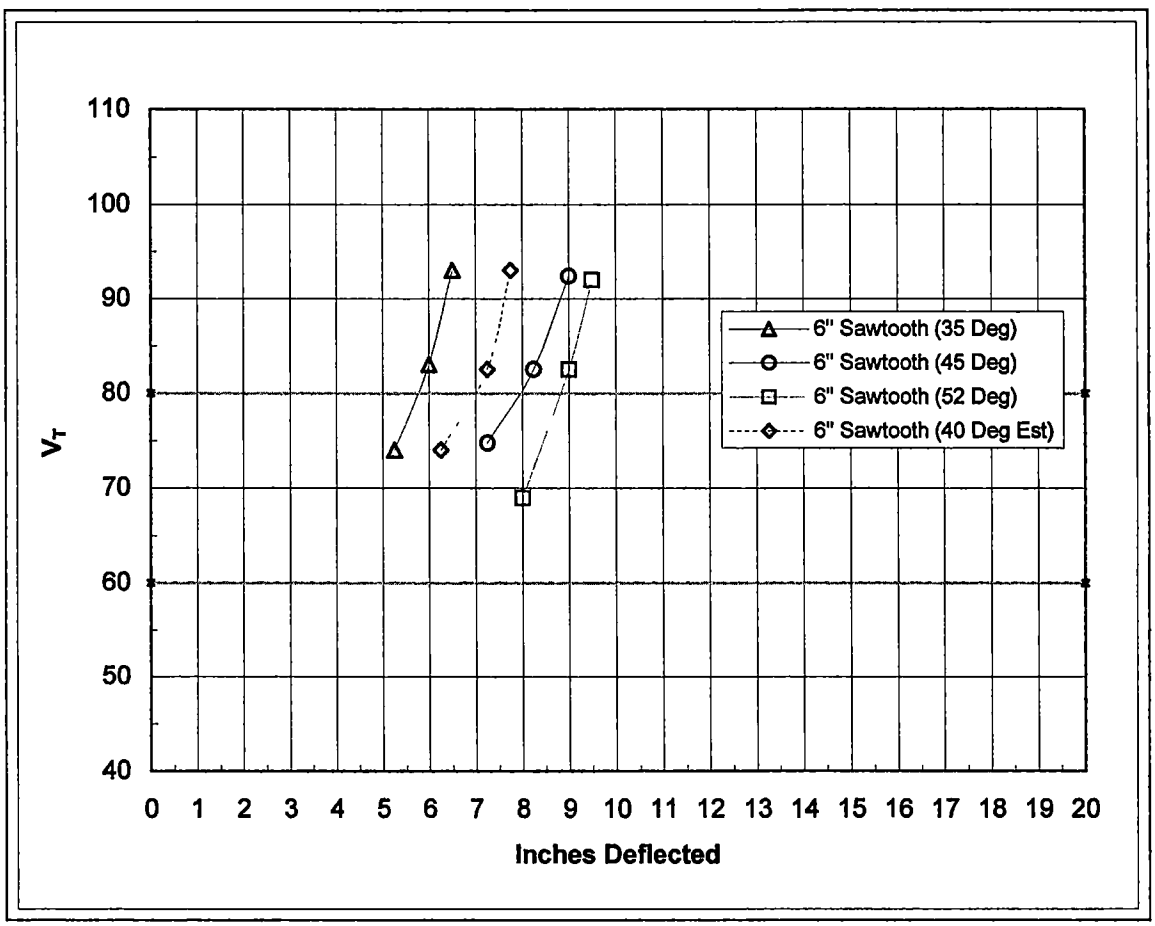


Figure C.3. True Airspeed vs. Inches Deflected, 6" Sawtooth Flow Diverters set at 35°, 45°, and 52°.

Aircraft:	OH-58A+	**Date:**	2 – 4 August 2000
Pilot:	Lewis	**FTE's:**	McDougall, Mulnik
Test:	6" Sawtooth Flow Diverters	**C_T:**	.0036

Configuration: High skid gear installed, Pitot static probe installed, All doors removed, W/σ 3600 lbs., Average CG 109.7.

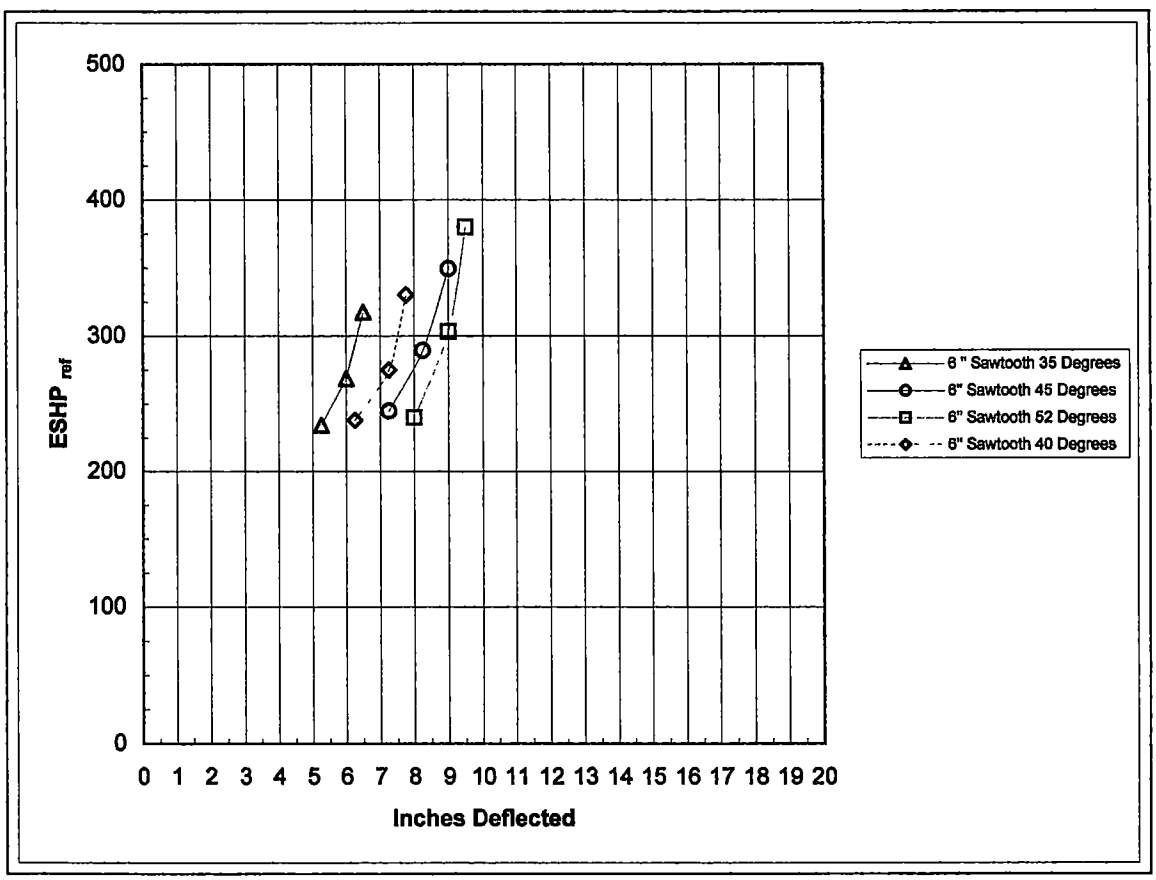


Figure C.4. $ESHP_{ref}$ vs. Inches Deflected, 6" Sawtooth Flow Diverters set at 35°, 45°, and 52°.

Aircraft:	OH-58A+	**Date:**	2 – 4 August 2000
Pilot:	Lewis	**FTE's:**	McDougall, Mulnik
Test:	6" Sawtooth Flow Diverters	**C_T:**	.0036

Configuration: High skid gear installed, Pitot static probe installed, All doors removed, W/σ 3600 lbs., Average CG 109.7.

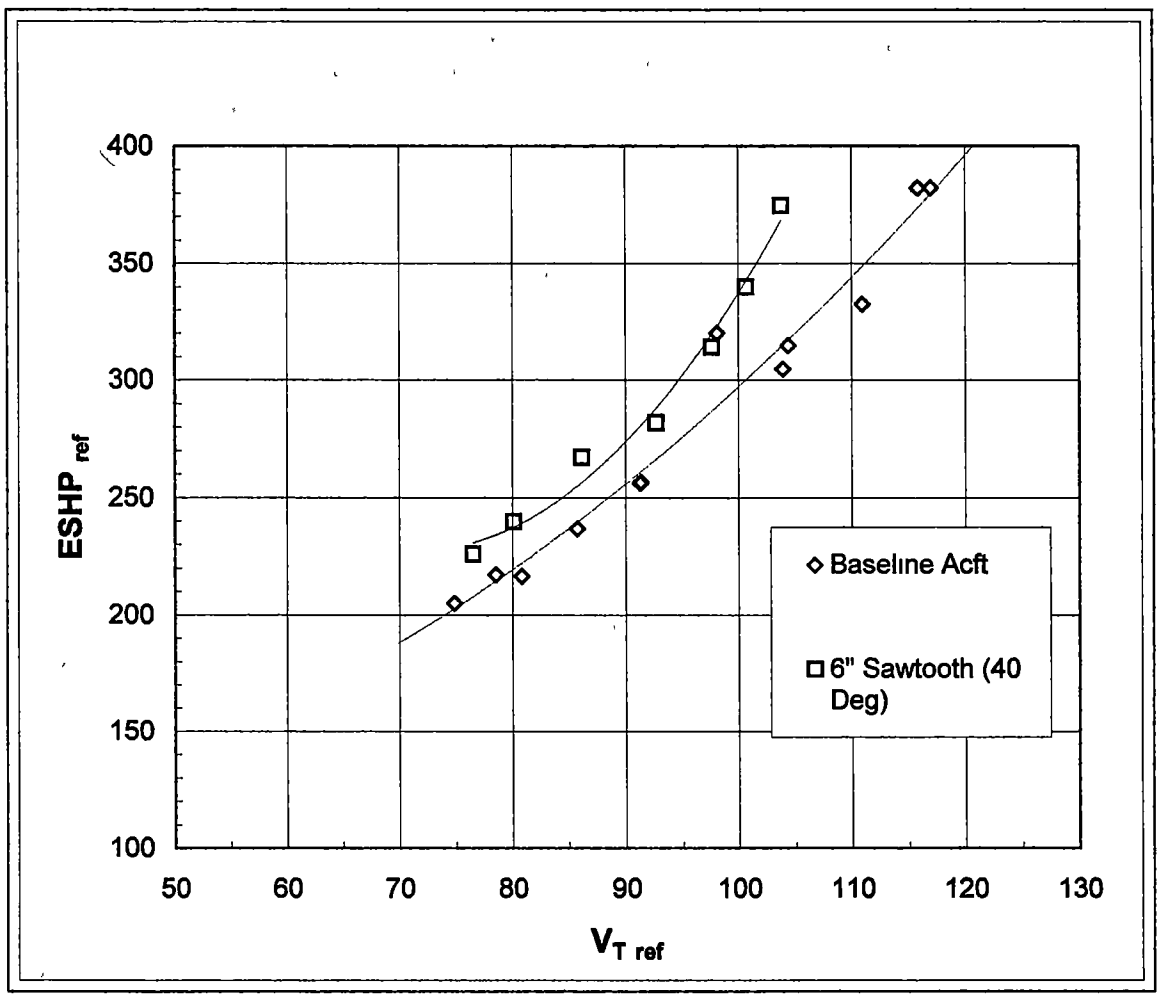


Figure C.5. Referred Level Flight Performance, 6" Sawtooth Flow Diverters set at 40°.

Aircraft:	OH-58A+	**Date:**	2 – 4 August 2000
Pilot:	Lewis	**FTE's:**	McDougall, Mulnik
Test:	6" Sawtooth Flow Diverters	**C_T:**	.0036

Configuration: High skid gear installed, Pitot static probe installed, All doors removed, W/σ 3600 lbs., Average CG 109.7.

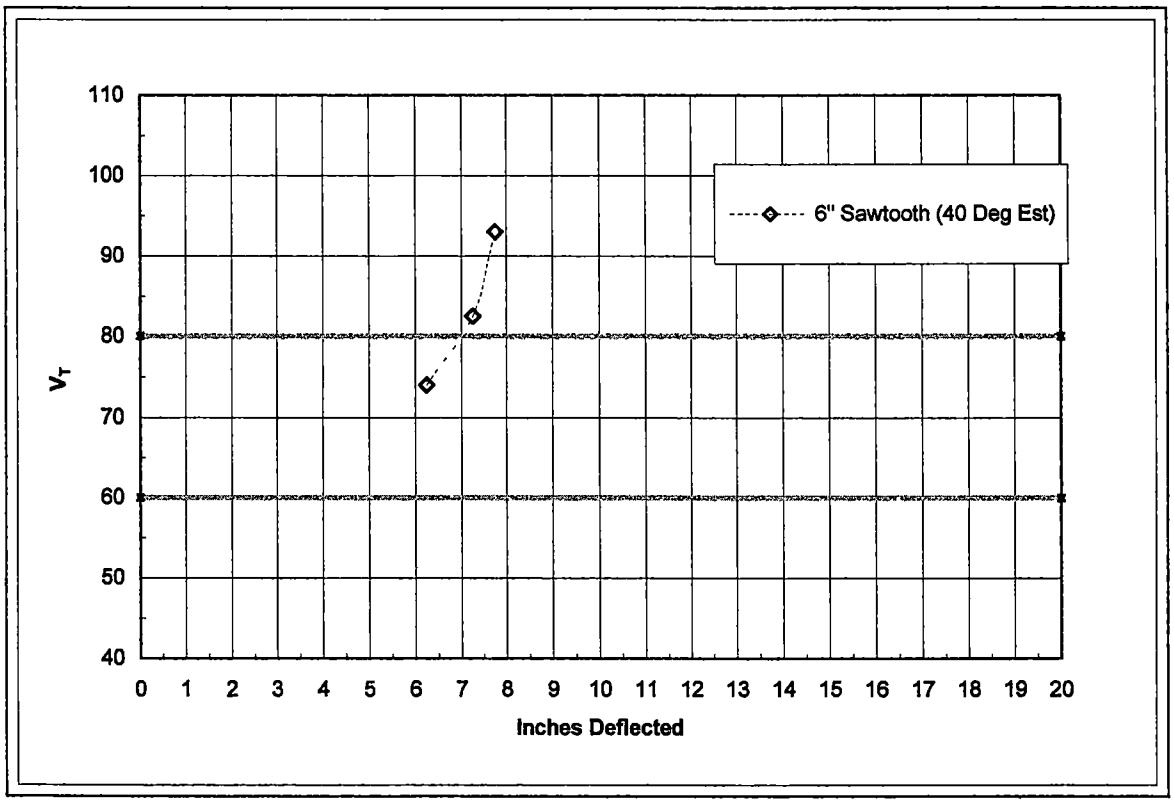


Figure C.6. True Airspeed vs. Inches Deflected, 6" Sawtooth Flow Diverters, set at 40°.

Aircraft:	OH-58A+	**Date:**	2 – 4 August 2000
Pilot:	Lewis	**FTE's:**	McDougall, Mulnik
Test:	6" Sawtooth Flow Diverters	C_T:	.0036

Configuration: High skid gear installed, Pitot static probe installed, All doors removed, W/σ 3600 lbs., Average CG 109.7.

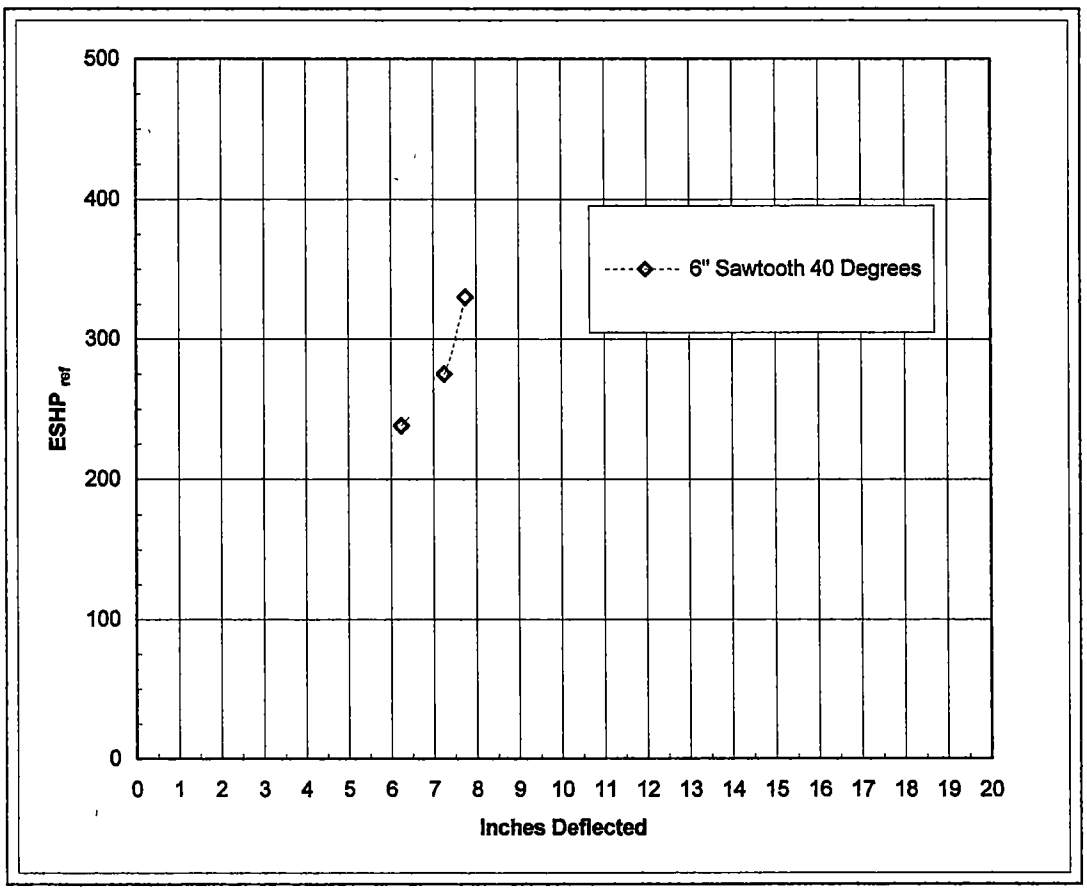


Figure C.7. $ESHP_{ref}$ vs. Inches Deflected, 6" Sawtooth Flow Diverters set at 40°.

Aircraft:	OH-58A+	**Date:**	2 – 4 August 2000
Pilot:	Lewis	**FTE's:**	McDougall, Mulnik
Test:	6" Sawtooth Flow Diverters	**C_T:**	.0036

Configuration: High skid gear installed, Pitot static probe installed, All doors removed, W/σ 3600 lbs., Average CG 109.7.

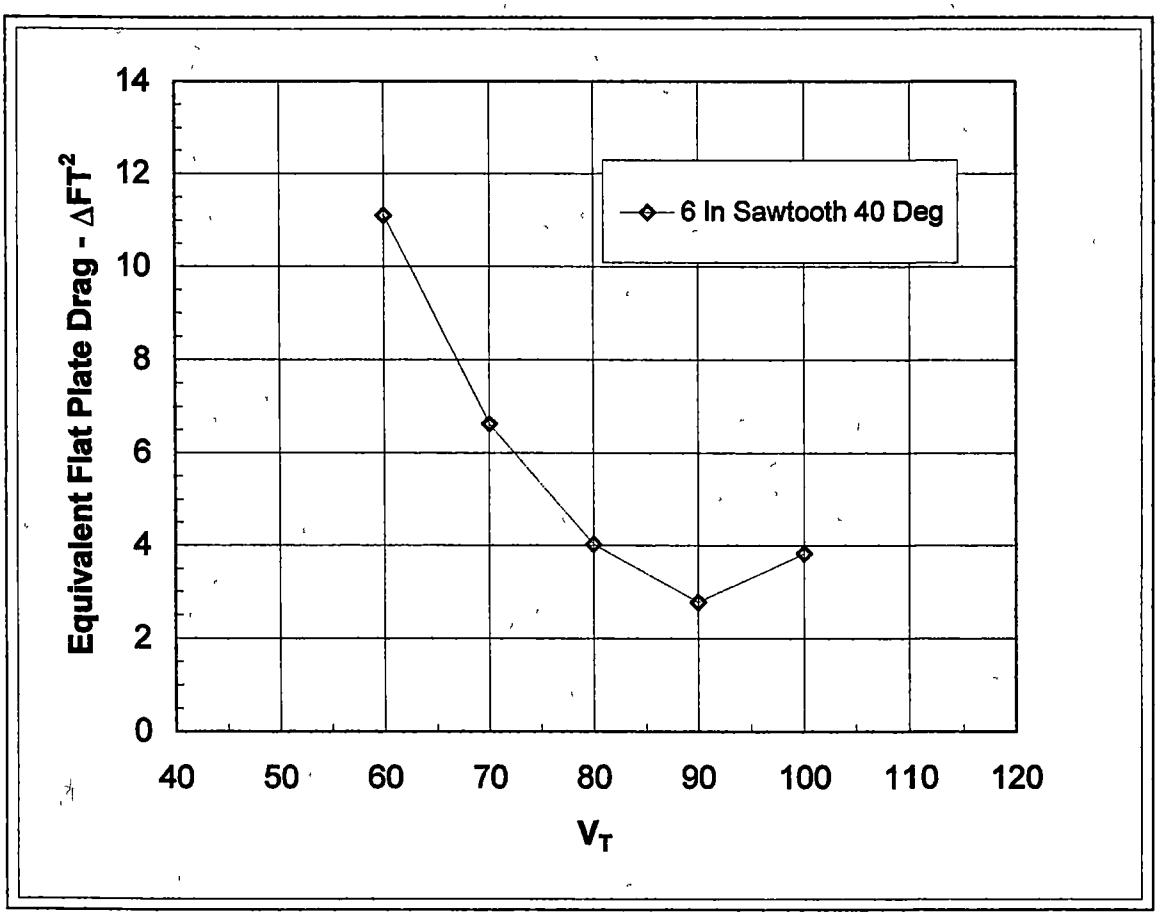


Figure C.8. Change in Equivalent Flat Plate Drag, 6" Sawtooth Flow Diverters, set at 40°.

Aircraft:	OH-58A+	**Date:**	20 – 24 August 2000
Pilot:	Lewis	**FTE's:**	McDougall, Mulnik
Test:	6" Flat Plate (with Vortex Generators) Flow Diverters		
C_T:	0036		

Configuration: High skid gear installed, Pitot static probe installed, All doors removed, W/σ 3600 lbs., Average CG 109.7.

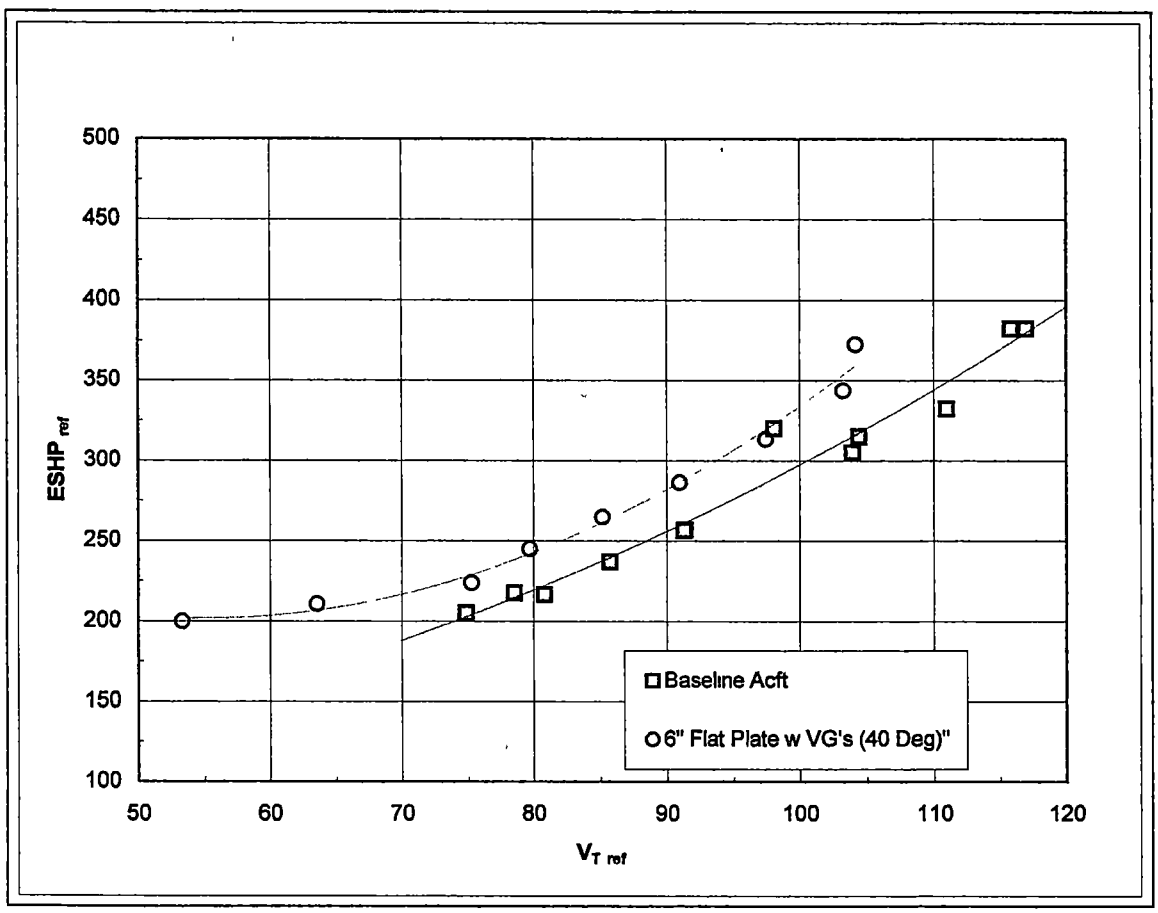


Figure C.9. Referred Level Flight Performance, 6" Flat Plate (with Vortex Generators) Flow Diverters set at 40°.

Aircraft:	OH-58A+	**Date:**	20-24 August 2000
Pilot:	Lewis	**FTE's:**	McDougall, Mulnik
Test:	6" Flat Plate (with Vortex Generators) Flow Diverters		
C_T:	.0036		

Configuration: High skid gear installed, Pitot static probe installed, All doors removed, W/σ 3600 lbs., Average CG 109.7.

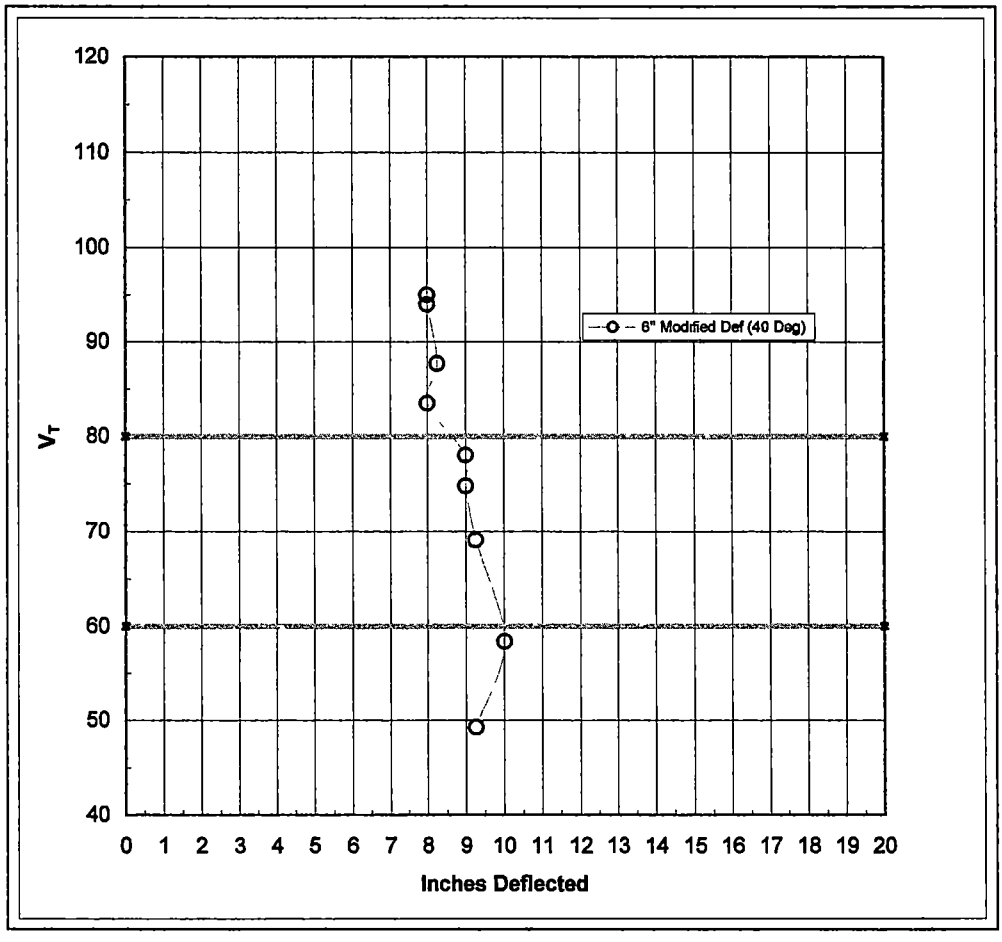


Figure C.10. True Airspeed vs. Inches Deflected, 6" Flat Plate (with Vortex Generators) Flow Diverters set at 40°.

Aircraft:	OH-58A+	**Date:**	20-24 August 2000
Pilot:	Lewis	**FTE's:**	McDougall, Mulnik
Test:	6" Flat Plate (with Vortex Generators) Flow Diverters		
C_T:	.0036		

Configuration: High skid gear installed, Pitot static probe installed, All doors removed, W/σ 3600 lbs., Average CG 109.7.

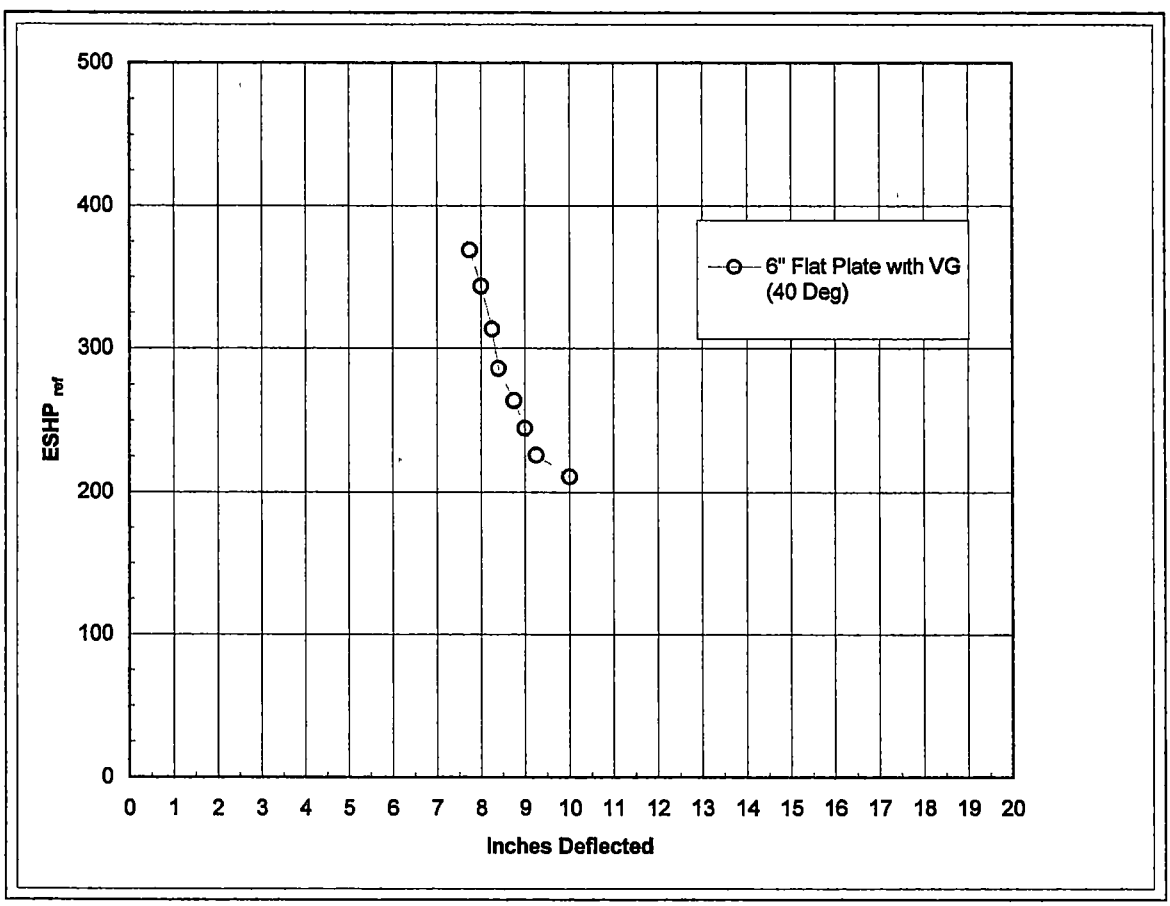


Figure C.11. True Airspeed vs. Inches Deflected, 6" Flat Plate (with Vortex Generators) Flow Diverters set at 40°.

Aircraft:	OH-58A+	**Date:**	20-24 August 2000
Pilot:	Lewis	**FTE's:**	McDougall, Mulnik
Test:	6" Flat Plate (with Vortex Generators) Flow Diverters		
C_T:	.0036		

Configuration: High skid gear installed, Pitot static probe installed, All doors removed, W/σ 3600 lbs., Average CG 109.7.

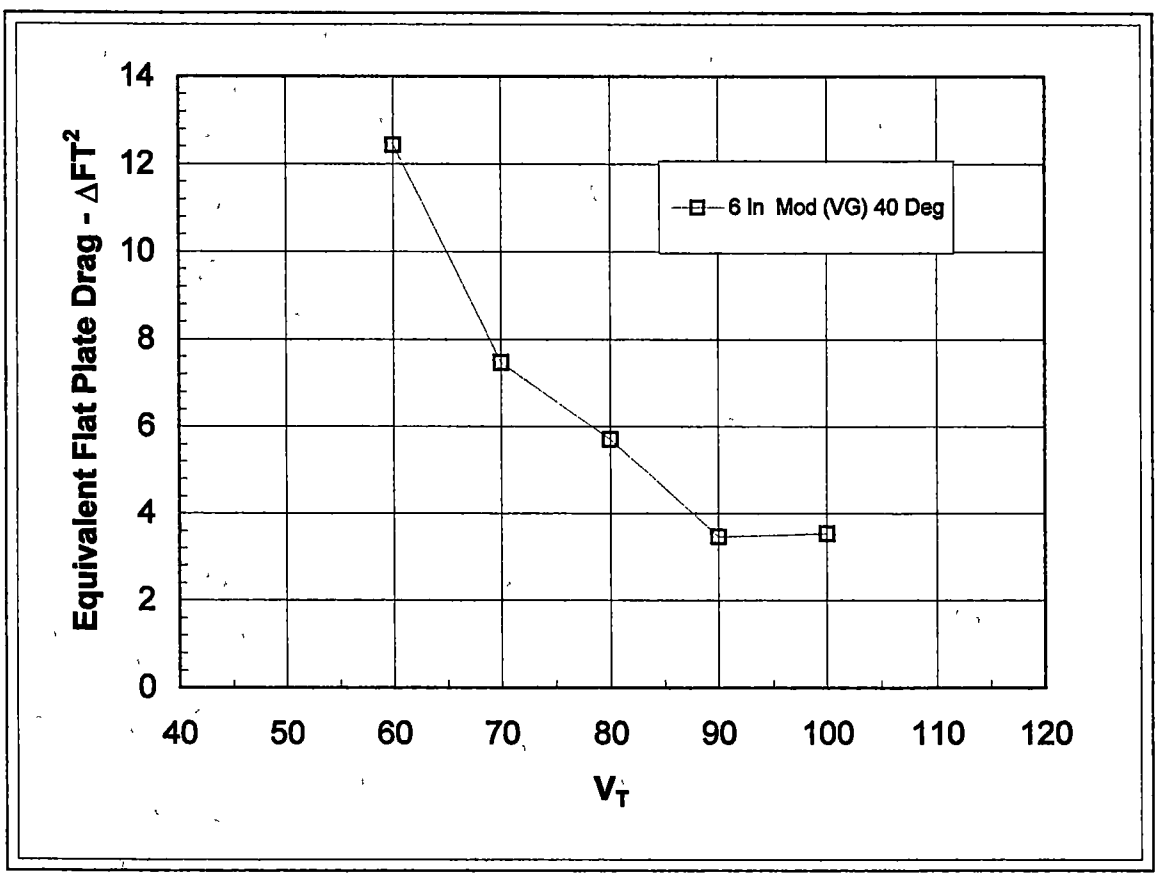


Figure C.12. Change in Equivalent Flat Plate Drag, 6" Flat Plate (with Vortex Generators) Flow Diverters set at 40°.

Aircraft:	OH-58A+	**Date:**	24-29 August 2000
Pilot:	Lewis	**FTE's:**	McDougall, Mulnik
Test:	8" Flat Plate (with Vortex Generators) Flow Diverter		
C_T:	.0036		

Configuration: High skid gear installed, Pitot static probe installed, All doors removed, W/σ 3600 lbs., Average CG 109.7

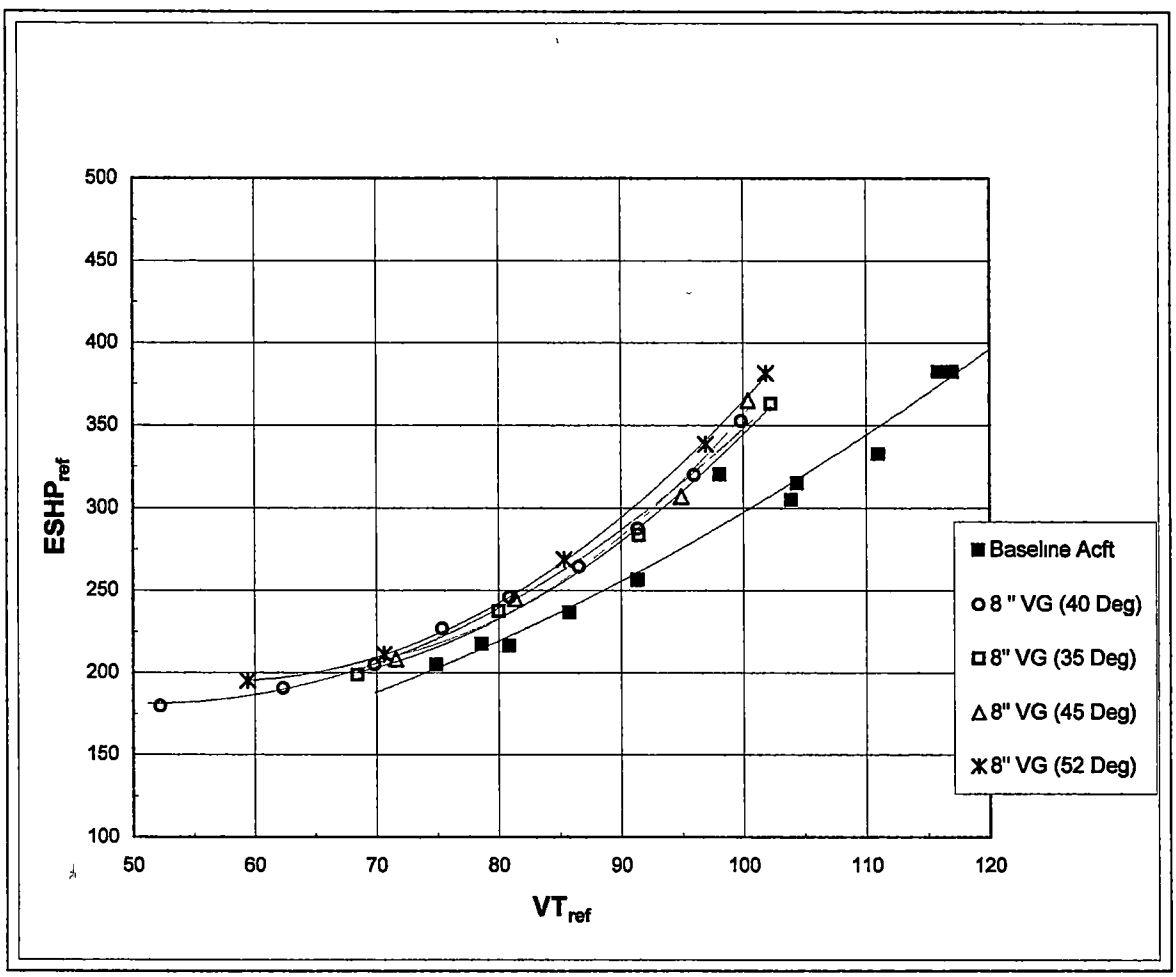


Figure C.13. Referred Level Flight Performance, 8" Flat Plate (with Vortex Generators) Flow Diverters, set at 35°, 40°, 45°, and 52°.

Aircraft:	OH-58A+	**Date:**	24-29 August 2000
Pilot:	Lewis	**FTE's:**	McDougall, Mulnik
Test:	8" Flat Plate (with Vortex Generators) Flow Diverter		
C_T:	.0036		

Configuration: High skid gear installed, Pitot static probe installed, All doors removed, W/σ 3600 lbs., Average CG 109 7.

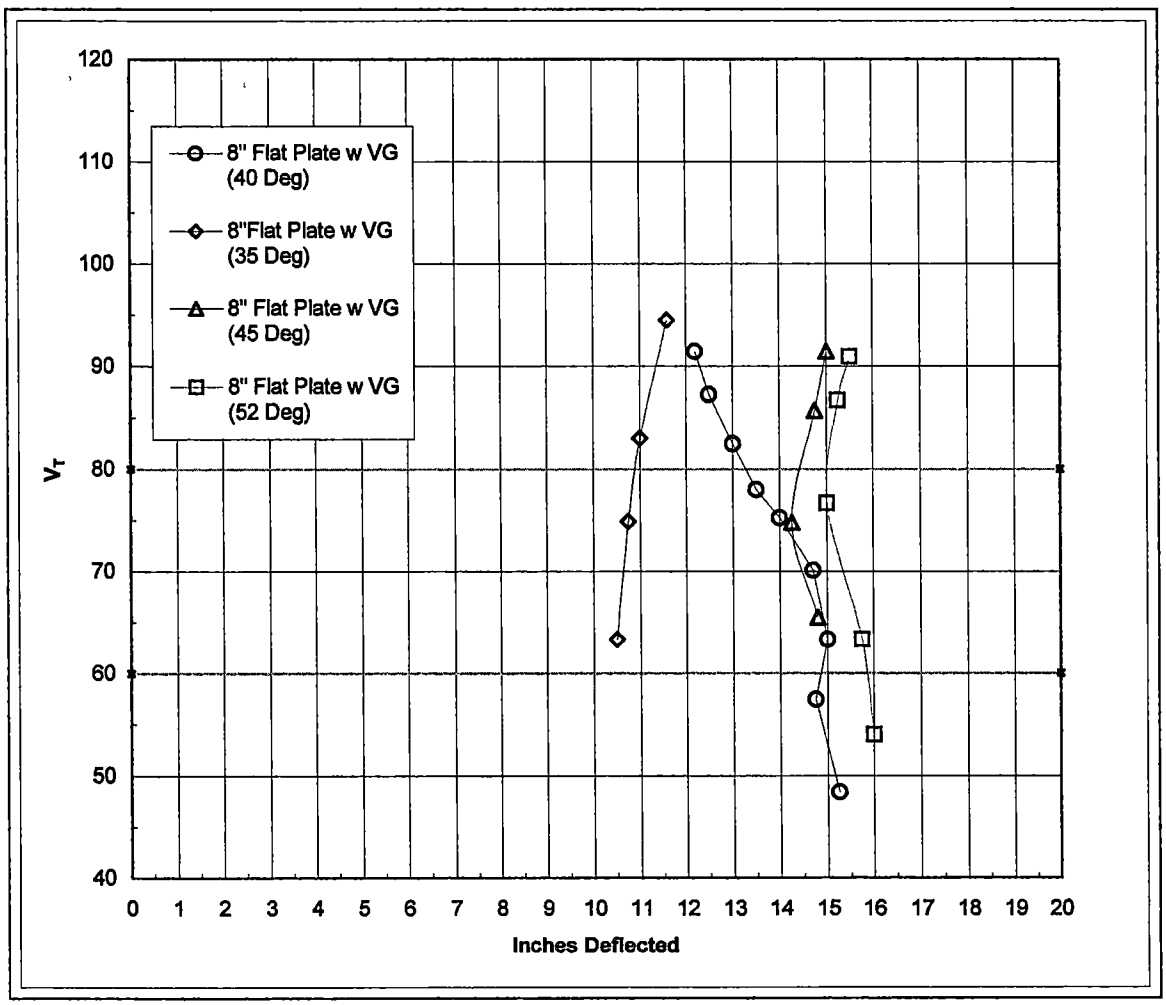


Figure C.14. True Velocity vs. Inches Deflected, 8" Flat Plate (with Vortex Generators) Flow Diverters, set at 35°, 40°, 45°, and 52°.

Aircraft:	OH-58A+	**Date:**	24-29 August 2000
Pilot:	Lewis	**FTE's:**	McDougall, Mulnik
Test:	8" Flat Plate (with Vortex Generators) Flow Diverter		
C_T:	0036		

Configuration: High skid gear installed, Pitot static probe installed, All doors removed, W/σ 3600 lbs., Average CG 109.7.

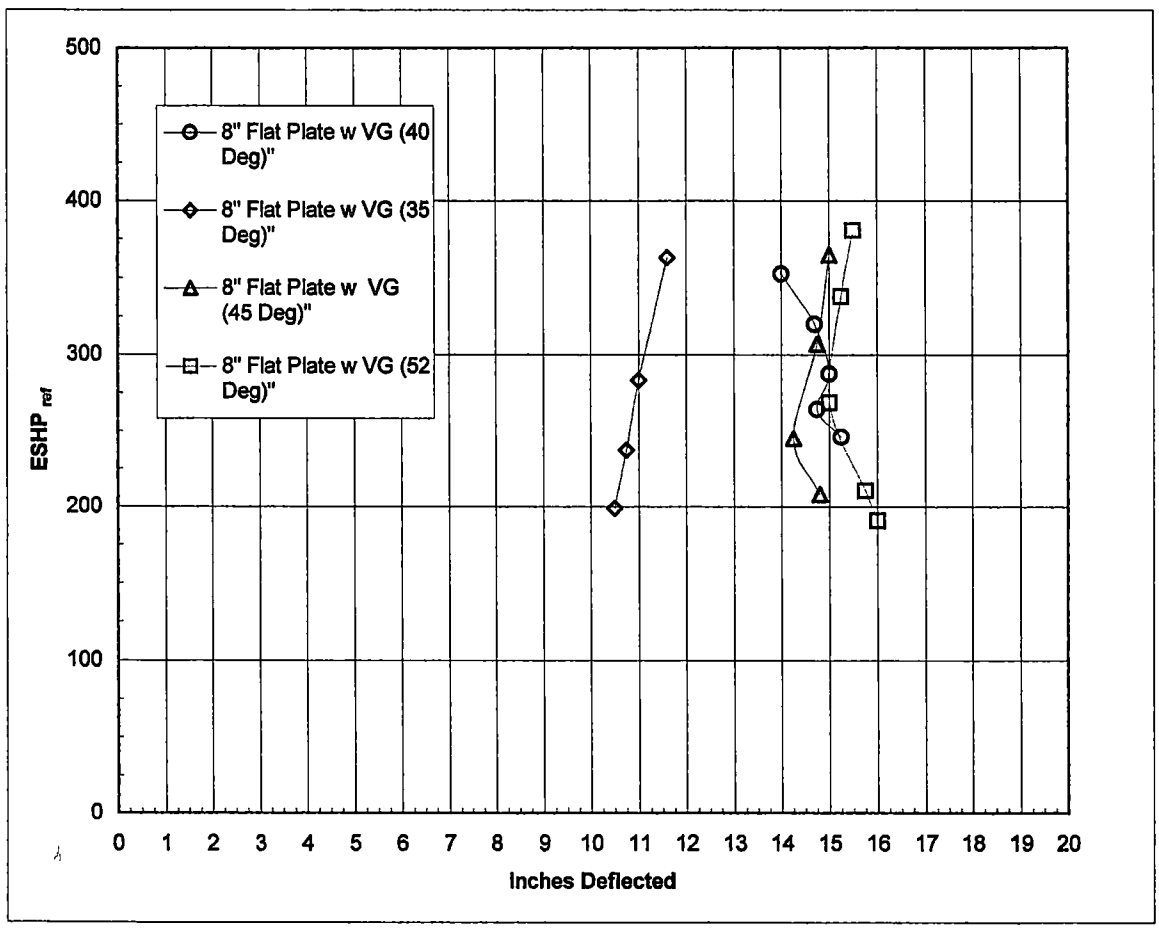


Figure C.15. ESHP referred vs. Inches Deflected, 8" Flat Plate (with Vortex Generators) Flow Diverters, set at 35°, 40°, 45°, and 52°.

Aircraft:	OH-58A+	**Date:**	24-29 August 2000
Pilot:	Lewis	**FTE's:**	McDougall, Mulnik
Test:	8" Flat Plate (with Vortex Generators) Flow Diverter		
C_T:	.0036		

Configuration: High skid gear installed, Pitot static probe installed, All doors removed, W/σ 3600 lbs., Average CG 109.7.

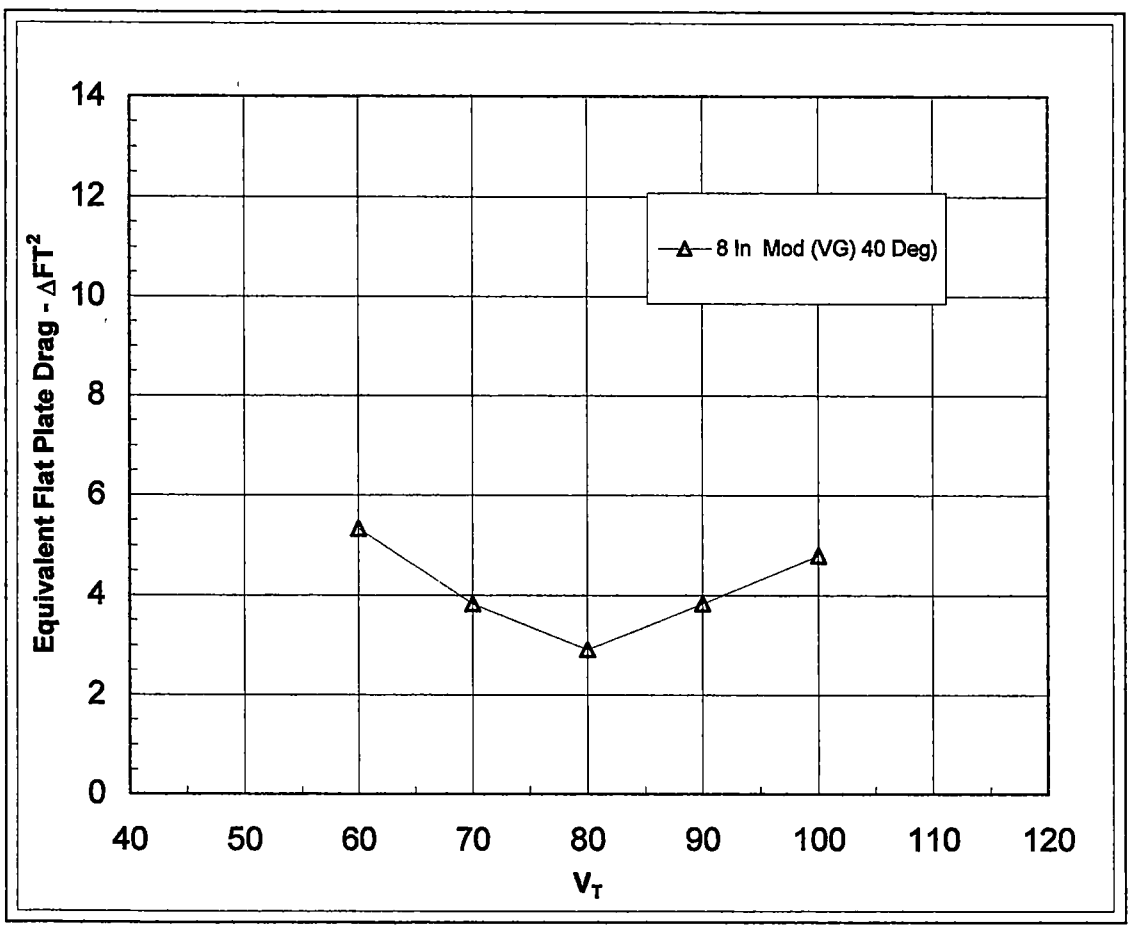


Figure C.16. Change in Equivalent Flat Plate Drag, 8" Flat Plate (with Vortex Generators) Flow Diverters, set at 40 Degrees.

Aircraft:	OH-58A+	**Date:**	24-29 August 2000
Pilot:	Lewis	**FTE's:**	McDougall, Mulnik
Test:	8" Flat Plate (with Vortex Generators) Flow Diverter		
C_T:	0036		

Configuration: High skid gear installed, Pitot static probe installed, All doors removed, W/σ 3600 lbs., Average CG 109.7.

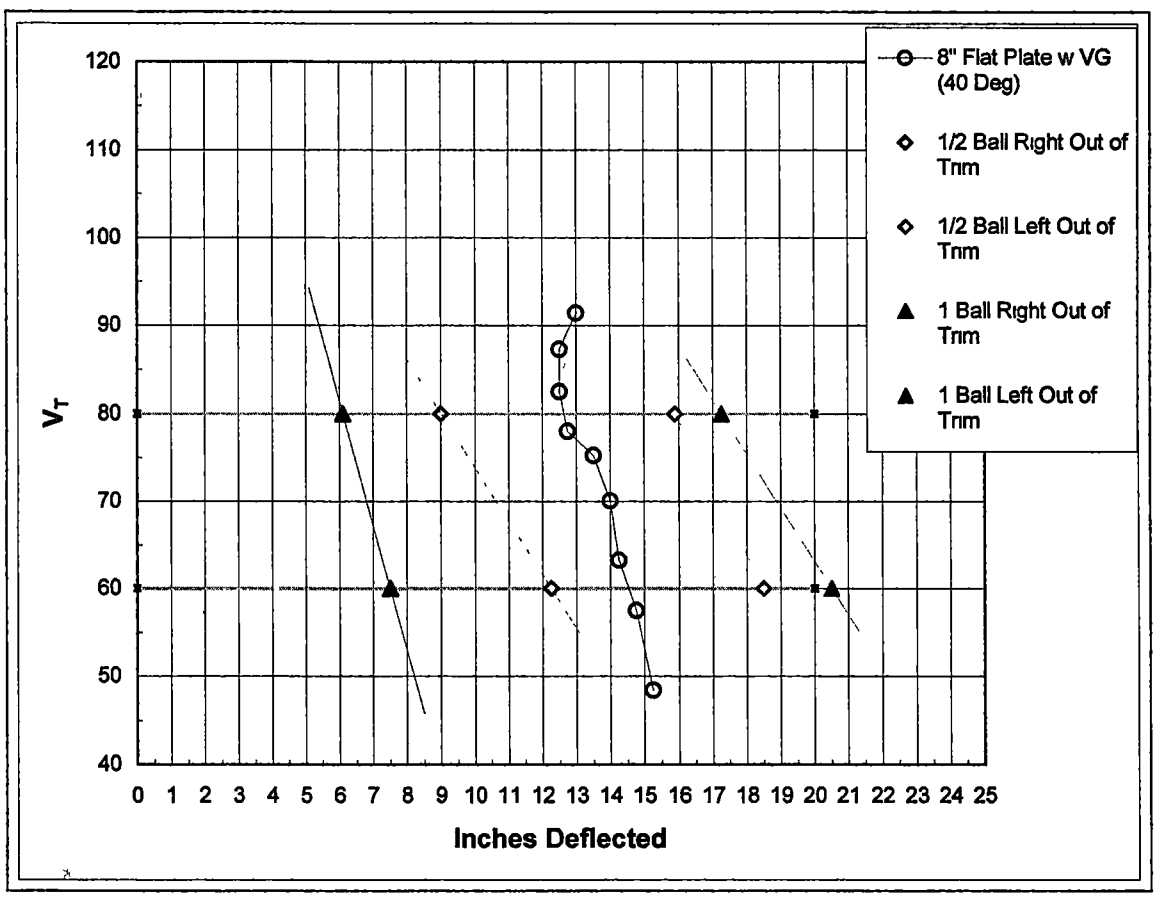


Figure C.17. Airspeed vs. Inches Deflected in Out of Trim Conditions with 8" Flat Plate Flow Diverters set at 40°.

Comparative Data Analysis

Aircraft:	OH-58A+	**Date:**	2-29 August 2000
Pilot:	Lewis	**FTE's:**	McDougall, Mulnik
Test:	LDO Baseline Aircraft and with Flow Diverter.		
C_T:	.0036		

Configuration: High skid gear installed, Pitot static probe installed, All doors removed, W_{ref} 3600 lbs., Average CG 109.7.

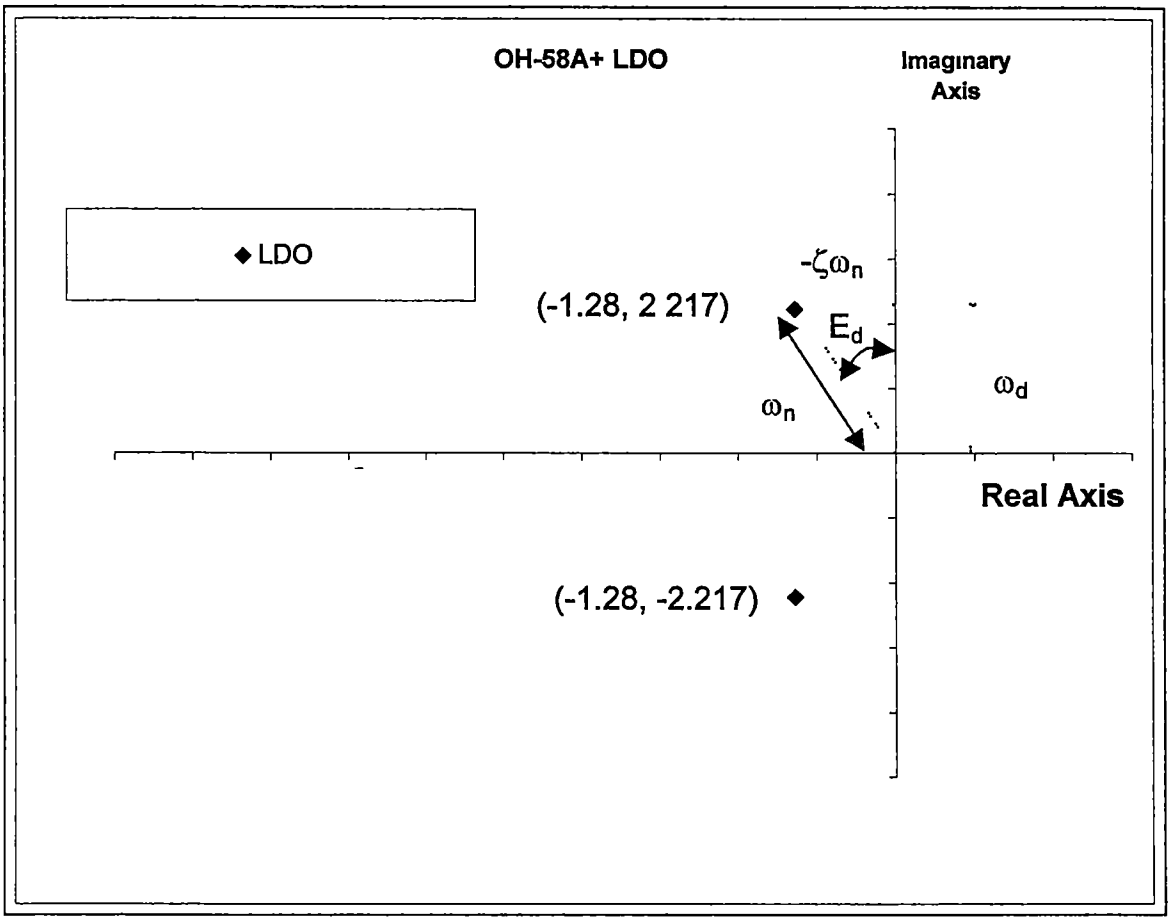


Figure C. 18. OH-58A+ Lateral Directional Oscillation Root Locus Plot.

Aircraft:	OH-58A+	**Date:**	24-29 August 2000
Pilot:	Lewis	**FTE's:**	McDougall, Mulnik
Test:	8" Flat Plate (with Vortex Generators) Flow Diverter		
C_T:	.0036		

Configuration: High skid gear installed, Pitot static probe installed, All doors removed, W/σ 3600 lbs., Average CG 109.7.

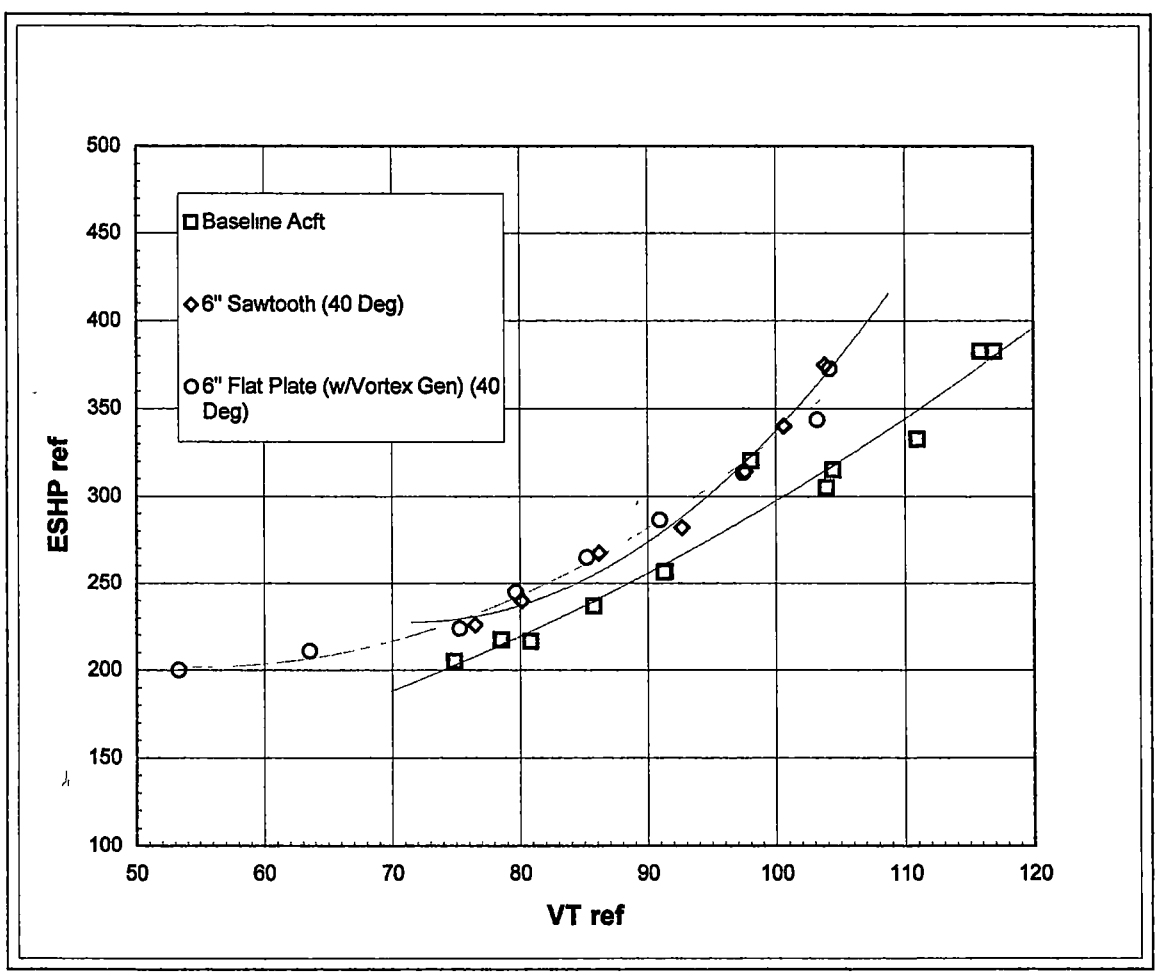


Figure C.19. 6" Sawtooth (40 Deg) and 6" Flat Plate (40 Deg) Referred Level Flight Performance.

Aircraft:	OH-58A+	**Date:**	24-29 August 2000
Pilot:	Lewis	**FTE's:**	McDougall, Mulnik
Test:	8" Flat Plate (with Vortex Generators) Flow Diverter		
C_T:	.0036		

Configuration: High skid gear installed, Pitot static probe installed, All doors removed, W/σ 3600 lbs., Average CG 109.7.

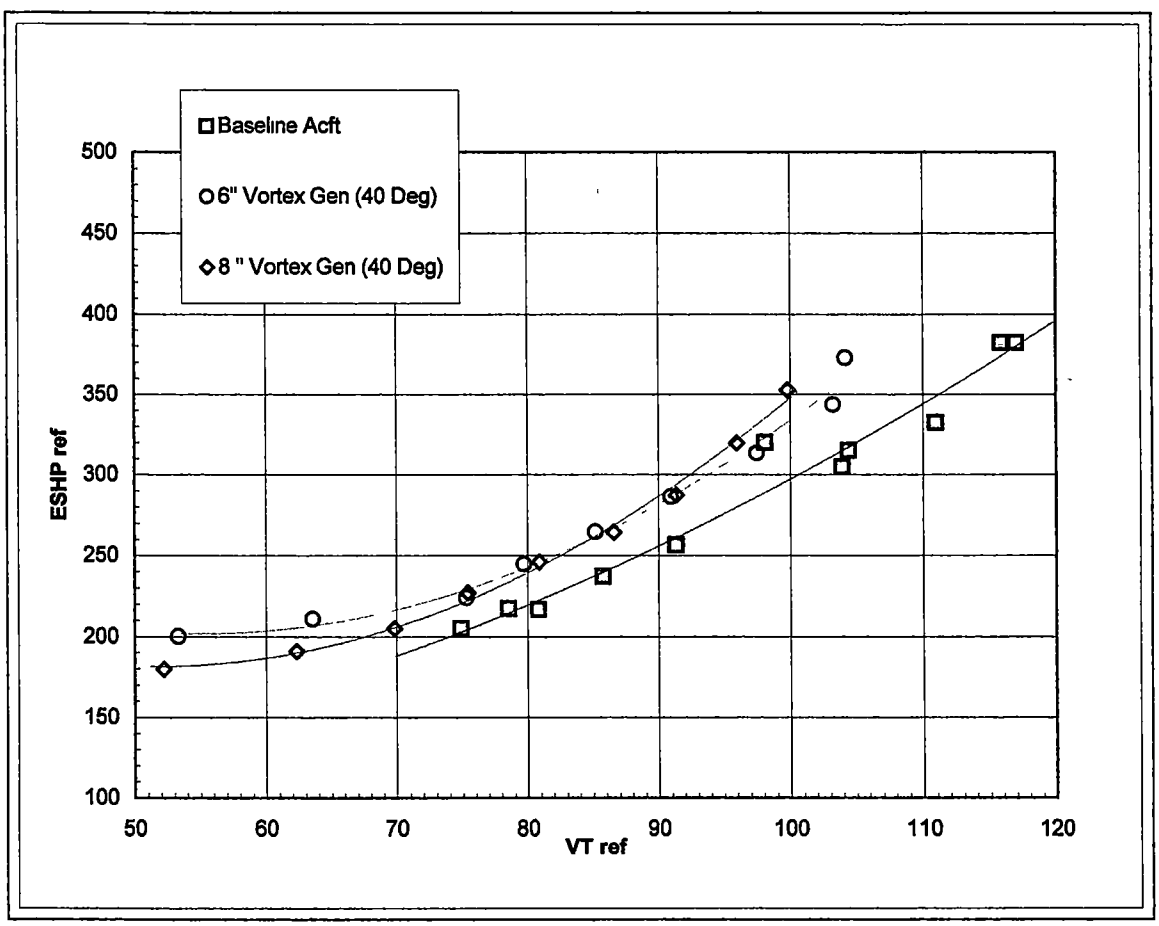


Figure C.20. 6" Flat Plate and 8" Flat Plate Referred Level Flight Performance.

Aircraft:	OH-58A+	**Date:**	24-29 August 2000
Pilot:	Lewis	**FTE's:**	McDougall, Mulnik
Test:	8" Flat Plate (with Vortex Generators) Flow Diverter		
C_T:	.0036		

Configuration: High skid gear installed, Pitot static probe installed, All doors removed, W/σ 3600 lbs., Average CG 109.7.

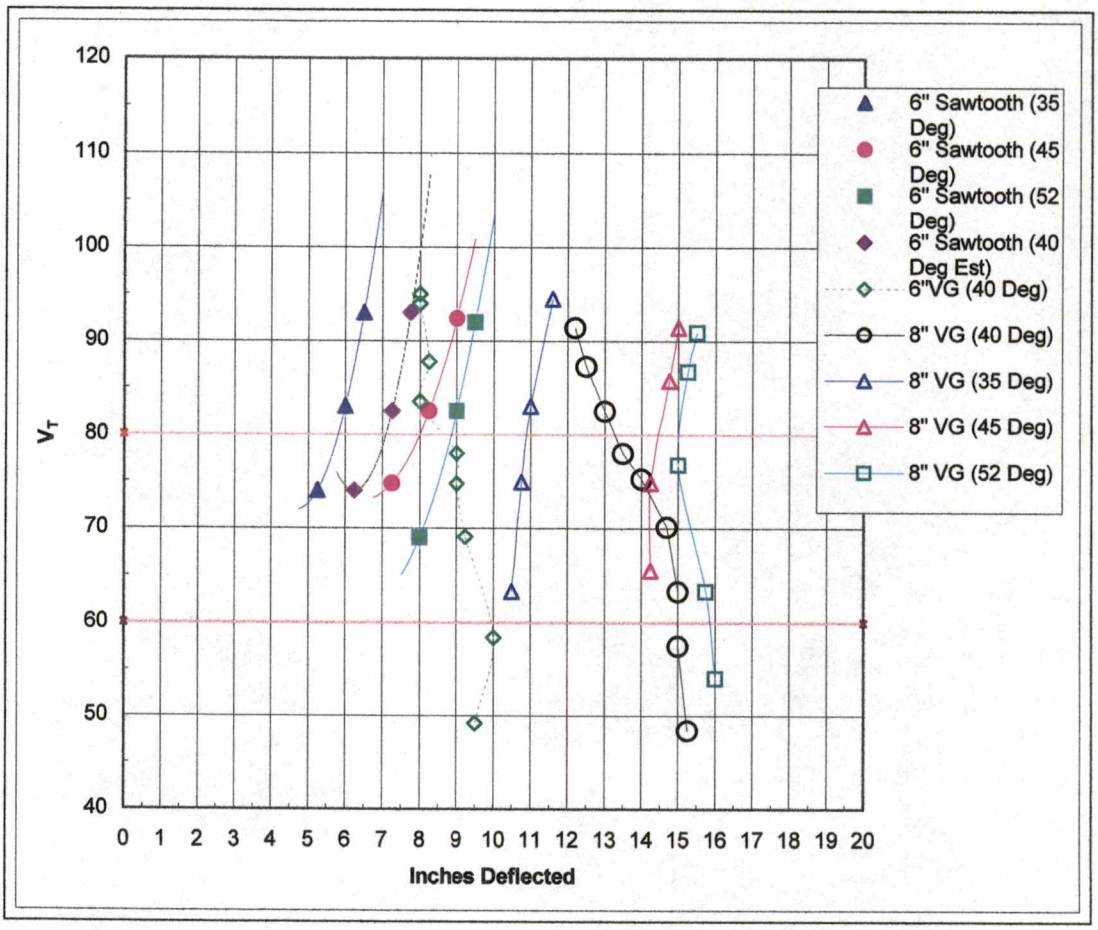


Figure C.21. All Diverters True Airspeed vs. Inches Deflected.

Aircraft:	OH-58A+	**Date:**	24-29 August 2000
Pilot:	Lewis	**FTE's:**	McDougall, Mulnik
Test:	8" Flat Plate (with Vortex Generators) Flow Diverter		
C_T:	.0036		

Configuration: High skid gear installed, Pitot static probe installed, All doors removed, W/σ 3600 lbs., Average CG 109.7.

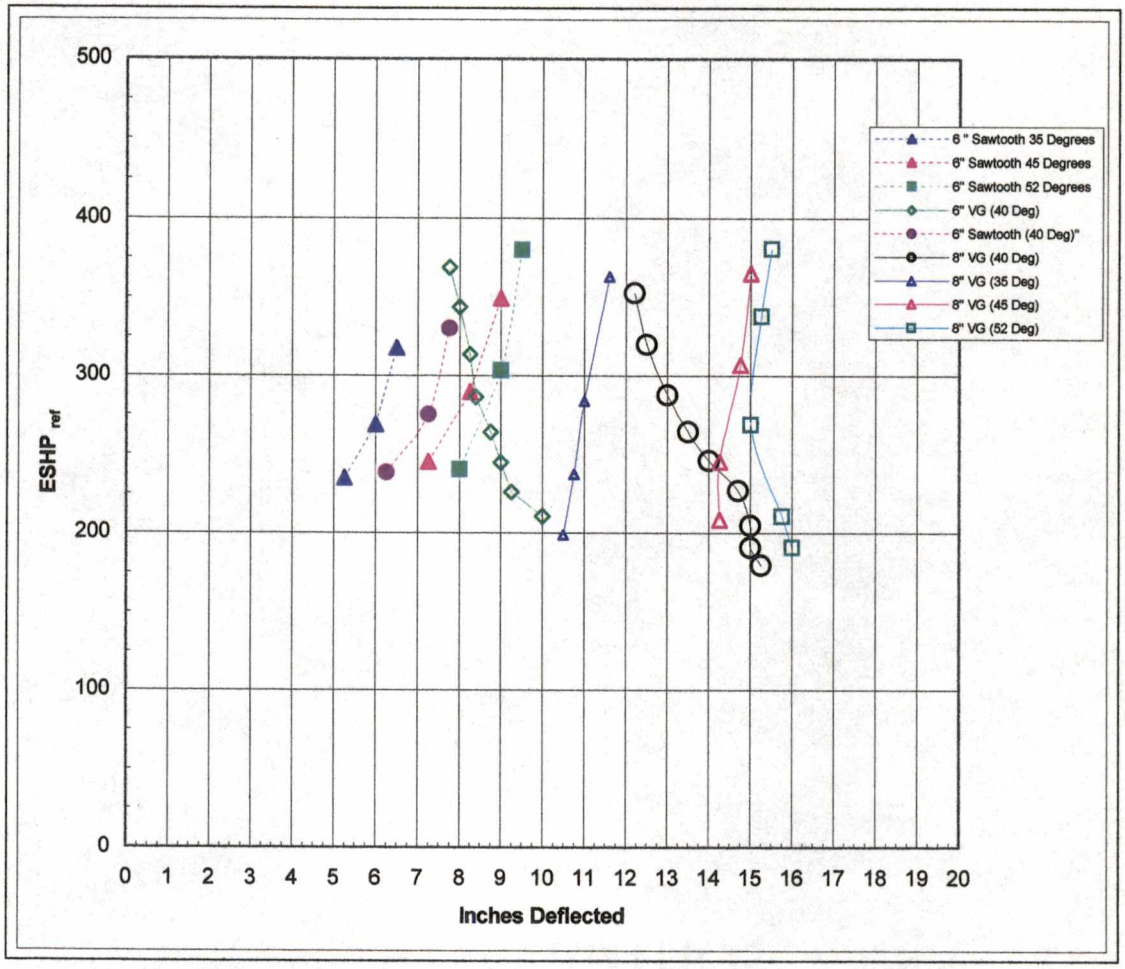


Figure C.22. All Diverters $ESHP_{ref}$ vs. Inches Deflected.

Aircraft:	OH-58A+	**Date:**	24-29 August 2000
Pilot:	Lewis	**FTE's:**	McDougall, Mulnik
Test:	8" Flat Plate (with Vortex Generators) Flow Diverter		
C_T:	.0036		

Configuration: High skid gear installed, Pitot static probe installed, All doors removed, W/σ 3600 lbs., Average CG 109.7.

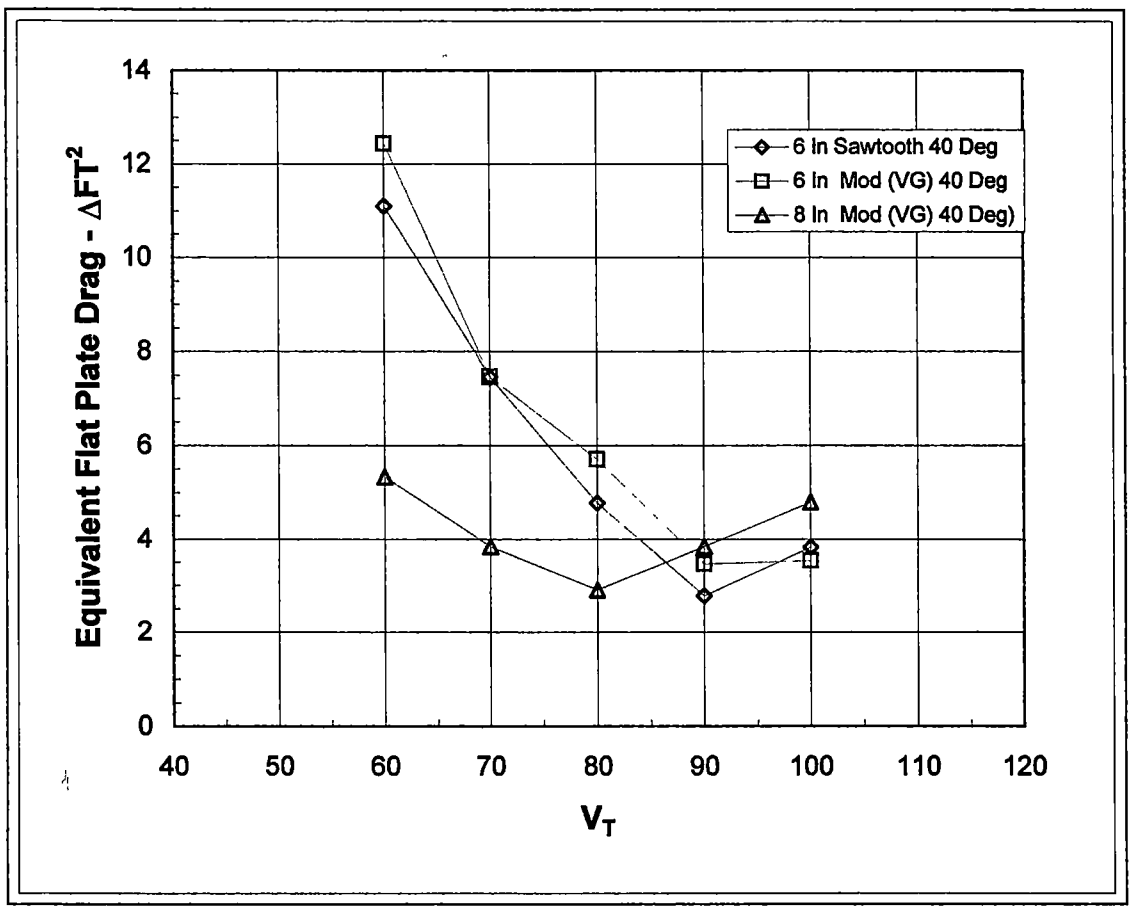


Figure C.23. All Diverters Change in Equivalent Flat Plate Drag.

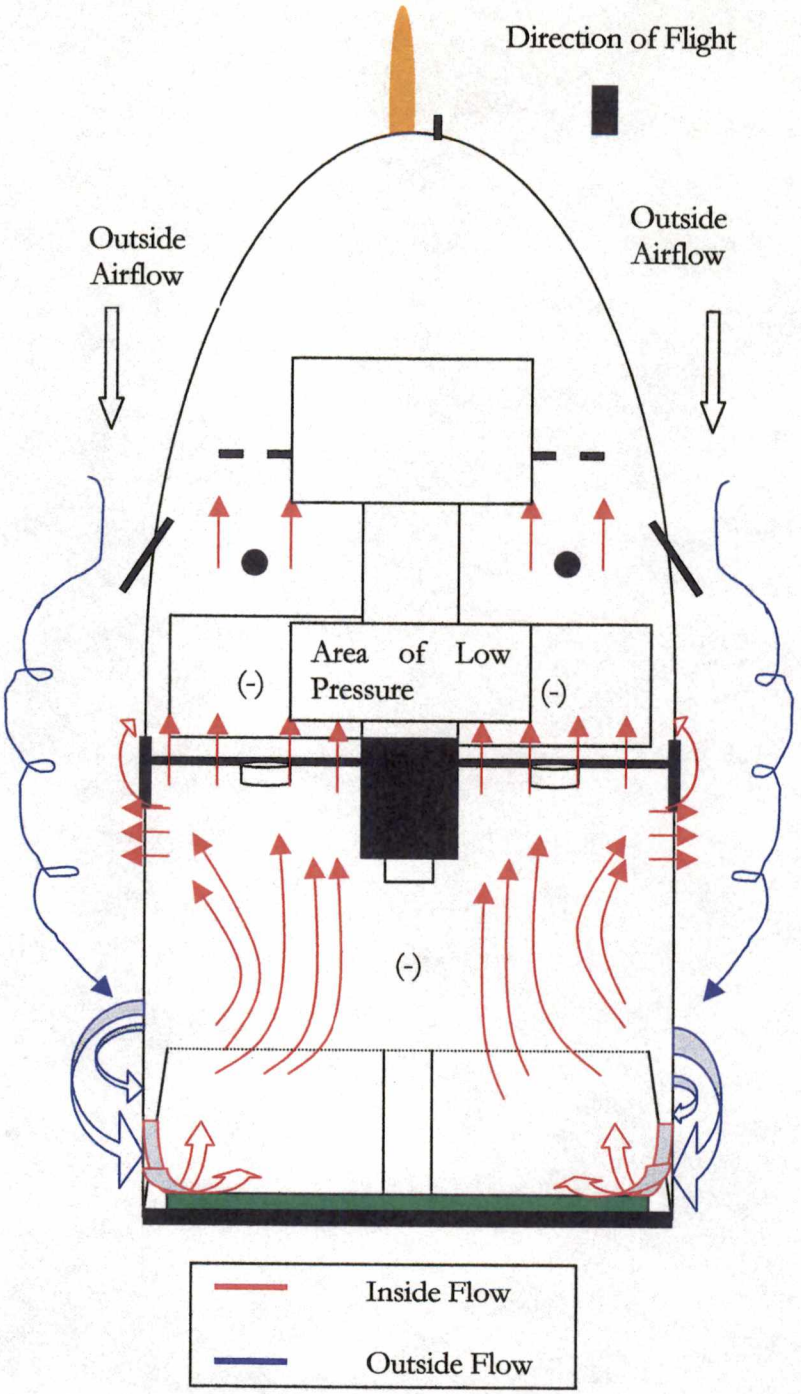


Figure C.24. OH-58A+ Projected Inside Airflow Pattern.

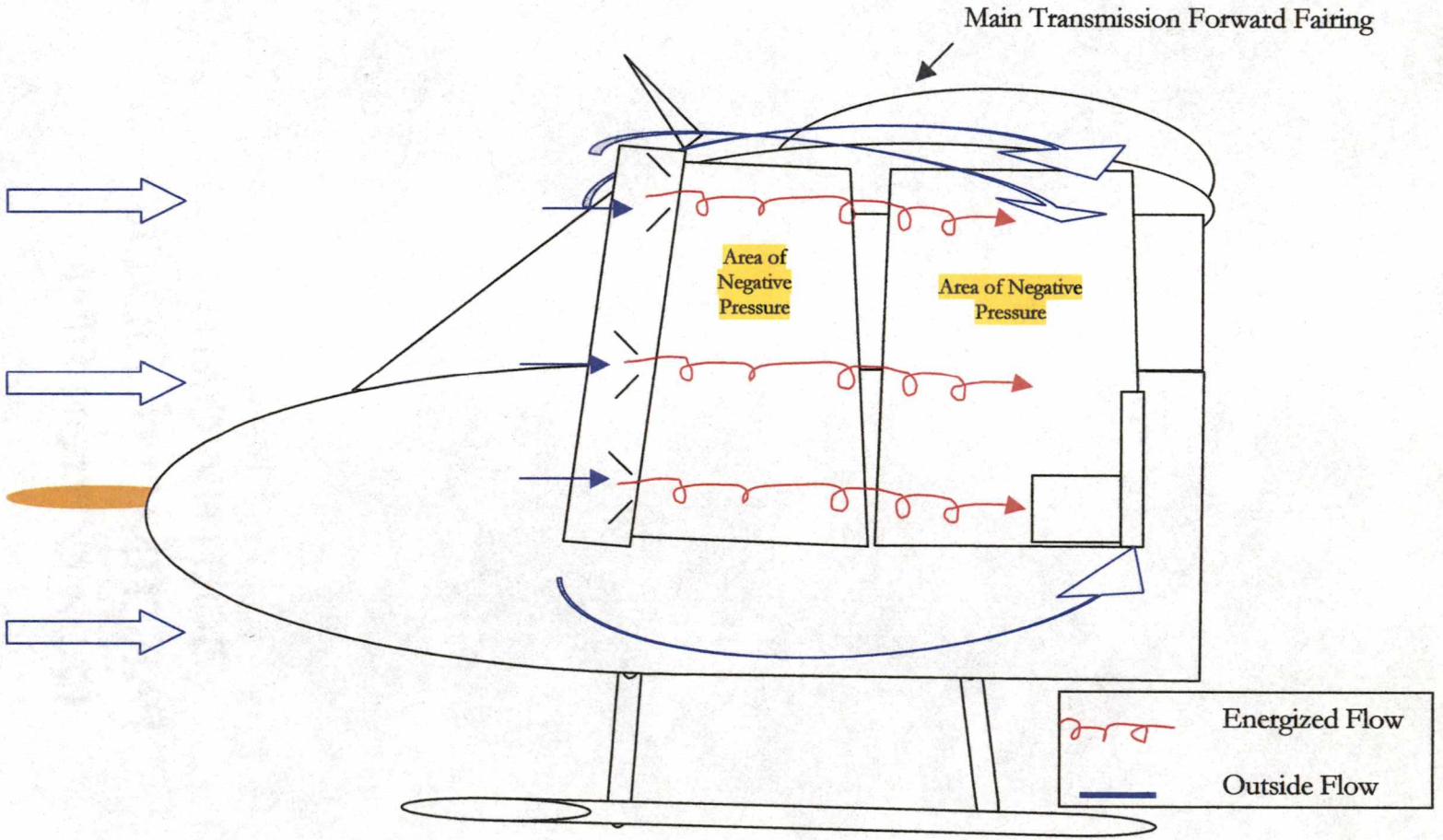


Figure C.25. OH-58A+ Projected Outside Airflow around the Diverters

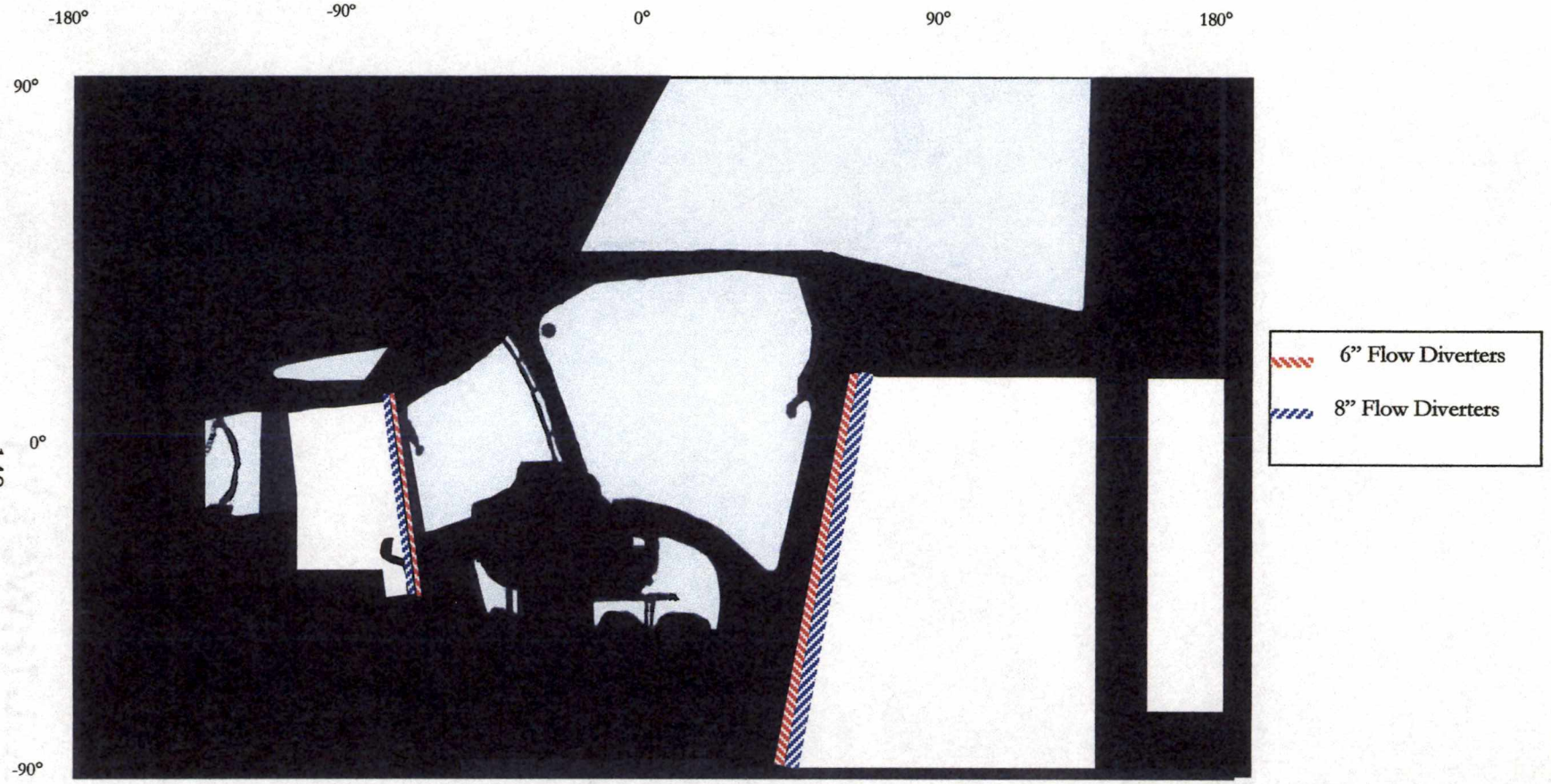


Figure C.26.
OH-58A+ Rectilinear Graph,
Doors Removed, 6" and 8" Flat Plate (with VG's) Flow Diverters Installed

APPENDIX D

AIRCRAFT WEIGHT AND BALANCE

OH-58A+ Weight & Balance
2-Aug-00

Crew: Lewis McDougall
Mulnik

	Weight	Arm/C G	Moment
Aircraft Basic Wt	2001		2368 0
Pilot	242	65	157 3
Copilot	200	65	130 0
Right Rear Seat	0	104	0 0
Left Rear Seat	218	104	226 7
Baggage Compartment	0	170	0 0
Misc Equip	25	105	26 3
Operating Wt	2686		2908 3
Fuel	480		560 4
Takeoff Condition	3166		3468 7
Corrections	38	85	32 3
Takeoff (Corrected)	3128	109 86	3436 4
Expendables			
Copilot		65	
Right Rear Pax		104	
Left Rear Pax		104	
Fuel 250 lbs Remain	-225		-255 8
Landing Condition	2903		3180 6
Corrections	0		0 0
Landing (Corrected)	2903	109 56	3180 6

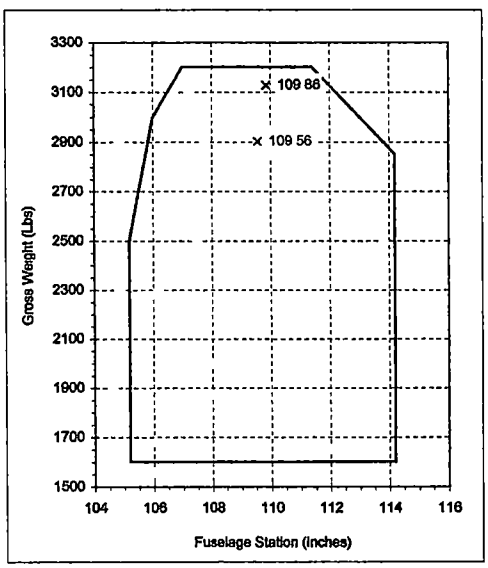


Figure D.1.
Weight and Balance
Pitot Statics and Baseline Testing

OH-58A+ Weight & Balance
4 Aug 00

Crew: Lewis Davis
Mulnik

	Weight	Arm/C G	Moment
Aircraft Basic Wt	2001		2368 0
Pilot	242	65	157 3
Copilot	200	65	130 0
Right Rear Seat		104	0 0
Left Rear Seat	218	104	226 7
	30	100	30 0
Operating Wt	2691		2912 0
Fuel	480		560 4
Takeoff Condition	3171		3472 5
Corrections	38	85	32 3
Takeoff (Corrected)	3133	109 80	3440 2
Expendables			
Copilot		65	
Right Rear Pax		104	
Left Rear Pax		104	
Fuel 100 lbs Remain	-200		-226 8
Landing Condition	2933		3213 4
Corrections	0		0 0
Landing (Corrected)	2933	109 56	3213 4

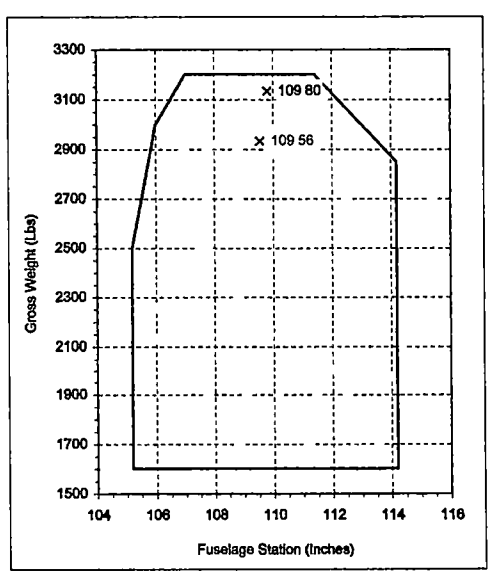


Figure D.2.
Weight and Balance
Best Angle Testing

OH-58A+ Weight & Balance
8-Aug-00

Crew: Lewis McDougall
Calendar

	Weight	Arm/C G	Moment
Aircraft Basic Wt	2001		2368 0
Pilot	242	65	157 3
Copilot	200	65	130 0
Right Rear Seat	0	104	0 0
Left Rear Seat	200	104	208 0
Baggage Compartment	0	170	0 0
Misc Equip	75	105	78 8
Operating Wt	2718		2942 1
Fuel	480		560 4
Takeoff Condition	3198		3502 5
Corrections	38	85	32 3
Takeoff (Corrected)	3160	109 82	3470 2
Expendables			
Copilot		65	
Right Rear Pax		104	
Left Rear Pax		104	
Fuel 250 lbs Remain	-225		-255 8
Landing Condition	2935		3214 4
Corrections	0		0 0
Landing (Corrected)	2935	109 52	3214 4

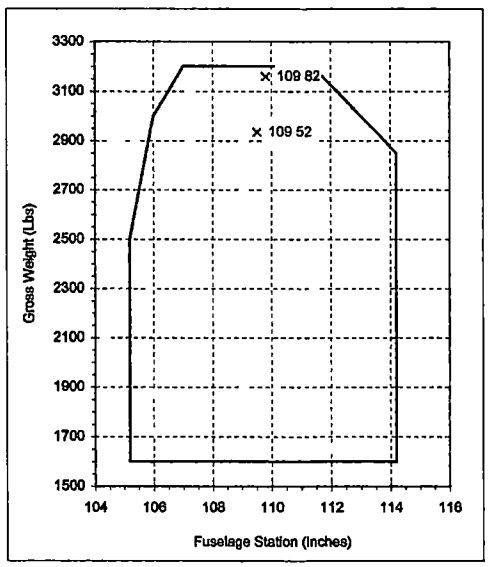


Figure D.3.
Weight and Balance
6" Sawtooth Level Flight Performance

OH-58A+ Weight & Balance
9 Aug 00

Crew: Lewis Davis
Deetman

	Weight	Arm/C G	Moment
Aircraft Basic Wt	2001		2368 0
Pilot	242	65	157 3
Copilot	200	65	130 0
Right Rear Seat		104	0 0
Left Rear Seat	185	104	192 4
	80	100	88 0
Operating Wt	2708		2935 7
Fuel	480		560 4
Takeoff Condition	3188		3496 1
Corrections	20	85	17 0
Takeoff (Corrected)	3168	109 82	3479 1
Expendables			
Copilot		65	
Right Rear Pax		104	
Left Rear Pax		104	
Fuel 100 lbs Remain	-100		-112 2
Landing Condition	3068		3366 9
Corrections	0		0 0
Landing (Corrected)	3068	109.74	3366 9

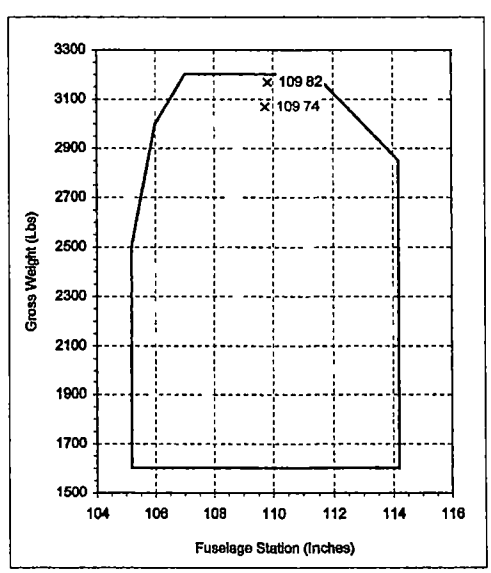


Figure D.4.
Weight and Balance
6" Sawtooth with Backdoors Installed

OH-58A+ Weight & Balance
11-Aug-00

Crew Lewis McDougall
Deetman

	Weight	Arm/C G	Moment
Aircraft Basic Wt	2001		2368 0
Pilot	242	65	157.3
Copilot	200	65	130 0
Right Rear Seat	0	104	0 0
Left Rear Seat	185	104	192 4
Baggage Compartment	0	170	0 0
Misc Equip	75	105	78 8
Operating Wt	2703		2926 5
Fuel	450		523 8
Takeoff Condition	3153		3450 3
Corrections	38	85	32 3
Takeoff (Corrected)	3115	109 73	3418 0
Expendables			
Copilot		65	
Right Rear Pax		104	
Left Rear Pax		104	
Fuel 250 lbs Remain	-225		-255 8
Landing Condition	2890		3162 1
Corrections	0		0 0
Landing (Corrected)	2890	109 42	3162 1

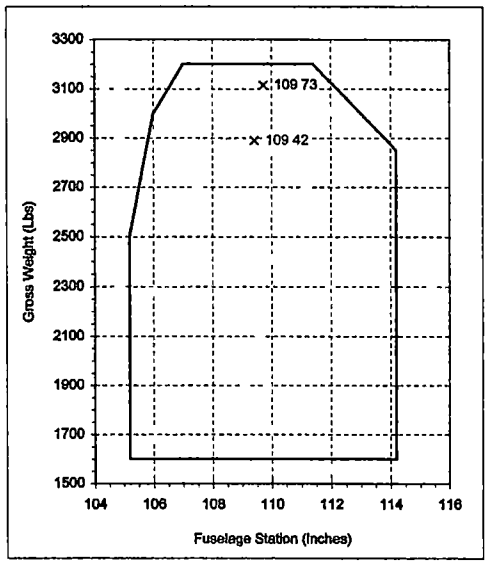


Figure D.5.
Weight and Balance
6" Flat Plate Level Flight Performance

OH-58A+ Weight & Balance
22 Aug 00

Crew Lewis Davis
Deetman

	Weight	Arm/C G	Moment
Aircraft Basic Wt	2001		2368 0
Pilot	242	65	157 3
Copilot	200	65	130 0
Right Rear Seat		104	0 0
Left Rear Seat	185	104	192 4
	80	100	84 0
Operating Wt	2708		2931 7
Fuel	480		560 4
Takeoff Condition	3188		3492 1
Corrections	38	85	32 3
Takeoff (Corrected)	3150	109 84	3459 8
Expendables			
Copilot		65	
Right Rear Pax		104	
Left Rear Pax		104	
Fuel 100 lbs Remain	-200		-226 8
Landing Condition	2950		3233 0
Corrections	0		0 0
Landing (Corrected)	2950	109 59	3233 0

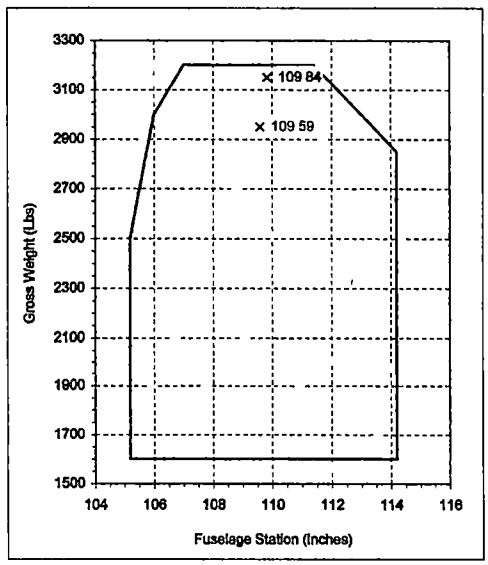


Figure D.6.
Weight and Balance
8" Flat Plate Level Flight Performance

OH-58A+ Weight & Balance
24-Aug-00

Crew: Lewis McDougall
Deetman

	Weight	Arm/C G	Moment
Aircraft Basic Wt.	2001		2368 0
Pilot	242	65	157 3
Copilot	200	65	130 0
Right Rear Seat	0	104	0 0
Left Rear Seat	185	104	192 4
Baggage Compartment	0	170	0 0
Misc Equip	75	105	78 8
Operating Wt	2703		2926 5
Fuel	450		523 8
Takeoff Condition	3153		3450 3
Corrections	38	85	32 3
Takeoff (Corrected)	3115	109 73	3418 0
Expendables			
Copilot		65	
Right Rear Pax		104	
Left Rear Pax		104	
Fuel 250 lbs Remain	-225		-255 8
Landing Condition	2890		3162 1
Corrections	0		0 0
Landing (Corrected)	2890	109 42	3162 1

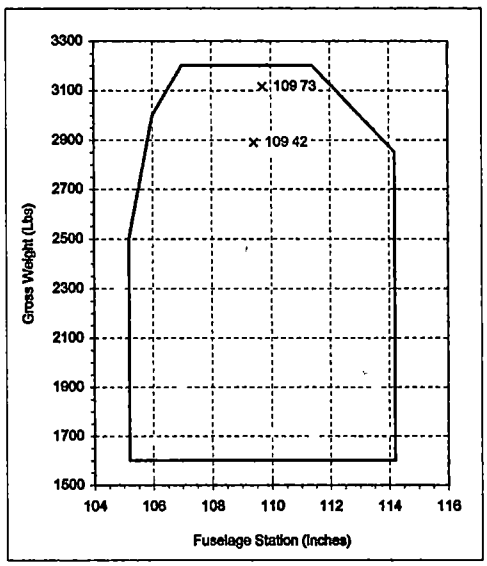


Figure D.7.
Weight and Balance
8" Flat Plate Level Flight Performance

OH-58A+ Weight & Balance
29 Aug 00

Crew: Lewis Davis
Deetman

	Weight	Arm/C G	Moment
Aircraft Basic Wt	2001		2368 0
Pilot	242	65	157 3
Copilot	200	65	130 0
Right Rear Seat		104	0 0
Left Rear Seat	0	104	0 0
	0	100	84 0
Operating Wt	2443		2739 3
Fuel	450		523 8
Takeoff Condition	2893		3263 1
Corrections	0	85	0 0
Takeoff (Corrected)	2893	112 79	3263 1
Expendables			
Copilot		65	
Right Rear Pax		104	
Left Rear Pax		104	
Fuel 100 lbs Remain	-250		-285 0
Landing Condition	2643		2978 1
Corrections	0		0 0
Landing (Corrected)	2643	112 68	2978 1

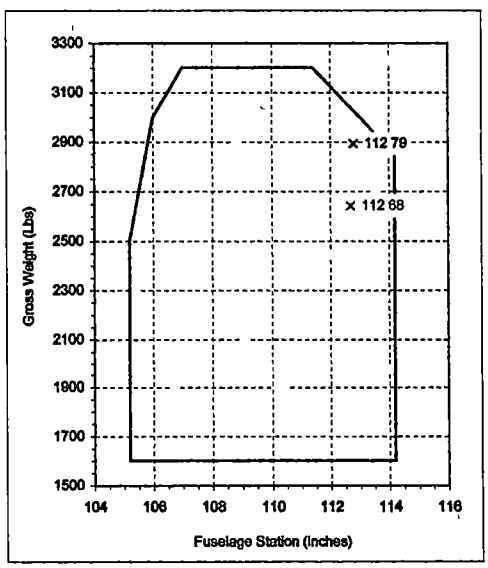


Figure D.8.
Weight and Balance
Flow Visualization Testing

OH-58A+ Weight & Balance
7-Sep-00

Crew: Lewis
Deetman

	Weight	Arm/C G	Moment
Aircraft Basic Wt	2001		2368 0
Pilot	242	65	157 3
Copilot	200	65	130 0
Right Rear Seat	0	104	0 0
Left Rear Seat		104	0 0
Baggage Compartment	0	170	0 0
Misc Equip	75	105	78 8
Operating Wt	2518		2734 1
Fuel	450		523 8
Takeoff Condition	2968		3257 9
Corrections	38	85	32 3
Takeoff (Corrected)	2930	110 09	3225 6
Expendables			
Copilot		65	
Right Rear Pax		104	
Left Rear Pax		104	
Fuel 250 lbs Remain	-150		-169 2
Landing Condition	2780		3056 4
Corrections	0		0 0
Landing (Corrected)	2780	109 94	3056 4

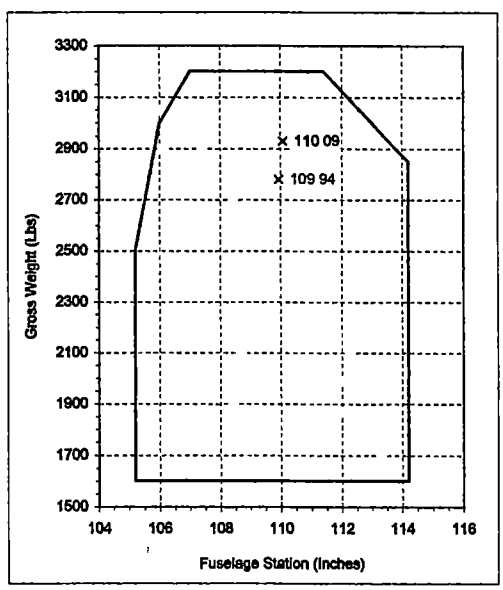


Figure D.9.
Weight and Balance
8" Flat Plate without Vortex Generators

APPENDIX E

TEST PLAN

TEST PLAN

Purpose

The purpose of this test is to evaluate the Flow Diverting Devices on the test helicopter with the doors removed for:

- Passenger Comfort
- Performance improvements
- Differences in handling qualities
- Validate water tunnel tests
- Validate Flight Test Technique

Scope of Tests

TESTS AND TEST CONDITIONS

The tests will be conducted in ten flights for a maximum of 12.0 flight hours. All flights will be conducted under daylight visual meteorological conditions (VMC) at Tullahoma Regional Airport, Tullahoma, Tennessee. The tests and test conditions matrix is presented as Table C.1. Appendix C.

TEST ENVELOPE

The test will be conducted within the limits of the Operator's Manual. The maximum altitude for level flight testing for the purpose of this test is 10,000 feet pressure altitude. Minimum test altitude will be 1000 feet above ground level (AGL). The V_{NE} limits will be 100 KIAS with the doors removed.

TEST LOADINGS

Flight-testing to determine level flight performance will be conducted at one thrust coefficient (C_T), 0.0036. Test loading will be varied only by the number of personnel aboard the aircraft and the amount of fuel used during the tests. The actual aircraft test gross weight will vary from 3109 to 2827 pounds, while the center of gravity (CG) varies from 109.5 to 110.5 inches. Test loading is included in Table C.1.

TEST CONFIGURATIONS

The aircraft configuration for all tests will be: Flight test pitot static system (Boom) installed, doors removed and all engine bleed air systems off.

Method of Tests

TEST METHODS AND PROCEDURES

Engineering tests will be conducted in accordance with USNTPS FTM-106. USNTPS FTM-107, and this test plan as described in the Tests and Test Conditions Table (Table C.1.) in order to assess the aircraft's performance and handling characteristics.

Pitot Static System Calibration

The calibration of the pitot and static systems will be accomplished using the Measured Course method. The pitot static system will be evaluated during a single flight of approximately 1.0 hour. Helicopter loading will be single pilot at the pilot station, one observer at the co-pilot station, and one observer in the passenger compartment, The center of gravity (CG) will be 109.5 inches, at the take-off gross weight (GW) of 3109 pounds.

Level Flight Performance Test & Handling Qualities (Clean)

Level flight performance will be evaluated at one (1) W/σ maintaining 100% Nr. The Level Flight Test (clean) will be evaluated during a single flight of approximately 1.0 hour. The initial pressure altitude will be approximately 4400 feet. The pressure altitude will be varied as necessary to maintain the desired W/σ. Helicopter loading will be single pilot at the pilot station, one observer at the co-pilot station, and one observer in the passenger compartment, The center of gravity (CG) will be 109.5 inches, at the take-off gross weight (GW) of 3109 pounds. Additionally, Lateral Directional Oscillations (LDO) will be evaluated at 90 KIAS.

Best Angle Test

The best angle test will be evaluated during a single flight of approximately 1.0 hour. The saw tooth flow deflectors will be installed for this test. The best air flow deflection

angle will be determined with a modified slide rule mounted in the passenger compartment behind the pilot seat as depicted in Figure 5.3. Helicopter loading will be single pilot at the pilot station, one observer at the co-pilot station, and one observer in the passenger compartment, The center of gravity (CG) will be 109.5 inches, at the take-off gross weight (GW) of 3109 pounds. The observer in the passenger compartment will operate the slide rule and record the distances that the airflow is deflected relative to the angle the flow deflectors are set. Additionally, the right front windscreen will be tufted with yarn strips to help define the relative wind across the flow-diverting device. The actual relative wind will help formulate the precise angle for the installation of the vortex generators on the modified flow diverting device during later testing.

Level Flight Test & Handling Qualities (Deflectors Installed)

Level flight performance will be evaluated at one (1) W/σ maintaining 100% Nr. The Level Flight Test (Flow Diverters installed) will be evaluated during a single flight of approximately 1.0 hour. The initial angle that the flow deflectors will be set at will be determined in the best angle test. The initial pressure altitude will be 4000 feet. The pressure altitude will be varied as necessary to maintain the desired W/σ. Helicopter loading will be single pilot at the pilot station, one observer at the co-pilot station, and one observer in the passenger compartment, The center of gravity (CG) will be 109.5 inches, at the take-off gross weight (GW) of 3109 pounds. Additionally, Lateral Directional Oscillations (LDO) will be evaluated at 90 KIAS.

Flow Visualization Test

Flow visualization flight-testing will be conducted during three flights totaling approximately 2.0 flight hours. This test involves the installation of non-standard equipment mounted on the left main landing gear on the test aircraft as depicted below in Figure 5.5. This equipment will help verify visually if the flow deflectors are working via the introduction of smoke into the airflow. Helicopter loading for the test aircraft will be single pilot at the pilot station, one FTE at the co-pilot station, and one FTE in the passenger compartment, The center of gravity (CG) will be 109.5 inches, at the take-off gross weight (GW) of 3109 pounds. The loading for the chase aircraft will be single pilot at the pilot station, and one observer at the co-pilot station. This test will require a chase aircraft with video recording capability.

INSTRUMENTATION AND DATA EXTRACTION/PROCESSING

Sensitive instrumentation and data recording equipment is installed onboard the test aircraft. Cockpit instrumentation will be used to acquire engine and flying parameters. Fuel flow data will be extracted from the Operator's Manual. A tufted screen will be installed in the right rear passenger door to assist in flow visualization. The external equipment required to collect the desired test data are: A programmable calculator, Stopwatch, GPS, Two Video Recorders and Portable Voice Recorders. Data will be recorded on a laptop computer, kneeboard cards by the observer, and on portable voice recorders. The data will be analyzed manually, using TPS computer programs or manual data reduction using an Excel spreadsheet and presented in the final report.

Where:

$$W_{ref} = \frac{W_T}{\sigma_T}\left(\frac{\Omega R_S}{\Omega R_T}\right)^3$$

$$C_T = \frac{\frac{W_T}{\sigma_T}}{\rho_{ssl} A_D (\Omega R)^2}$$

W_{ref} - Referred weight

W_T - Test weight

σ_T - Density ratio

ΩR_S - Standard RPM blade rotational velocity

ΩR_T - Test RPM blade rotational velocity

V_{NE} - Never exceed velocity
(Note: VNE is 100 knots with doors removed)

H_d - Density altitude

M_{TIP} - Blade tip Mach number

V_c - Calibrated airspeed

a - Speed of sound at test conditions

The data will be recorded on hand-held data cards and micro cassette recorders. The following will be taken at each data point:

Vo - Ship observed airspeed.

Q - Ship torque.

N_R - Rotor RPM.

Fuel - Fuel remaining.

H_P - Pressure altitude.

OAT - Observed outside air temperature.

The following is a list of data requirements:

Stabilize on data for 60 seconds prior to recording data.

V_o - ± 1 knot.

H_P - ± 20 feet.

N_R - ± 0.5%.

Lateral-Directional Oscillation

The following data will be taken at each data point:

δlat - Lateral cyclic position.

δlong - Longitudinal cyclic position.

δped - Pedal position.

δcol - Collective position.

Vo - Velocity observed.

Hpo - Altitude observed.

To - Temperature observed.

Vv - Vertical velocity (climb and descent).

θ - Pitch angle.

ϕ - Roll angle.

β - Side slip angle.

Q - Ship torque.

NR - Rotor RPM.

Fuel - Fuel remaining.

The following is a list of test criteria:

Ball centered, balanced flight at trim.
Longitudinal, lateral, and pedal controls fixed (at trim) and or free
Collective fixed.

The following is a list of the data requirements:

Hpo ± 1000 ft of the target test altitude.

NR ± 0.5 %.

Vo ± 2 kn.

The data will be reduced manually.

Special Precautions

SAFETY CONSIDERATIONS

Both the Level Flight and Flow Visualization Flight Tests involve mounting of non-standard equipment on the test aircraft. The test crew must have a thorough knowledge of aircraft limitations. All level flight testing shall be conducted within the established flight envelope and normal operating limitations contained in the Aircraft Operator's Manual. Particular attention and caution will be used when flow visualization and flow diverting devices are installed on the test aircraft. A chase aircraft will be required for all Flow Visualization Flight Tests. A training flight will be conducted to practice formation flying, test procedures, and emergency breakup procedures prior to the actual test flight. The crew will terminate the test in the event of any unusual handling characteristics or vibrations. A thorough review of smoke and fume elimination and fuselage fire in flight emergency procedures will be conducted during the flight briefings. During all tests the crew must remain vigilant to air traffic and obstacle avoidance.

RISK MANAGEMENT

The flight shall be conducted in VFR conditions during daylight. Emergency actions will be developed and briefed by the aircrew prior to the installation of experimental (non-standard) equipment. Consideration will be given to a formation training flight prior to the Flow Visualization Flight Tests. The overall risk associated with the conduct of this test is assessed to be low. However, with the exception of formation flight which is assessed as a medium risk.

Management

SCHEDULE/MILESTONES

Coordination meeting for the Flow Deflector Project is scheduled on 19 July 2000 (1530 hours) at the UTSI hangar facility for all personnel concerned in the flight test. The first flight test is scheduled to be conducted on 21 August 2000 pending approval of the test plan by the project advisor.

Test Plan approval	19 July 2000
Flight Brief	18 August 2000
Pitot Static System Calibration Flight Test	21 August 2000
Baseline Level Flight Performance Test	21 & 22 August 2000
Installation of Flow Deflectors	22 August 2000
Flight Briefing	22 August 2000
Best Angle Flight Test	23 August 2000
Level Flight Performance with Flow Deflectors	23 August 2000
Flight Briefing	23 August 2000
Level Flight Performance (modified Deflectors)	24 August 2000
Flight Briefing	25 August 2000
Formation Training Flight with Chase Acft	25 August 2000

Flow Visualization Flight Test 25 August 2000

PERSONNEL ASSIGNMENT

Dr. Lewis is assigned as the aircraft pilot-in-command of the test aircraft and project advisor. Professor Stellar is designated pilot-in-command of the chase aircraft. CW4 McDougall is assigned as the test director and FTE for each of the tests. Mr. Mulnik is assigned as an FTE as well as technical advisor for the installation of experimental equipment. Mr. Leigh is designated as the technical advisor for all instrumentation. Mr. Heatherly is designated chief of maintenance.

REPORTS

An individual Report of Test Results will be completed as soon as practicable after the successful completion of the flight tests. The report will:

- Determine if passenger comfort will be enhanced with the flow deflectors installed.
- Summarize the differences in the level flight performance of the OH-58A+ with and without flow diverting devices installed with the doors removed.
- Report any handling quality differences observed during the testing.
- Validate the water tunnel test results from a previous study conducted at UTSI in 1997.

Table E.1.
Test and Test Conditions

Event #	Description	Crew	Target W/σ [1]	Estimated Pressure Altitude (ft) [2]	Estimated Gross Weight (lbs) [3]	Airspeed (KOAS) [4]
1	Pitot Static Calibration	1 pilot, 2 FTE's	3600	1500-6500	3070	40 - 100 knots
2	Baseline testing & Handling Qualities (LDO)	1 pilot, 2 FTE's	3600	2900-6500 Initial target Alt. ≈ 4400	≈ 3070	70 - 100 knots
3	Best Angle Testing	1 pilot, 2 FTE's	3600	≈ 2000	≈ 3070	90 knots
4	Flow Diverting Device Testing & Handling Qualities (LDO)	1 pilot, 2 FTE's	3600	2900-6500 Initial target Alt. ≈ 4400	≈ 3070	70 - 100 knots
5	Modified Flow Diverting Devices & Handling Qualities (LDO)	1 pilot, 2 FTE's	3600	2900-6500 Initial target Alt. ≈ 4400	≈ 3070	70 to 100 knots
6	Formation Training Flight	**Test Acft** 1 pilot, 1 FTE's **Chase Acft** 1 pilot, 2 FTE's	N/A	≈ 4400	3070	70-100 knots
7	Flow Visualization	**Test Acft** 1 pilot, 1FTE's **Chase Acft** 1 pilot, 2 FTE's	N/A	≈ 4400	≈3070	70 - 100 knots
8	Flow Visualization	**Test Acft** 1 pilot, 1 FTE's **Chase Acft** 1 pilot, 2 FTE's	N/A	≈ 4400	≈3070	70 - 100 knots

Notes:

1. Referred Gross Weights are computed allowing 50 pounds fuel burn to initial data point using a non-standard temperature of 21° C with a standard lapse rate.
2. The initial pressure altitude of 4400 feet and σ, are calculated for a non-standard day (21° C) with a standard lapse rate.
3. Average Center of Gravity will be approximately 109.2 inches.
4. Maximum airspeed tested shall be limited by VNE with doors removed (100 KIAS).

TABLE E.2. OH-58A/C EMERGENCY PROCEDURES

Engine Failure-Hover
Autorotate

Eng Fail-Low Alt/Low Airspd or Cruise
1. Autorotate
2. EMER SHUTDOWN

Engine Restart-During Flight
1. Throttle-Close
2. Attempt Start
3. Land ASAP

Engine Compressor Stall
1. Collective-Reduce
2. ENG DEICE and HTR-OFF
3. Land ASAP

Engine Overspeed
1. Collective-Increase
2. Throttle-Adjust
3. Land ASAP

If RPM cannot be controlled manually:
4. Autorotate
5. EMER SHUTDOWN

Engine Underspeed
a. If powered flight w/ rotor in green
Land ASAP
b. Engine underspeed below 94% N2
1. Autorotate
2. EMER SHUTDOWN

Engine Surges
1. GOV RPM switch-INCR
landing
2. Throttle-Adjust to 98% N2
3. Land ASAP

If engine surges are not controlled:
4. Autorotate
ON
5. EMER SHUTDOWN

Flight Control Malfunctions
1. Land ASAP
2. EMER SHUTDOWN after landing

Loss of Tail Rotor Effectiveness
1. Pedal-Full Left
2. Cyclic-Forward

Main Driveshaft Failure
1. Autorotate-maintain power
2. EMER SHUTDOWN-after landing

Clutch Fails to Disengage
1. Throttle-Open
2. Land ASAP

Mast Bumping
Land ASAP

Hot Start
1. STARTER switch-Press
2. Throttle-Close

Engine/Fuselage/Elec. Fire-Ground
EMER SHUTDOWN

Engine/Fuselage Fire-In Flight
If Power-On landing:
1. Land ASAP
2. EMER SHUTDOWN after landing

If Power-Off landing:
1. Autorotate
2. EMER SHUTDOWN

Electrical Fire-In Flight
1. BAT and GEN switches-OFF
2. Land ASAP
3. EMER SHUTDOWN after

Smoke and Fume Elimination
1. Vents-Open
2. DEFOG & VENT switches-

Overheated Battery
1. BAT switch-OFF
2. Land ASAP
3. EMER SHUTDOWN after landing

APPENDIX F

FLOW DIVERTERS AND INSTRUMENTATION INSTALLATION

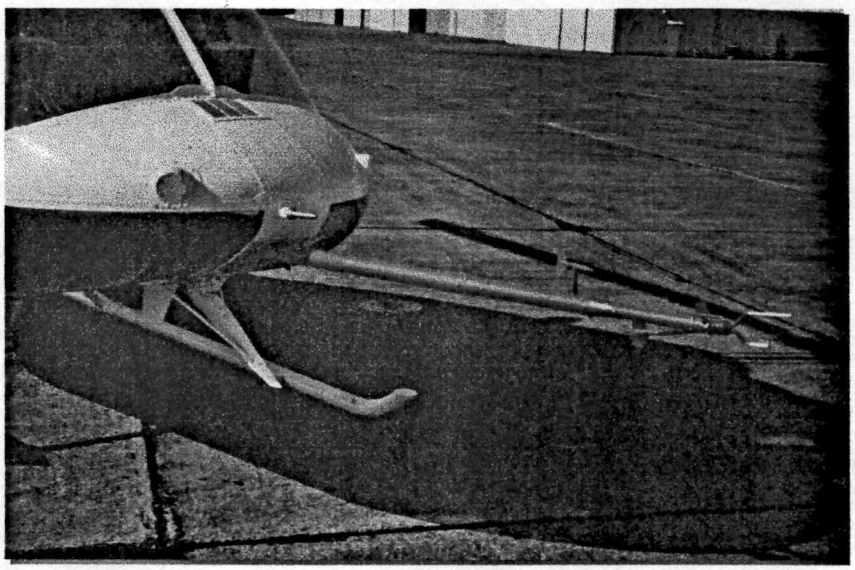


Figure F.1. Pitot Static Boom.

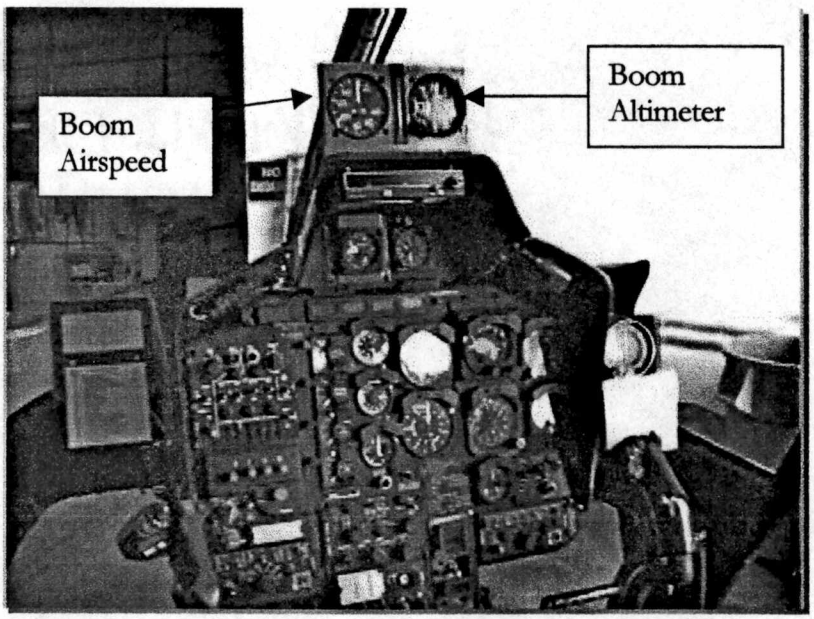


Figure F.2. Boom Airspeed and Altimeter Instruments.

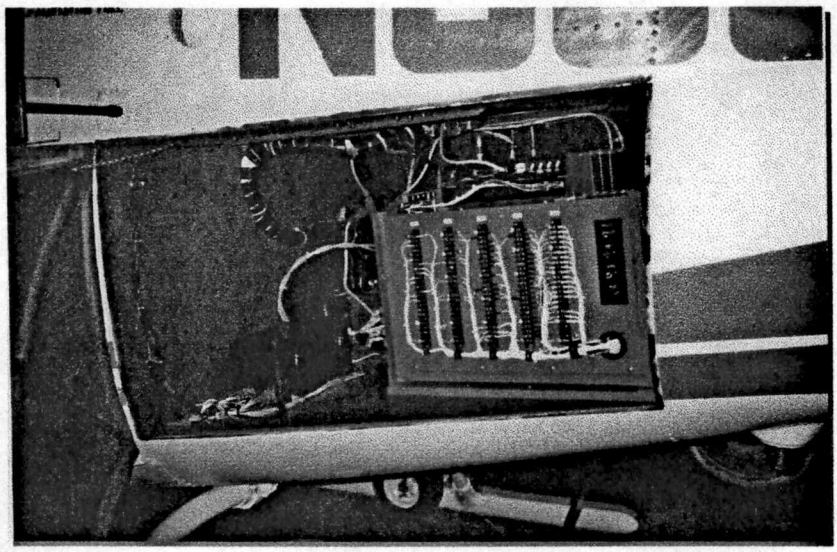
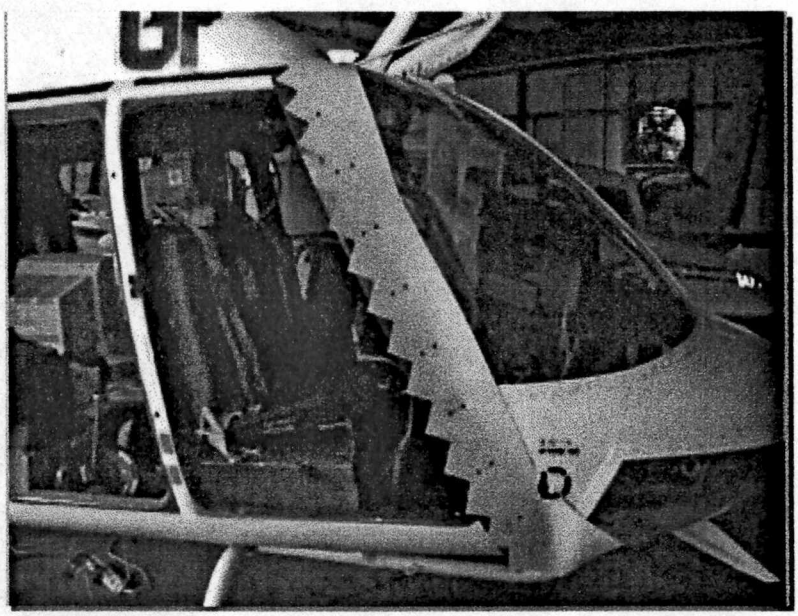


Figure F.3. Data Acquisition Pallet Installation.



F.4. 6" Sawtooth Flow Diverter

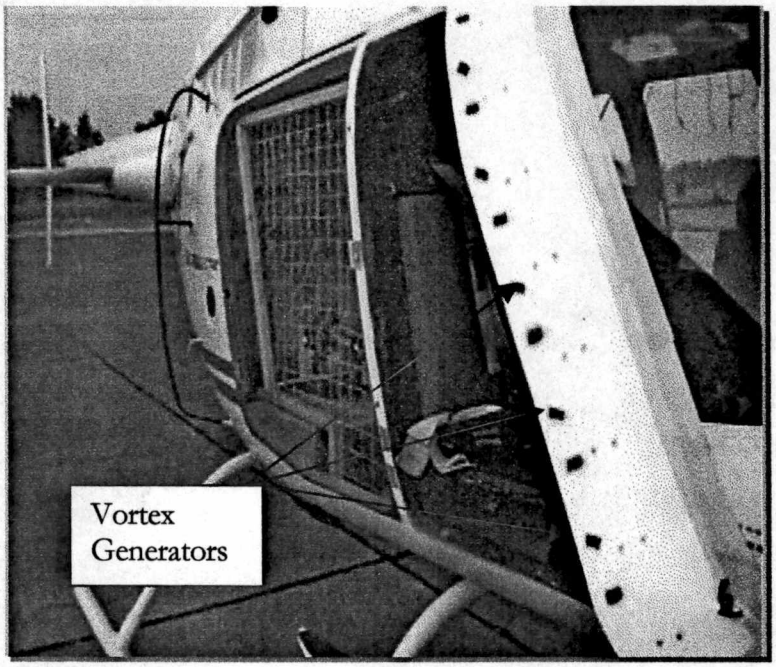
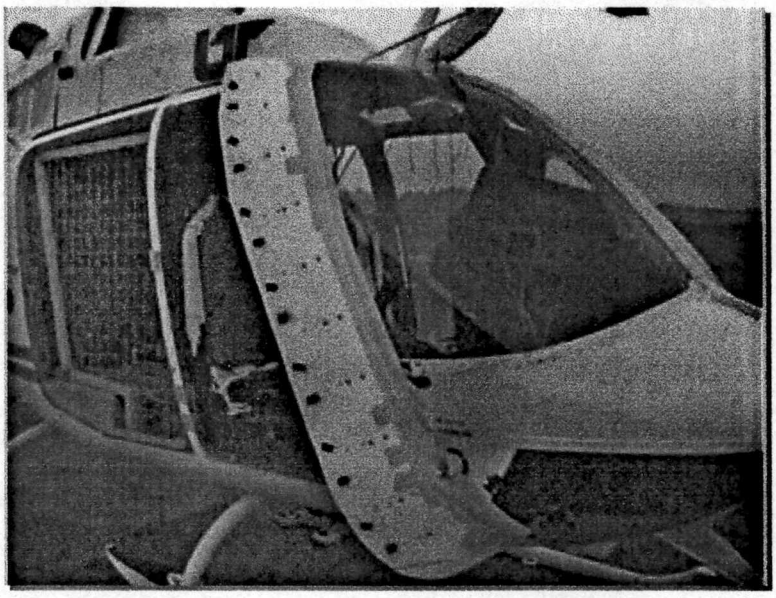


Figure F.5. 6" Flat Plate (with Vortex Generators) Flow Diverter.



F.6. 8" Flat Plate (with Vortex Generators) Flow Diverter.

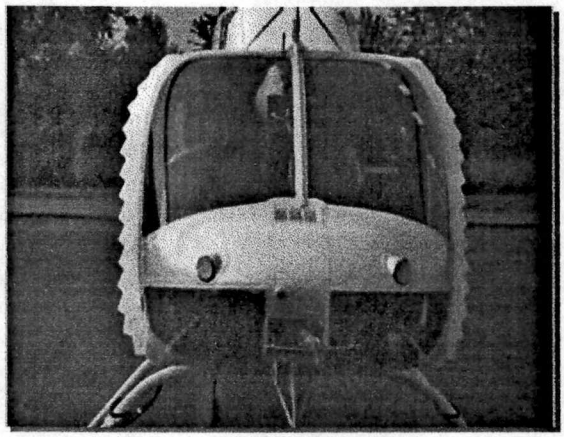


Figure F.7. 6" Sawtooth Flow Diverters Installed.

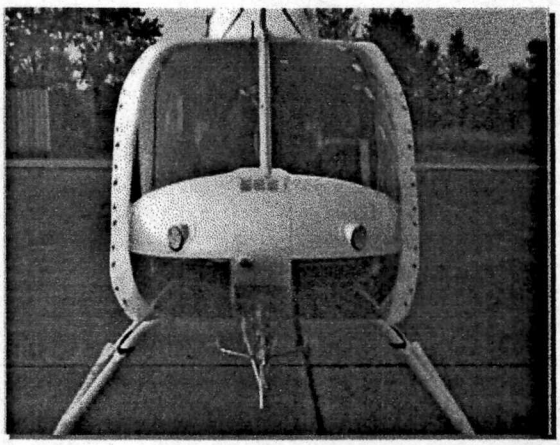


Figure F.8. 6" Flat Plate Flow Diverters Installed.

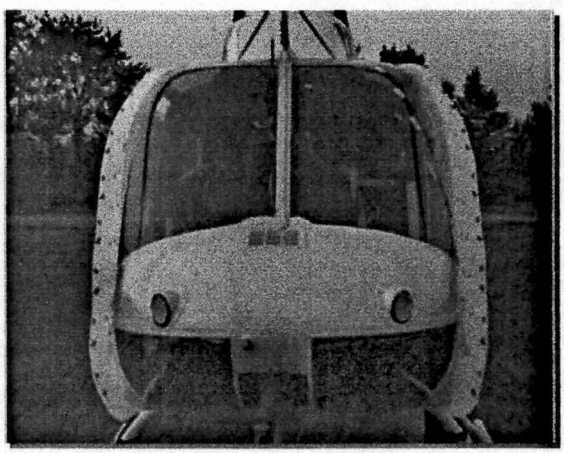


Figure F.9. 8" Flat Plate Flow Diverters Installed.

APPENDIX G

FLOW VISUALIZATION INSTALLATION

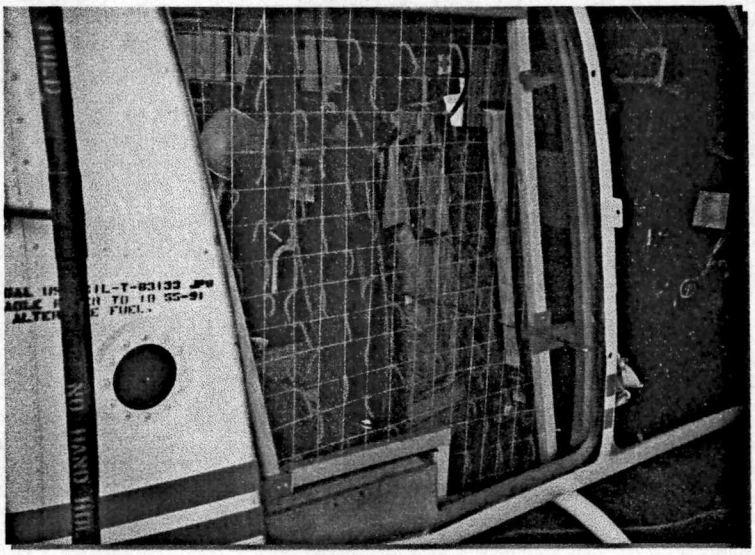


Figure G.1. Tufted Screen Installed.

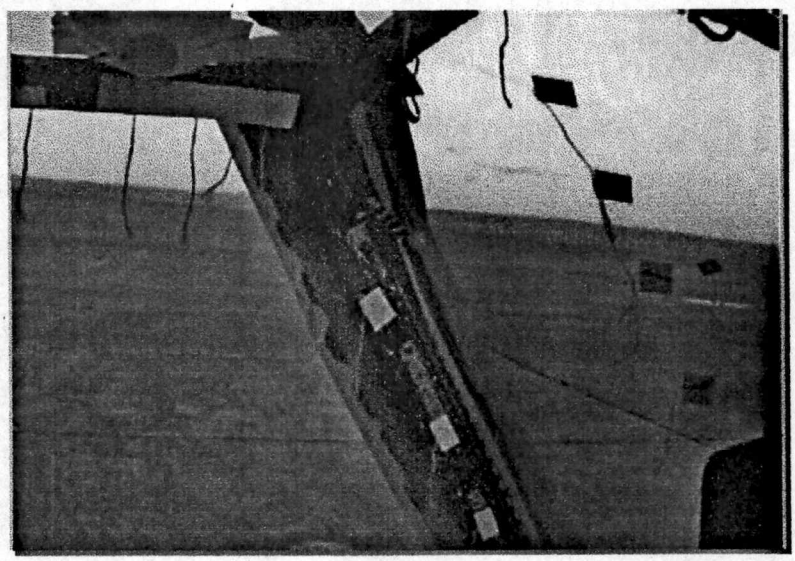
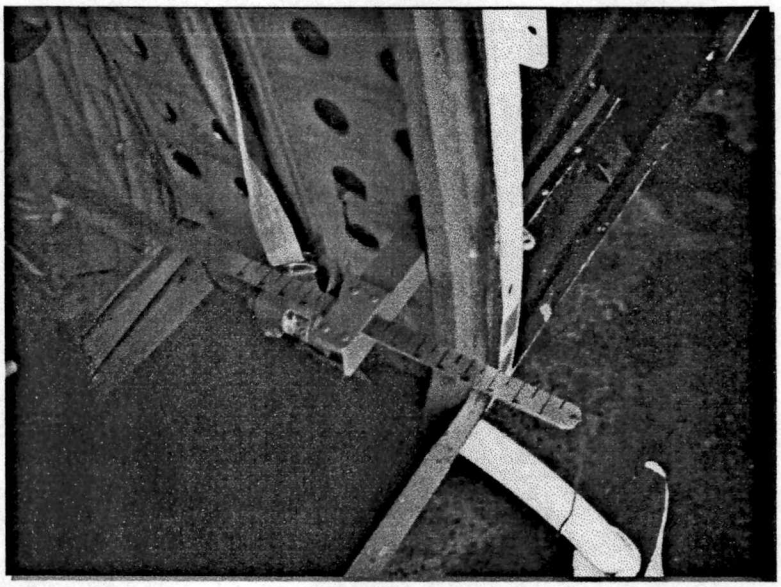


Figure G.2. Inside and Outside Windscreen Tufts.



G.3. Best Angle Measuring Device.

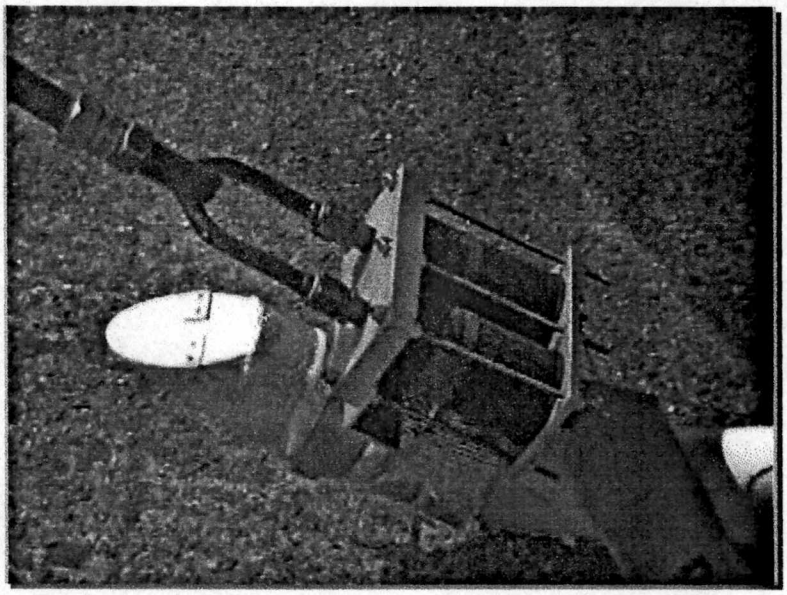


Figure G.4. Smoke Canister Mounting (Left Skid).

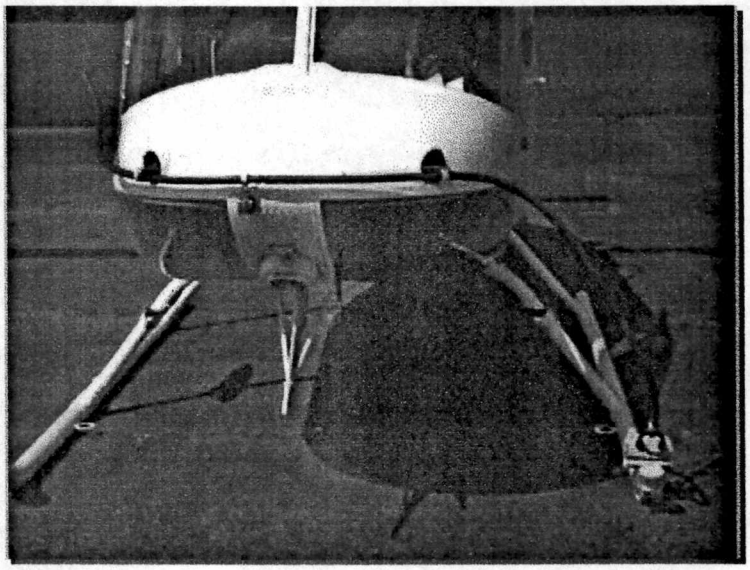


Figure G.5. Smoke Generator System Installed.



Figure G.6. Representative 18" Flow Diverter.

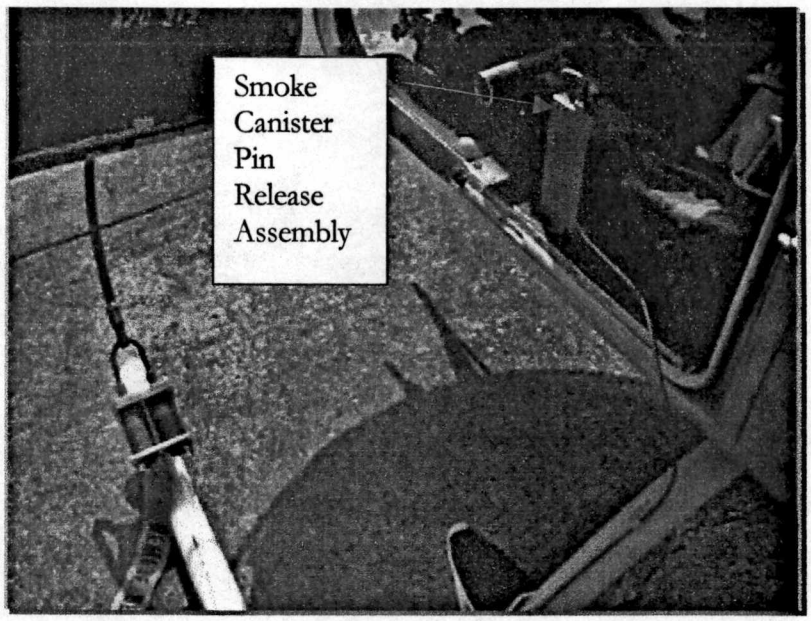


Figure G.7. Smoke Generator System Pin Release Assembly.

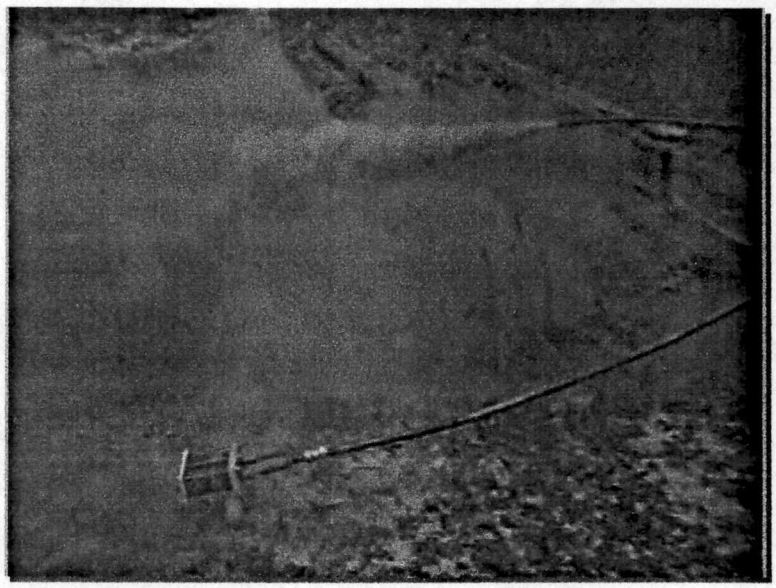


Figure G.8. Smoke Generator System Ground Test.

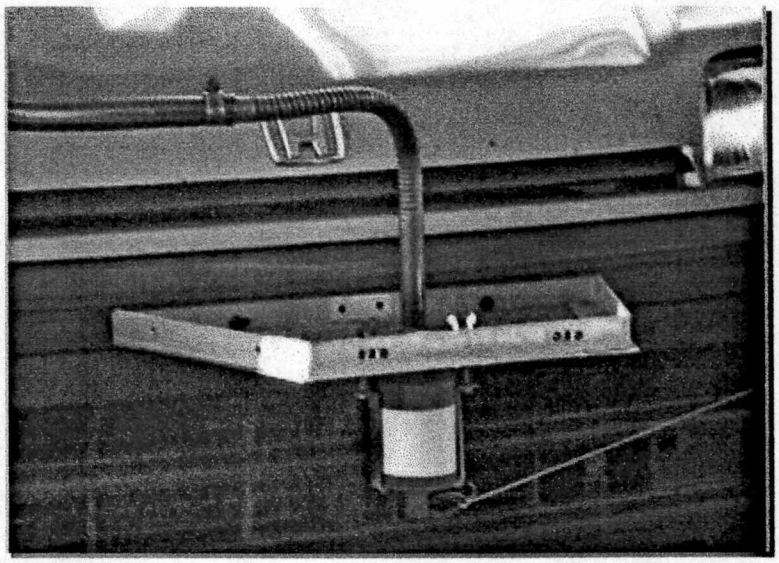


Figure G.9. Smoke Generator System Ground Test Installation.

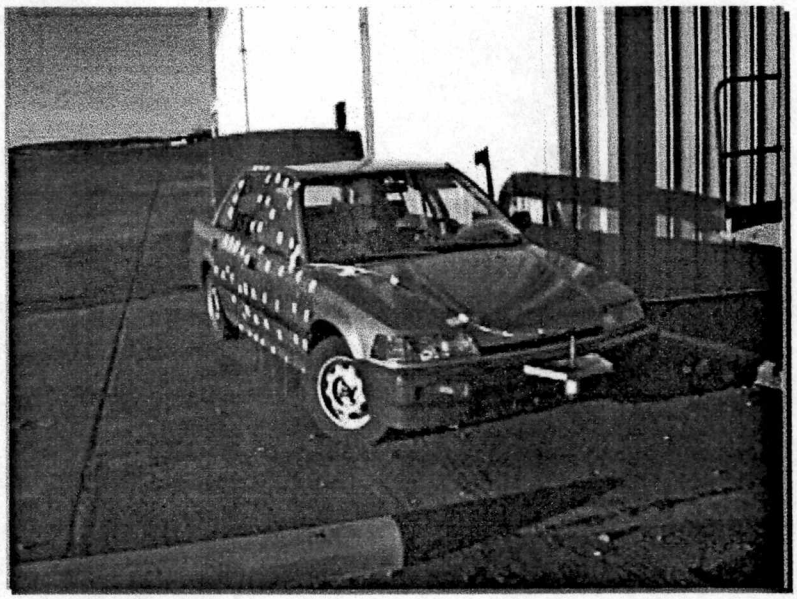


Figure G.10. Smoke Generator System and Tufts for Ground Test.

VITA

Kelly E. McDougall was born to Edith and Patrick McDougall in September 1960 in the town of Bloomington, Minnesota. He graduated from Lincoln High School in 1978. He enlisted in the United States Army in the Airborne Infantry in 1979. After jumping from many different aircraft during his first assignment at Fort Bragg, North Carolina, he was accepted to the United States Army's Initial Entry Rotary Wing Course. He graduated from flight school in December 1983 as an honor graduate, and flew a variety of aircraft, both rotary and fixed wing, throughout the next seventeen years. During this time, he had numerous assignments including serving with the 160th SOAR as a Flight Lead, Fully Mission Qualified, MH-6E, H & J Instructor Pilot from 1987 - 1992. Additionally, during this time, he earned a Bachelor of Science Degree in Professional Aeronautics, from Embry-Riddle Aeronautical University. He earned his Commercial and Instrument Pilot certificate for both single and multi-engine airplanes and helicopters and an Airline Transport Pilot rating for helicopters. He is a veteran of Operation Just Cause (Panama 1989), Operations Desert Shield and Storm, and operation Uphold Democracy (Haiti 1994). In November 1989, he married Mary Glenn of Wayne, New Jersey. They now have two children, Kaely and Bradley. Kelly graduated from the University of Tennessee Space Institute in December 2000 with a Master of Science degree in Aviation Systems with a follow on assignment to attend the U.S. Naval Engineering Test Pilot School at Patuxent River, Maryland.